VILNIUS UNIVERSITY

Vytautas Ašeris

COMPUTATIONAL MODELLING OF BIOSENSORS UTILIZING INTERMEDIATE SUBSTANCES

Doctoral dissertation
Physical sciences, informatics (09 P)

Vilnius, 2013

Doctoral dissertation was prepared in 2009–2013 at Vilnius University.

Scientific supervisor:

prof. dr. Romas Baronas (Vilnius University, Physical Sciences, Informatics – 09 P).

VILNIAUS UNIVERSITETAS

Vytautas Ašeris

TARPINES MEDŽIAGAS NAUDOJANČIŲ BIOJUTIKLIŲ KOMPIUTERINIS MODELIAVIMAS

Daktaro disertacija
Fiziniai mokslai, informatika (09 P)

Vilnius, 2013

Disertacija rengta 2009–2013 metais Vilniaus universitete.

Mokslinis vadovas:

prof. dr. Romas Baronas (Vilniaus universitetas, fiziniai mokslai, informatika – 09 P).

Acknowledgements

I would like to express my deepest gratitude towards all the people who, in one way or another, influenced me in a positive way. It was a long journey of keeping in touch with science.

First of all, I would like to thank my parents and my grandparents for being patient and answering every question I had came up with in my childhood. I strongly believe that if my inquisitiveness was not encouraged so much, I would not be defending this dissertation.

Secondly, I would like to thank my mathematics and informatics teachers, J.Budzilaitė and B.Budvytis, for getting me interested in research in general sense. I would like to thank physics schools "Fotonas" and "Fizikos Olimpas", and everyone involved with them, for showing how little I understand about science.

Thirdly, I would like to thank my scientific supervisor prof. R.Baronas, for getting me interested in science again, as I lost almost all the interest during my first few years in the University. Not only topic-related assistance, but numerous discussions, advices, recommendations and encouragements are greatly appreciated. On the same note, I would like to thank Research Council of Lithuania and association "Infobalt" for their financial support.

I had a real break-through with my research after the group of "Biomoda" was assembled. I am grateful to everyone within this group, from prof. J.Kulys and his highly professional advices, to my young (but already doctoral) colleagues - Evelina, Dainius and Karolis, for their friendly help.

Finally, I would like to express my most hearty gratitude towards my wife Giedrė for the patience and understanding, especially during the last few months. Solicitude from my mother and grandmother was always felt and appreciated.

Contents

Introduction

Research context and motivation

Various auxiliary equipment items are being constantly created, modified and applied to improve the quality of life. The use of mechanical, electronic, biochemical and other devices is an inseparable part of everydays life of humanity. Biosensors play an integral part in medicine, ecology and environmental monitoring [1].

Biosensors are sensing devices that transform a biological recognition into a detectable signal [2, 3]. During the biosensor operation the substrate to be analysed is biochemically converted to a product. The biosensor response, in most cases, is directly proportional to the concentration of the reaction product [4].

According to the report by Global Industry Analysts, the global demand for biosensors in medical devices is forecasted to reach US$16.5 billion by the year 2017 [5]. The largest market for biosensors globally is in the US, followed by Europe, with the largest growing market (expected to be, due arising health-related concerns) in Asia-Pacific.

Various types of biosensors are currently being developed and used. The most common of them are potentiometric, optical and amperometric [6–8]. This research concentrates on the investigation of enzymatic amperometric biosensors, which have proved to be reliable and low-cost in various analytical systems with applications in medicine, food technology and the environmental industry [9–11]. The response of such biosensors is measured as anodic or cathodic current [12].

However, amperometric biosensors possess a number of serious drawbacks. One of the main reasons restricting wider use of the biosensors is a relatively short linear range of the calibration curve [4, 11]. Increasing

the concentration range of detectable substrate and the sensitivity of the detection event improves the prospects for commercializing biosensors [13, 14].

One way of overcoming those problems is to use intermediate substances. Due to the appropriate combination of substances used for biochemical reaction, the biosensor sensitivity may be considerably enhanced [15, 16]. The context of this research is optimization and research of new possibilities for the development of biosensors by using intermediate substances (either by using mediators, either by coupling enzymes to use additional substrates as intermediates) [17–19].

The understanding of the kinetic peculiarities of the biosensors is of crucial importance for their design and optimization. In order to optimize the biosensor configuration the mathematical modelling is rather often used instead of expensive physical experiments [20–23]. For almost half a century the mathematical modelling is successfully used to study the characteristics of the biosensors and to optimize their configuration [24–28]. The digital simulation of more general reaction-diffusion systems began as early as 1969 [29, 30].

In many cases analytical solutions of the developed mathematical models exist only for specific conditions, due the non-linear term in governing equations [28, 31]. Computational modelling is the only way to solve the problem in general case [32, 33]. However this is a complicated and time-consuming task [33–35]. In most cases the finite difference technique is employed and the software implementing the computational model is created [33, 36].

Various finite difference schemes have been analysed and compared to model the behaviour of the classical Michaelis-Menten biosensor [37, 38]. The improvement of the finite difference schemes to solve related biochemical problems was presented by Bieniasz in the 16 part series from [39] to [40] and Britz [41, 42]. The mathematical models developed in this work are solved by using finite difference technique [43–46] with calculations being carried out in a computational grid [47] to improve their performance.

Aim and objectives of the thesis

The aim of this work was to develop an algorithms and a software tool, which would simulate the behaviour of the biosensors utilizing intermediate substances and to investigate the peculiarities of analysed biosensors.

The aim is further divided into the following tasks:

1. Develop and investigate practical mathematical models of the biosensor with chemically modified electrode and the biosensor utilizing parallel substrates conversion.

2. Suggest improvements to the mathematical and computational models, which would increase calculation speeds for a specific model configurations.

3. Develop a tool to automate the process of the biosensors peculiarities investigation by using parameter sweep approach on a computational grid.

4. Investigate kinetic peculiarities of both biosensors utilizing intermediate substances by using developed tool.

Research approach and method

Mathematical models presented in this thesis are formulated by non-linear reaction-diffusion partial differential equations of parabolic type. Models were approximated by using finite difference technique by applying explicit and Cranck-Nicolson computational schemes. Software tools implementing computational schemes were developed in C++ programming language. Computational grid was used to improve the speed of calculations by applying parameter sweep approach.

Scientific novelty and results

1. An existing mathematical model with quasi-steady-state assumption of biosensor with chemically modified electrode was generalized. Proposed transient mathematical model was proved to be more accurate

than the existing one at a practically meaningful set of parameter values.

2. Mathematical model with application of catalase and peroxidase realizing parallel substrates conversion was developed. The simulated results of this model significantly approached the ones received in the experiments with the suggested application of the partition of compounds between the layers.

3. Parameter values were determined under which the efficient diffusion coefficient can be used to merge the dialysis and diffusion layers of the biosensor utilizing parallel substrates conversion and the biosensor with chemically modified electrode.

4. The half-maximal effective concentration signifying the efficiency of the analysed biosensors was determined for various parameter values of both analysed biosensors.

5. Computational grid was used to efficiently investigate the biosensor behaviour by applying parameter sweep approach.

Practical significance of the results

The mathematical models presented in this thesis describe real-life biosensors action. The developed and implemented computational models can be used to numerically investigate the behaviour of the biosensors. The conditions were determined, when the calculations can be done faster with desired loss of accuracy by applying quasi-steady-state assumption (for biosensor with chemically modified electrode) and effective diffusion coefficient (for both analysed biosensors).

By using developed tool to model biosensor action on a computational grid, the dependency of half maximal concentration on various parameters was investigated. The obtained results show the optimal configuration of both analysed biosensors at various physical conditions.

The investigation of various other peculiarities described in this thesis can be applied for creation and development of biosensors utilizing intermediate substances.

Some of the results obtained during the research presented in this

thesis [A5] were already used when analysing biosensors behaviour experimentally [A7].

The results presented in this thesis were used in reaching the goals of the following projects:

- "Development of bioelectrocatalysis for synthesis and analysis (BIOSA)" funded by a grant (No. PBT-04/2010) from the Research Council of Lithuania (2008-2010).

- "Developing computational techniques, algorithms and tools for efficient simulation and optimization of biosensors of complex geometry" (project no. VP1-3.1-ŠMM-07-K-01-073/MTDS-110000-583) funded by the European Social Fund under measure VP1-3.1-ŠMM-07-K "Support to Research of Scientists and Other Researchers (Global Grant)"(2011-2015).

Statements promoted to defend

1. The quasi-steady-state assumption (QSSA) can be applied to computational modelling and investigating the peculiarities of the biosensor with chemically modified electrode. The assumption affects response the most for the relatively small diffusion module and relatively large Biot number.

2. Three-layered one-dimensional in space mathematical model can be successfully applied to investigate the kinetic peculiarities of the biosensor with parallel substrates conversion. The most efficiently operating biosensor configuration is at the relatively low ratio of the catalase to the peroxidase and the relatively high concentrations of hydrogen peroxide.

3. The partition coefficient should be included when describing the biosensor behaviour mathematically. The partition coefficient impacts the response and sensitivity, but does not change general tendencies in the biosensor behaviour.

4. Effective diffusion coefficient can be successfully applied to merge two diffusion-based regions into one for both analysed mathematical models. Numerical investigation showed that in most cases the error of the merger is less than 10%.

Results approbation

Three articles were published in the journals with citation index in Thomson Reuters Web of Knowledge database [A5, A7, A8]. The contribution of the thesis author in the published papers covers the development of numerical models and the software solving these models, validation of the models, digital investigation processes, analysis of the results and varying in scope text preparation process.

Additionally, results were presented in five conference proceedings [A1–A4, A6].

Contributed talks were given at six international and five national conferences:

1. KODI 2013 (Šiauliai, Lithuania): *Kompiuterininkų dienos – 2013.* 19-21st September, 2013.

2. DSL 2013 (Madrid, Spain): *9th International Conference on Diffusion in Solids and Liquids.* 24-28th June, 2013.

3. NUMTA 2013 (Falerna, Italy): *Numerical Computations: Theory and Algorithms. International Conference and Summer School.* 17-23rd June, 2013.

4. ECCOMAS 2012 (Vienna, Austria): *6th European Congress on Computational Methods in Applied Sciences and Engineering.* 10-14th September, 2012.

5. LMD 2012 (Klaipėda, Lithuania): *Lietuvos Matematikų Draugijos 53-oji konferencija.* 11-12th June, 2012.

6. MMA 2012 (Talin, Estonia): *Mathematical Modelling and Analysis 2012.* 6-9th June, 2012.

7. KODI 2011 (Klaipėda, Lithuania): *Kompiuterininkų dienos – 2011.* 22–24th September, 2011.

8. MMA 2011 (Sigulda, Latvia): *Mathematical Modelling and Analysis 2011.* 25–28th May, 2011.

9. LMA 2011 (Vilnius, Lithuania): *LMA pirmoji jaunųjų mokslininkų konferencija.* 25th May, 2011.

10. ECCOMAS CFD 2010 (Lisbon, Portugal): *V European Conference on*

Computational Fluid Dynamics. 14–17th June, 2010.

11. KODI 2009 (Kaunas, Lithuania): *Kompiuterininkų dienos – 2009.* 25–26th September, 2009.

Structure of the thesis

Thesis consists of four chapters. In the first chapter overview of the researched area is presented: an introduction to the biosensors, their peculiarities and classification, an overview of the mathematical possibilities to model their behaviour, as well as methods and tools used to carry out the simulation processes. Chapter 2 presents the mathematical models of the biosensors utilizing intermediate substances: biosensor with chemically modified electrode and biosensor utilizing parallel substrates conversion. Solving of these mathematical models are presented in Chapter 3. Analytical solutions, utilization of variable time step in the computational schemes as well as the use of computational grid are presented. In Chapter 4 the peculiarities of the biosensors utilizing intermediate substances are presented, with a special emphasis on the comparison with the experimental data (for the biosensor utilizing parallel substrates conversion) and the half maximal effective concentration.

Chapter 1

Theoretical framework

1.1. Biosensors

Leland C. Clark published an article on what became known as the Clark's Electrode in 1953 [48]. The first demonstration of the biosensor concept, as we understand it today, was given by the same Leland C. Clark Jr. in 1962 [49]. Since then various biosensors have been developed and applied in point-of-care testing, home diagnostics, environmental monitoring, research laboratories, process industry, security and biodefense and others [11, 50]. In the medical field, a majority of biosensors are included in glucose meters, blood gas analysers, electrolyte analysers, metabolite analysers and various drug detectors [1–4].

Biosensors are widely applied in the above mentioned areas, because they are relatively cheap to construct, reliable and highly sensitive devices. Biosensor consist of three major parts: sensitive biological element (bioreceptor), element that transforms the signal of interaction between substrate and biological element into another signal (transducer element) and associated electronic device which displays the result. As a result of this separation by parts, biosensors are classified according to bioreceptor and transducer elements.

Three classes of bioreceptors are distinguished: biocatalytic, bioaffinity and hybrid receptors. Biocatalytic receptors are systems containing enzyme (single or multiple enzymes might be used), whole cells (bacteria, fungi, eukaryotic cells, yeast), cells organelles and tissues (plant or animal) [51]. Enzyme biosensors, analysed in this research, work by immobilization of the enzyme system onto a transducer. The enzymes used in the biosensors are

specifically chosen for the desired molecules and catalyze generation of the product, which is then directly determined using the transducer element.

According to the transducer type, biosensors are classified into electrochemical, electrical, optical, piezoelectric, thermometric. In the electrochemical biosensors, analysed in this thesis, chemical reactions between immobilized bioreactors and target substrate produce or consume ions or electrons, which affects measurable electrical properties of the solution, such an electric current (for amperometric biosensors) or potential (for potentiometric biosensors) [52]. Amperometric biosensors are simple, have an extensive variety of redox reaction for construction of the biosensors, and facility for miniaturize [10]. They are widely applied to detect glucose, galactose, lactate, sucrose, aspartame, acetic acid, glycerides, biological oxygen demand, cadaverine, histamine, etc. Two of the most serious drawbacks are their low sensitivity and short linear parts of the calibration curves. The application of intermediate substances is investigated in this thesis as a perspective way to minimize these disadvantages of enzymatic amperometric biosensors.

In the following sections of this chapter, a physical processes taking place inside the biosensor are presented. Methods and tools used for the investigation of these processes are analysed.

1.1.1. Enzymatic processes in biosensor systems

Two physical phenomenons are unusually analysed when investigating the behaviour of the enzymatic biosensors: enzyme kinetics and diffusion. One of the simplest and best-known approaches to model the kinetic action is the Michaelis-Menten kinetics, described in 1913 [53]. The assumption is made, that enzyme binds the substrate to form an intermediate complex ES,

$$\mathrm{E + S} \underset{k_{-1}}{\overset{k_1}{\rightleftharpoons}} \mathrm{ES} \overset{k_2}{\longrightarrow} \mathrm{E + P}, \tag{1.1}$$
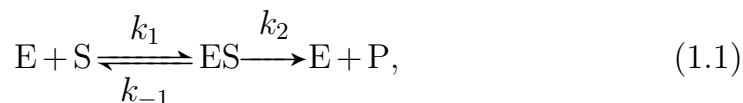
where substrate S binds reversibly to an enzyme E to form an enzyme-substrate complex ES (reaction rate constants denoted as k_1 and k_{-1}), which then reacts irreversibly to generate a product P and to regenerate the free enzyme E (with reaction rate constant of k_2). Some degree of reversibility in the product formation in many biochemical reactions might be noticeable, however in most cases (including Michaelis-Menten kinetics) it is neglected.

The quasi-steady-state assumption (QSSA) was presented in 1925 [54]

and is widely used up to this day. Concentration of complex ES will not change significantly after an initial burst phase, until a significant amount of substrate has been consumed,

$$\frac{\partial e_s}{\partial t} = k_1 es - (k_2 + k_{-1})e_s = 0, \tag{1.2}$$

where s and e_s are concentrations of S and ES.

By extracting e_s from (1.2) and multiplying it by reaction rate of k_2 and by substituting $e = e_0 - e_s$ (e_0 is the initial concentration of the enzyme), the rate v of the product formation can expressed as follows:

$$\frac{\partial p}{\partial t} = v = k_2 e_s = \frac{k_2 e_0 s}{\frac{k_{-1}+k_2}{k_1} + s} = \frac{V_M s}{K_M + s}, \tag{1.3}$$

where $V_M = k_2 e_s$ (when $e_s = e_0$) is the reaction velocity at saturating substrate concentration, $K_M = (k_{-1} + k_2)/k_1$ is the Michaelis-Menten constant, unique for each enzyme-substrate pair. One can notice, that when $s = K_M$, then $v = V_M/2$, meaning that K_M can be interpreted as the substrate concentration, at which the half-maximal reaction rate is achieved. The lower the values of K_M represent more effective enzyme at low substrate concentrations.

Free substrate concentration, represented by s in (1.3), is usually assumed to be close to the total substrate concentration present in the system ($s \approx s_0$). This assumption (as well as the whole quasi-steady-state assumption) is valid when $e_0 \ll s_0 + K_M$ [55].

1.1.2. Diffusion processes

The diffusion is the second physical phenomenon taking place in the analysed biosensors. It is described as one of the several transport mechanisms (alongside with convection and advection) that occur in nature. An overview of diffusion is presented in this section with accordance to the related research works of the biosensor mathematical modelling.

1.1.2.1. Diffusion of compounds in multi-layered domain

Diffusion is described by a partial differential equation, describing density dynamics in a material in which diffusion processes take place. In case

of diffusion in two or more dimensions, a diffusion of mass during time can be described by generalized Fick's Second Law (which is analogous to the heat equation):

$$\frac{\partial c}{\partial t} = D \nabla^2 c, \tag{1.4}$$

where t is time, ∇ represents the differential operator which generalises the first spatial derivative, c is the concentration of compound C in dimensions of [(amount of substance) $\times$ length^{-3}], D is the diffusion coefficient of compound C in dimensions of [length$^2 \times$ time^{-1}]. In more general case a diffusion coefficient can be a function, but in case of biosensors, it is considered to be a constant, which depends on the molecule size, temperature, pressure and other properties of the diffusing substance. Larger diffusion coefficient represents better diffusivity (for example gas diffusion in gas medium would have relatively large diffusion coefficient), while the lower diffusion coefficient represents greater resistance (e.g. gas diffusion in liquid media).

When biosensor action is described in one dimensional space, the following diffusion equation is used:

$$\frac{\partial c}{\partial t} = D \frac{\partial^2 c}{\partial x^2}, \tag{1.5}$$

where x is space coordinate. One-dimensional in space diffusion is analysed in this thesis, as it is known to be accurate enough for the most biosensor models. Therefore further equations and definitions are provided in the same manner.

In most of the mathematical models found in the literature, a multi-layered approach of biosensor is usually taken. Different regions are represented by distinct diffusion coefficients for different compounds, meaning that physical diffusion processes in various layers are different.

In case neighbouring layers are non-reflective to the analysed compound (the compound is able to diffuse from one layer to another), it is considered, that the flux of compound C entering from $l+1$-th layer to l layer (see boundary $x = a_l$ in Fig. 1.1) is equal to the corresponding flux of the same compound entering the surface of layer l,

$$D_c^{(l)} \frac{\partial c^{(l)}}{\partial x}\bigg|_{x=a_l} = D_c^{(l+1)} \frac{\partial c^{(l+1)}}{\partial x}\bigg|_{x=a_l}, \tag{1.6}$$

$$c^{(l)}\big|_{x=a_l} = c^{(l+1)}\big|_{x=a_l}, \tag{1.7}$$

where $D_c^{(l)}$, $D_c^{(l+1)}$ are the diffusion coefficients and $c^{(l)}$, $c^{(l+1)}$ are the concentrations of compound C in layers l and $l+1$.
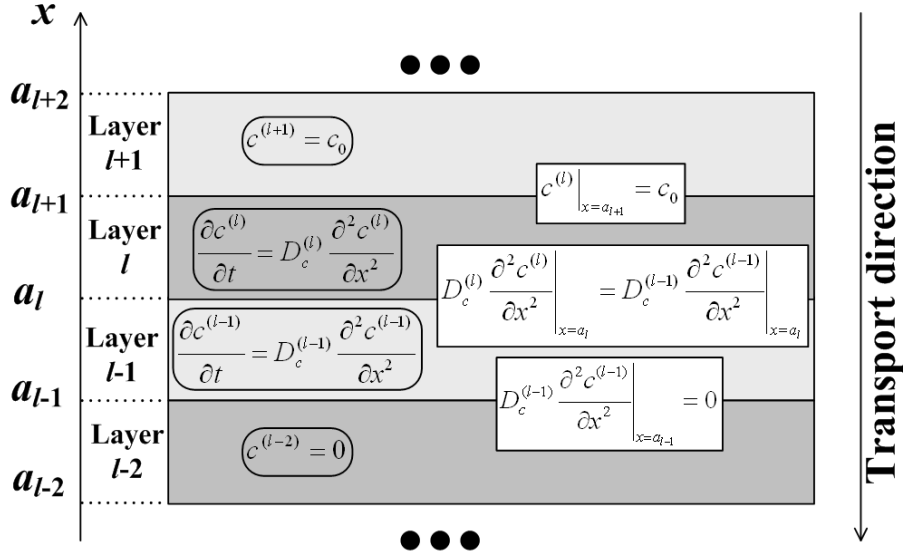
Figure 1.1. The graphical illustration of the diffusion through different layers. Equations in rounded boxes describe the diffusion inside the layers, while boxed ones display the diffusion processes at the boundaries.

If the concentration of compound C is kept constant (with a value of $c^{(l+1)} = c_0$) in layer $l+1$, and transport direction is from layer $l+1$ to layer l, then Dirichlet boundary condition is applied at the boundary of $x = a_{l+1}$,

$$c^{(l)}|_{x=a_{l+1}} = c_0. \tag{1.8}$$

If the compound does not diffuse from layer $l-1$ to layer $l-2$ (at the boundary of $x = a_{l-1}$) because of the non-permeability, Neumann boundary condition is applied,

$$D_s^{(l-1)} \frac{\partial s^{(l-1)}}{\partial x}\bigg|_{x=a_{l-1}} = 0. \tag{1.9}$$

Illustrations of the described conditions are presented in Fig. 1.1: concentration c of compound C in layer $l+1$ is constant, while in layers l and $l-1$ it is described by the diffusion equation (1.5) with according diffusion coefficients. Direchlet boundary condition is applied at the boundary $x = a_{l+1}$, the equation (1.6) describing the steadiness of fluxes is applied at boundary $x = a_l$ and Neumann boundary condition is applied at the boundary of $x = a_{l-1}$, which results concentration of $c^{(l-2)} = 0$ for the layer

$l - 2$.

1.1.2.2. Partition coefficient

Partition coefficient commonly refers to the equilibrium partition of a single compound between two solvent and immiscible phases separated by a boundary and is a measure of hydrophobic/hydrophilic properties of a given molecule. Water and octanol are typically the solvents in the context of drug detection. Partition coefficient, sometimes referred as partition constant or partition ratio, depends on the temperature and pressure, but should not vary with composition [56].

The partition coefficient $K_c^{(l),(l+1)}$ between layers l and $l+1$ at $x = a_l$ is calculated by the following ratio [57]:

$$K_c^{(l),(l+1)} = \frac{c^{(l)}\big|_{a_l}}{c^{(l+1)}\big|_{a_l}}, \tag{1.10}$$

where $c^{(l)}$ and $c^{(l+1)}$ are concentrations of compound C in corresponding layers l and $l+1$ near the boundary of $x = a_l$. The logarithm of the concentrations ratio (1.10) in the solvents is frequently expressed as logarithm of K. The log K value (more often denoted as log P) is also known as a measure of lipophilicity [58].

The partition coefficient sometimes is called as a distribution coefficient, however, while not differing drastically, two coefficients have different meanings [58]. A ratio of the concentrations of the non-ionised compound between two different solutions is displayed by the partition coefficient, while the distribution coefficient is the ratio of the sum of the concentrations for both forms of the compound (ionised and non-ionised).

The partition coefficient was applied in analysis of various diffusion-related researches [59, 60] and when analysing the behaviour of the biosensors [61–63]. However the impact of the partition coefficient on the biosensor response was not analysed exclusively. Therefore, the impact of the partition coefficient was extensively analysed in this thesis for biosensor utilizing parallel substrates conversion while comparing digitally obtained results to the experimental ones.

1.1.2.3. Effective diffusion coefficient

In order to minimize the number of the model parameters, the effective diffusion coefficient might be applied to merge some of the model layers, where only the mass transport by diffusion takes place. An efficient diffusion coefficient $D^{(ij)}$ can be used to merge two neighbouring layers (enumerated as i-th and j-th layers), with diffusion coefficients $D^{(i)}$ and $D^{(j)}$ [64–66],

$$\frac{D^{(i)}D^{(j)}}{v_{ij}D^{(j)} + (1 - v_{ij})D^{(i)}} \leq D^{(ij)} \leq v_{ij}D^{(i)} + (1 - v_{ij})D^{(j)}, \qquad (1.11)$$

where v_{ij} is the relative thickness of the i-th layer as compared to the sum of both layer thicknesses,

$$v = d_i/(d_i + d_j). \qquad (1.12)$$

The effective diffusion coefficient was successfully applied to model the biosensors with a perforated membrane, by considering the right side of the (1.11) equation to be accurate expression of the efficient diffusion coefficient for two neighbouring areas [67, 68],

$$D^{(ij)} = v_{ij}D^{(i)} + (1 - v_{ij})D^{(j)}. \qquad (1.13)$$

By using the efficient diffusion coefficient (1.13), the one-dimensional mathematical model with two or more diffusion-based layers can be simplified by merging those layers. The diffusion coefficient of the merged layer is $D^{(ij)}$ and thickness is $d_{ij} = d_i + d_j$. When analysing mathematical models described in two-dimensional or three-dimensional space, the same approach can be applied not only for a flat layers, but for an areas with a more complex geometry.

In this research the application of the efficient diffusion coefficient was investigated for the biosensor with chemically modified electrode (Section 4.1), as well as for the biosensor utilizing parallel substrates conversion (Section 4.2).

1.2. Mathematical modelling of biosensors

Mathematical modelling is widely used in various research areas nowadays, especially in the area of applied applications [69], as the emergence of new fields of research after the sixties expanded even more [70]. One of the many areas, where mathematical modelling can be applied is solving various systems of differential equations [71]. Biochemistry and electrochemistry are areas, where mathematical modelling also found it's rightful mark [24, 72].

Various mathematical models of biosensors were developed and later investigated digitally in Vilnius University since 2000: a biosensor with partially blocked electrodes [73], a sensor with array of enzyme microreactors [74, 75], a carbon nanotube based biosensor [76], a biosensor based on synergistic substrates determination [77], a synergistic action of laccase-based biosensor [78] and many others.

Mathematical modelling is also widely applied outside Vilnius University, as various research works are done by quite a few researchers: a layer by layer assembling approach of glucose biosensor modelling was presented in [62], another glucose biosensor is modelled in [79]. Models of a biosensors with modified [80] and bienzyme [81] electrodes, based on bioluminescent E.Coli [21] and cantilever [82], microbioreactor-based [63], working under flow injection [83] and many others [31, 84–87] were developed.

A research group in Dublin Institute of Technology is working in the same area of mathematical models and methods of biosensor action investigation, as two dissertations [88, 89] were recently defended as well as several articles were published [90, 91].

An overview of modelling biosensor responses is given in [92] and overview of the mathematical modelling of biosensors is presented in [33].

1.2.1. Development of biosensor mathematical model

Michaelis-Menten kinetics [53] is a most common fundamental base for the mathematical modelling of biosensors [7, 22, 87–90, 93–99]. Commonly, the domain describing the geometry of a mathematical model of the biosensor is divided into a physically meaningful regions: enzymatic region, diffusion-based region, dialysis and selective membranes, etc.

1.2.1.1. Governing equations

In case of enzymatic biosensors, one of the regions is an enzymatic layer, and in presence of the Michelis-Menten kinetics the region is described by combining enzymatic reaction rate (1.3) and diffusion equation (1.5). A classical system of non-linear reaction-diffusion equations is obtained for layer $l = 1$,

$$\frac{\partial s^{(1)}}{\partial t} = D_s^{(1)} \frac{\partial^2 s^{(1)}}{\partial x^2} - \frac{V_M s^{(1)}}{K_M + s^{(1)}}, \quad \frac{\partial p^{(1)}}{\partial t} = D_p^{(1)} \frac{\partial^2 p^{(1)}}{\partial x^2} + \frac{V_M s^{(1)}}{K_M + s^{(1)}}, \quad (1.14)$$

where $s^{(1)}(x,t)$ denotes concentration of the substrate S and $p^{(1)}(x,t)$ denotes the concentration of the product P in layer $l = 1$ (marked as (1) in superscript). If the model is not analysed according to the Michaelis-Menten kinetics, reaction term is replaced by a corresponding reduction reaction term.

Various multiple layers might be added to the mathematical model, by using other reaction equations as well as diffusion equations presented in Section 1.1.2.1. A diffusion limiting region, where only the mass transport by diffusion takes place is usually added when modelling biosensors working under bath regime. A convective region is located outside the diffusion layer, where the substrate concentration is maintained constant with a help of stirring.

The thickness of the diffusion layer is inversely proportional to the intensity of stirring of the solution. The more intense stirring corresponds to the thinner diffusion layer. This diffusion layer, also known as the Nerst layer, practically does not depend upon the enzyme membrane thickness. The Nerst layer may be practically minimized up to 2×10^{-6} m, but no zero thickness can be achieved [100].

1.2.1.2. Initial, boundary and matching conditions

In order for the mathematical model to be a well-posed problem, a sufficient amount of boundary, governing and matching conditions must be described:

- *Initial conditions* describe the initial state of the biosensor, by describing the concentrations of all compounds at time moment $t = 0$.

- *Boundary conditions* describe the concentrations at the boundaries of

the domain during the biosensor operation $(t > 0)$. Direchlet (1.8) and Neumann (1.9) conditions are used in most analysed cases.

- *Matching conditions* describe the mass transport between the layers during the biosensor operation $(t > 0)$. In most cases they are described using (1.6) and (1.7) equations.

1.2.1.3. Biosensor response

The anodic or cathodic current is assumed as the response of the amperometric biosensor [92] and is, in one way or another, the main interest of the researchers. In this research, electrode is placed below the enzymatic layer, at the boundary of $x = a_0$. The current density $i(t)$ is obtained according to Fick's and Faraday's laws [4], and is proportional to the gradient of product concentration p at the electrode surface $(x = a_0)$,

$$i_1(t) = n_e F D_p^{(1)} \frac{\partial p^{(1)}}{\partial x}\bigg|_{x=a_0}, \qquad (1.15)$$

where F is Faraday's constant $(F = 96.485 \times 10^6 \, \text{CM}^{-1}\text{m}^{-3})$, n_e is a number of electrons involved in the electrochemical reaction.

Mathematical model approaches the steady-state as $t \to \infty$,

$$i_s = \lim_{t \to \infty} i(t). \qquad (1.16)$$

Analytical solution for the mathematical model with a non-linear reaction term (marked as v in (1.3)) exists when this term can be linearised. In case of Michaelis-Menten kinetics (described by the governing equations (1.14)), the linearisation is possible in two cases:

1. $s_0 \ll K_M$, then $v \approx V_M s / K_M$.

2. $s_0 \gg K_M$, then $v \approx V_M$.

Analytical solutions in most cases are used only for the validation purposes, as they solve the model only for the very limited set of parameter values. Analytical expressions of concentrations for one-layered and two-layered models for some cases with linear reaction term also exist [12, 28].

1.2.2. Dimensionless mathematical models

Dimensionless parameters and dimensionless mathematical modelling describing various real-life systems are used quite often [101–103].

The non-dimensioning approach in the area of enzyme kinetics was applied as early as 1967 [104]. The same approach was used in 1989 to study quasi-steady-state assumption (QSSA) in biochemistry [55]. By deriving the dimensionless model the main governing parameters impacting the behaviour of the biosensor can be determined [33]. The dimensionless model approach is applied not only to model biosensor action [89, 105, 106], but to model other biochemical [107–111] and non-biochemical [69] processes as well.

When non-dimensioning the mathematical model of the biosensor, the parameters of spatial and time coordinates, as well as diffusion coefficients are nondimensionalized in the following manner:

$$X = \frac{x}{d_1}, \quad T = t\frac{D_s^{(1)}}{d_1^2}, \quad \Phi_C^{(l)} = \frac{D_c^{(l)}}{D_g^{(1)}}, \tag{1.17}$$

where X and T are dimensionless space and time parameters, $\Phi_C^{(l)}$ is dimensionless diffusion coefficient of compound C in layer l and $D_g^{(1)}$ is freely chosen diffusion coefficient of compound g in layer $l = 1$.

However, no universal solution exists describing how to obtain the remaining dimensionless parameters (concentrations of the compounds and reaction-related parameters). By extracting the corresponding dimensional parameters from (1.17) and by inserting them to the governing equations (e.g. 1.14) one will obtain the equations needed for further derivation of the dimensionless parameters.

In case of Michaelis-Menten kinetics, the remaining concentrations are normalized by K_M, and equations (1.14) take the following dimensionless form:

$$\frac{\partial S^{(1)}}{\partial t} = \frac{\partial^2 S^{(1)}}{\partial X^2} - \sigma^2 \frac{S^{(1)}}{1+S^{(1)}}, \quad \frac{\partial P^{(1)}}{\partial t} = \Phi_P^{(1)}\frac{\partial^2 P^{(1)}}{\partial X^2} + \sigma^2 \frac{S^{(1)}}{1+S^{(1)}}, \tag{1.18}$$

where $\sigma^2 = V_M d_1^2 / D_s^{(1)} K_M$ is also a dimensionless parameter, known as the diffusion modulus (see Section 1.2.3).

1.2.3. Parameters used for the investigation

The sensitivity is a characteristic indicating how properly the biosensor responds to the concentration changes of the substance to be analysed [1, 11]. The sensitivity is defined as the gradient of the steady-state current i_s (1.16) with respect to the concentration (s_0) of the substrate to be determined [2, 33],

$$b_s = \frac{di_s(s_0)}{ds_0}. \tag{1.19}$$

Since substrate concentration and steady-state response usually varies in few orders of magnitude, the dimensionless sensitivity sometimes is preferred [106, 112, 113],

$$B_s = \frac{s_0}{i_s(s_0)} \times \frac{di_s(s_0)}{ds_0}. \tag{1.20}$$

In case of a sensitive biosensor, a relatively small increase in the substrate concentration leads to a relatively large alteration in the biosensors response.

When analysing two-layered mathematical model, the thicknesses of the enzymatic and diffusion layers highly affect the biosensor behaviour in a complex manner [112, 114]. The Biot number includes the thicknesses of both layers and is widely used to investigate the behaviour of the biosensor action [28, 60, 93, 115–117],

$$Bi = \frac{d_1}{D_s^{(1)}} \times \frac{D_s^{(2)}}{d_2}, \tag{1.21}$$

where $D_s^{(1)}$ and $D_s^{(2)}$ are the diffusion coefficients of substrate in enzymatic and diffusion layers. As one can see the Biot number Bi expresses the ratio of the internal mass transfer resistance to the external one. The thickness d_2 of the diffusion layer, which is treated as the Nernst layer, is practically independent upon the enzyme membrane thickness d_1 [34].

The steady-state current might be normalized in the following manner, because of high sensitivity of the maximal biosensor current to the thickness of the enzyme layer:

$$I_N = \frac{i_s(Bi)}{i_s(\infty)}, \tag{1.22}$$

where Bi is the Biot number described in (1.21), $i_s(Bi)$ is the steady-state current, calculated at given Bi and $i_s(\infty)$ is the steady-state current, calcu-

lated when the $Bi \to \infty$ (when analysing the thicknesses it usually means slightly increasing d_1 and decreasing d_2 as much as possible [115, 118]).

Dialysis membrane and external diffusion layer can be merged using effective diffusion coefficient as described in Section 1.1.2.3. The relative error of the two-layered mathematical model response is expressed as follows:

$$\eta = \frac{|i_{s3} - i_{s2}|}{i_{s3}}, \tag{1.23}$$

where i_{s3} is the steady-state current of the tree-layered model (considered as the accurate one), and i_{s2} is the steady-state current of the two-layered model.
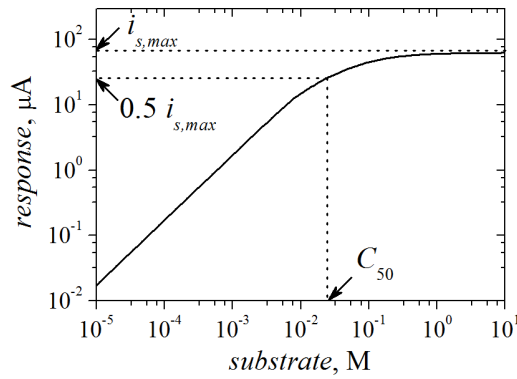
Figure 1.2. The graphical illustration of C_{50} concentration.

The half maximal effective concentration C_{50} of the substrate to be determined is also important characteristic of the biosensor [119]. A greater value of C_{50} corresponds to a longer linear part of the calibration curve (see Fig. 1.2). In some cases (especially when exhibiting the Michaelis–Menten kinetics [99, 120]), the concentration C_{50} is called the apparent Michaelis–Menten constant, denoted as K_M^{app} [121, 122]. The half maximal effective concentration is expressed as follows:

$$C_{50} = \left\{ s_0^* : i_s(s_0^*) = 0.5 \lim_{s_0 \to \infty} i_s(s_0) \right\}, \tag{1.24}$$

where $i_s(s_0)$ is the steady-state current (1.16) achieved at the concentration s_0 of the substrate S.

Diffusion module (sometimes referred as diffusion modulus [97] or Damköhler number [11]) is another important characteristic. The parameter is derived from dimensionless mathematical models (see section 1.2.2), but with a significant physical meaning [87, 123, 124]. In case of Michaelis-

Menten kinetics, the diffusion module is expressed as follows:

$$\sigma^2 = \frac{V_M d_1^2}{D_s^{(1)} K_M}.$$

(1.25)

As one can see, diffusion module essentially compares the rate of enzyme reaction (V_M/K_M) with the diffusion through the enzyme layer $(D_s^{(1)}/d_1)$.

1.3. Computational modelling of the biosensors

The computational modelling is applied in various scientific areas, including more theoretical ones (alternating direction method for solving Poisson [125] and parabolic equations [126, 127]) as well as for solving applied problems when modelling blood glucose dynamics [128], anisotropic media [129], moisture diffusion in wood [130], piezoelectric and ultrasound actuators [131, 132], protein spot detection [133] and others.

Computational modelling is the only way to solve the problems presented by the mathematical models of the biosensors (see Section 1.2.1), since the analytical solutions exist only at extreme set of parameter values. Most of the mathematical models overviewed in Section 1.2 are solved numerically in one way or another.

1.3.1. Numerical approximation

In order to solve the problem presented by the mathematical model of the biosensor, numerical approximation must be applied. Finite volume method [134] and finite element method [85, 135] are applicable in the research area, as they are capable of solving complex geometries in an integrated fashion, making it perspective for the two-dimensional and three-dimensional models. However, in most cases one-dimensional in space geometry is sufficient enough to investigate the behaviour of the biosensor, thus finite difference method can be used [43, 44, 46].

In one-dimensional biosensor with L layers, space and time variables x and t are defined in domain $\Omega = \{a_0 \leq x \leq a_L, 0 \leq t \leq T\}$, where T is the total simulated time. One of the most commonly used solutions is to replace the continuous domain of Ω with a discrete uniform mesh [33, 43,

45, 46],

$$\Omega_{h\tau} = \{(x_i^{(l)}, t_j) : x_i^{(l)} = h_l i + \sum_{ii=1}^{l-1} a_{ii}; \ t_j = j\tau; \ i = 1, ..., N_l, \ j = 1, ..., M\},$$

(1.26)

where h_l and τ are constant mesh sizes in space and time directions, M is the total time step count $\tau M = T$ and N_l is the space step count in layer l, that $h_l N_l = d_l$, $l = 1, 2, ..., L$.

To solve the problem in the numerical manner, the functions $s^{(l)}(x, t)$ and $p^{(l)}(x, t)$ of the continuous arguments introduced in (1.14), need to be replaced by the functions of the discrete arguments mesh points, e.g. $s^{(l)}(x_i^{(l)}, t_j) = s_{i,j}^{(l)}$ and $p^{(l)}(x_i^{(l)}, t_j) = p_{i,j}^{(l)}$.

In case of finite difference method, finite differences are used to approximate the derivatives in the mathematical models. Various orders of accuracy can be applied using finite difference approximations [136], however, first-order accuracy is considered as sufficiently accurate when modelling biosensor behaviour. For the first space derivative, left-sided and right-sided approximations are described as follows ($c = s, p$):

$$\frac{\partial c^{(l)}}{\partial x}\bigg|_{x=x_i^-} \approx \frac{c_{i,j}^{(l)} - c_{i-1,j}^{(l)}}{h_l}, \quad \frac{\partial c^{(l)}}{\partial x}\bigg|_{x=x_i^+} \approx \frac{c_{i+1,j}^{(l)} - c_{i,j}^{(l)}}{h_l}.$$

(1.27)

Both expressions are used for the approximation of boundary and matching conditions defined in Section 1.1.2.1. First time derivative is approximated in the same manner as in (1.27). Left-handed time derivative is used for explicit schemes, while right-handed is used for implicit ones.

First order accuracy central finite difference of the second order space derivative is used to approximate the diffusion term,

$$\frac{\partial^2 c^{(l)}}{\partial x^2} \approx \frac{c_{i+1,j}^{(l)} - 2c_{i,j}^{(l)} + c_{i-1,j}^{(l)}}{h_l^2}.$$

(1.28)

By applying approximations (1.27) and (1.28) to the derivatives in the mathematical model and by replacing the remaining occurrences of the functions with continuous arguments $s^{(l)}(x, t)$ and $p^{(l)}(x, t)$ with the ones of discrete arguments mesh points $s_{i,j}^{(l)}$ and $p_{i,j}^{(l)}$, mathematical model is completely discretized. The computations are started by applying the initial conditions at time $t = 0$ and then by calculating inner points of the mesh

for governing equations and boundary conditions for the boundary of the mesh for each new time step ($t = j\tau$, $j = 1, 2, ..., M$).

Various finite difference methods exist, but the most commonly used in the computational modelling of biosensors are explicit, implicit and Crank-Nicolson. Explicit finite difference scheme is obtained by applying left-handed approximation of the first time derivative. It is simple to implement (therefore, it is error-free compared to the implicit methods) and has low computational cost, because it gives value of the solution for the new time step explicitly in terms of values at the previous time step. Method is recommended for the problems where accuracy is not a significant factor but the speed is [38].

The convergence of the finite difference scheme is a compulsory feature, and it has to be implemented in order for one to apply the scheme practically [43, 45, 46]. The scheme is convergent if

$$\lim_{\tau, h_l \to 0} |c^{(l)}(x_i^{(l)}, t_j) - c_{i,j}^{(l)}| = 0. \tag{1.29}$$

The convergence of a difference scheme depends on the smoothness of a solution of the differential problem, the choice of a mesh grid and the stability of a difference scheme [33]. The scheme is called stable if initial errors are not magnified by the ones arising during the course of the calculation. The explicit scheme for the diffusion equation (1.5) is only conditionally stable, as the time step is restrained be the space step,

$$\tau < \frac{h_l^2}{2D_c^{(l)}}, \quad \forall l = 1, 2, ..., L, \quad c = s, p. \tag{1.30}$$

In case of implicit method the variables in the upper time step can not be explicitly calculated from the lower time step. When reaction term is linear, the reaction-diffusion equation approximated by implicit scheme can be solved by solving the system of linear equations. Since the equations form tridiagonal matrix, the system is efficiently solved by tridiagonal matrix algorithm [43, 46]. However, in case of non-linear reaction term, the values of the upper time step variables can only be calculated by the method of iterations or by linearising the non-linear term. Usually, as it is also the case for this thesis, the later option is applied.

Crank-Nicolson method is based on average in time of explicit and implicit schemes, therefore it is second order accurate space and in time (for

the diffusion equation it is $O(h^2 + \tau^2))$, compared to the implicit method, which is only first order accurate in time: $O(h^2 + \tau)$.

While implicit and Crank-Nicolson methods applied for the diffusion equation are unconditionally stable, reaction terms add stability limitations. However no analytical expression for the stability inequality for such approximations can be obtained, therefore initial time step is usually defined experimentally. Since the biosensor reaches the steady-state when $t \to \infty$, an increasing step size in the time direction can be applied.

1.3.2. Steady-state response detection

Time t_r is used to describe the time when the response reaches the steady-state with accuracy of ε:

$$t_r = \min_{i(t)>0} \left\{ t : \frac{t}{i(t)} \left| \frac{di(t)}{dt} \right| < \varepsilon \right\}, \quad i(t_r) \approx i_s, \tag{1.31}$$

where t_r is the assumed response time at the steady-state of the second operational phase of the biosensor. The decay rate ε highly influences the response time, when $\varepsilon \to 0$, $t_r \to \infty$.

1.3.3. Computational improvements

Bieniasz sixteen part series (from [39] to [40]) entitled "Use of dynamically adaptive grid techniques for the solution of electrochemical kinetic equations" focuses on moving computational grid points. Various examples are analysed, as most of the problems solved in the series are for linear reaction terms and few with non-linear ones. However, techniques presented in the series are strongly complicated and requires additional investigation for each newly presented mathematical problem.

A less complicated approach was used to model the behaviour of the biosensor with chemically modified electrode [112]. Instead of using a discrete uniform mesh, the space step size away from the boundaries was increased. However, the efficiency of variable time step was not analysed, as well as the accuracy issue was not investigated. The investigation of the variable space step calculation accuracy to model the biosensor with chemically modified electrode is analysed in Chapter 3 of this thesis.

Another possible improvement of computations is to use existing parallel methods in order of performing single calculation in parallel [137–140] as they were successfully applied to solve heat equation [141] and biochemical processes [142]. Explicit finite difference method can be easily parallelized by dividing the domain of concentration points and solving them separately, as no intersections occur. Wang's algorithm can be effectively used to parallelize the solving of tridiagonal equations appearing in implicit finite difference methods [143]. Parallel computational methods were not researched or applied in this dissertation, as the computational grids were used to parallelize the simulations.

1.4. Tools and environments

Various tools and environments exist to solve numerical problems, starting with Maple and MatLab [144] and finishing with a problem-specific software tools [145]. Efficiency of the tool to be used always raises a question, as what can be done to improve it's performance. Parallelization is one of the most common approaches to improve the performance of calculations, as it can be applied on a local machine for a single simulation task (as it was described in previous section) or by using computational grids [47].

1.4.1. Tools for automated modelling of biosensors

The digital investigation processes of various biosensors and biosensor systems can be summarized in the following steps:

1. Gathering of information on the biochemical background and structure.

2. Development of the mathematical model.

3. Development of the computational model according to the mathematical one.

4. Building a software tool, which solves the problem presented by the mathematical model.

5. Using the developed tool to investigate the peculiarities of the biosensor.

Various approaches can be taken when trying to automate the above mentioned processes. An automated generation of computer model code in JAVA is described in [146]. The model is described by SBML (Systems Biology Markup Language) document [147], which is considered standard for representing computational models in systems biology [148]. However, SBML language lacks depth in the description of geometric properties, as the proposed geometry representation [149] was not implemented since the last release (Level 3 Version 1) of SBML language in 2010 [150].

A solution for the problem of geometric representation was presented in [151]. By using XML language various biosensor geometries can be described in one-dimensional and two-dimensional Cartesian coordinate system, as well as in cylindrical coordinate system [152].

A tool for automated modelling of biosensors based on substrate synergy and inhibition effects is presented in [153]. The tool is based on the universal mathematical and corresponding computational models presented in the mentioned thesis.

Before-mentioned approaches and tools aim to build a mathematically described model in an automated way, e.g. automate the Steps 2-4 described in the beginning of this Section. However, when simulating the biosensors, building the model is only the part of the big picture. The tedious processes take place after the model is already developed, as the investigation of the biosensor peculiarities (marked as Step 5) is carried out by changing various model parameter values in various ways. The single simulation process, with one set of parameter values can take up to few days of time when simulating two-dimensional biosensor [68]. However, there is always a possibility, that the results obtained by the simulation must be recalculated.

One of the approaches is to visualise intermediate calculation results and let the researcher decide, whether to continue the simulation or to start a new one. A tool called *FDVis* with interactive visualization and steering environment for the computational processes using the finite difference method is presented in [154]. Through a user-friendly interface a researcher can submit simulation parameters and the intermediate results are presented in the graphical output panel, leaving the researcher with the final decision to make according to the received visual data.

However, since thousands of different computations with various sets of the parameter values might be needed to properly investigate biosensor behaviour, one could not relate only to the visualisations when determin-

ing the significance of the received results. The following approaches can be used to improve, speed-up and automate the investigation processes of biosensor behaviour:

1. Use improved formation of the computational scheme grid mesh points (described in the first part of Section 1.3.3).

2. Solve the equations presented by the computational schemes quicker by using various parallel algorithms [137, 138]. One of the most common is Wang's algorithm used to parallelize the tridiagonal matrix algorithm [143].

3. Employ the computational grids.

4. Automate the analysis of transitional results obtained with lower orders of accuracy.

In the further research presented in this thesis, approaches 1, 3 and 4 are analysed in Chapter 3 in different details and scopes.

1.4.2. Usage of the computational grids

The computational grid is a system that coordinates resources that are not subject to centralized control using standard, open, general-purpose protocols and interfaces to deliver non-trivial qualities of service [155]. The computer software designed to solve problems of parametrized computer modelling already exists [156–159].

The computational grids are used in a wide variety of scientific researches – molecular physics, thermodynamics, cosmology and other areas. Usually, analysed characteristic's dependency on the initial parameters during simulation process can be described as follows [160]:

$$y = f(p_1, p_2, ..., p_N), \tag{1.32}$$

where y stands for the above mentioned specific characteristic, N – the number of parameters, $Q = p_1, p_2, ..., p_n$ – the parameter queue where values p_1, $p_2, ..., p_n$ affects the investigated characteristic y, f denotes the simulation process.

In many cases of the comprehensive analysis the simulations are carried out with different sets of parameters called the parameter sweep - a collection of different parameter queues [158]. The parameter sweep can be

created by enumerating particular values of parameters or can be generated. When generating the parameter sweep of parameter queues the following values must be specified [161]:

- The interval of parameter values,

$$p_A \leq p_i \leq p_B, \tag{1.33}$$

  where p_A stands for the starting value of the concrete parameter, p_B – last value, and p_i – any parameter from the parameter queue, $i = 1$, $2, ..., N$.

- The progression type to define whether arithmetic or geometric progression is used to generate the parameter. Plain enumeration of the parameter values or keeping them constant are other possibilities.

1.5. Research and modelling of the biosensors utilizing intermediate substances

A comprehensive review on the modelling of amperometric biosensors has been presented in [28, 33]. Numerous intermediate substances can be used to increase biosensors sensitivity and selectivity (thus their overall quality) [15, 16]. In this thesis the behaviour of two biosensors utilizing intermediate substances is analysed digitally: biosensor with chemically modified electrode and biosensor utilizing parallel substrates conversion.

1.5.1. Biosensor with chemically modified electrode

Various chemically modified electrodes (CME) have been proposed more than three decades ago [17, 19]. Mathematical modelling has been also successfully applied for specific sensors based on the CME [122, 162, 163]. A mathematical model of a generic amperometric biosensor based on the CME has been proposed in 2008 [112]. The biosensor was considered as a flat electrode with a thin layer of the low soluble mediator and covered with an enzyme membrane. The biosensor response was numerically modelled under quasi-steady-state assumption, which usually holds, as it was proved mathematically [164].

One of the tasks in this thesis was to develop a transient mathematical

and corresponding numerical models of the biosensor based on the CME, where no quasi-steady-state assumption is applied. By using the developed models conditions were evaluated at which the biosensor action can be simulated under quasi-steady-state approximation (QSSA) for an accurate prediction of the biosensor response.

The initial model of CME biosensor proposed in [112] consists of two layers (enzymatic and diffusion), with a dialysis membrane not present in that research. In this work, the missing layer of the dialysis membrane is added to the mathematical model. By using effective diffusion coefficient, two outer layers (dialysis membrane and diffusion layer) are merged in the mathematical model. The task was to determine at which parameter values three layered model (3L) can be replaced with two-layered model (2L) and to determine the accuracy of the 2L model.

The impact of the mediator concentration on the half maximal effective concentration is investigated, as well as the impact of the *Biot* number.

1.5.2. Biosensor utilizing parallel substrates conversion

Medicine industry is one of the significant areas, where biosensors are applied, as the detection and distinction of various chemical drugs in blood is needed. As an example, one of the analgetics, i.e. acetaminophen (N-acetyl-paminophenol or paracetamol) is used to reduce fever and as a pain-killer for backache, headache and arthritis [165].

An acetaminophen overdose, however, can lead to accumulation of toxic metabolites, which may cause severe or fatal hepatotoxicity and nephrotoxicity related to renal failure [166, 167]. The use of acetaminophen for children is limited due to a possible increase in rhino conjunctivitis, asthma and eczema [168]. Therefore, the control of this compound in pharmaceutical formulations and real biological liquids is topical. Usually, a rather unspecific electrochemical method is used for the determination of this compound [169, 170].

Catalase and peroxidase biosensor, designed to detect acetaminophen is analysed in this thesis. The application of these enzymes allows to construct the biosensor realizing parallel substrate conversion and this dual biocatalytical system has some interesting possibilities. At first, the product of catalase reaction (i.e. dioxygen) can be detected with an exceptionally selective Clark-type electrode [48]. Second, redox active drugs, e.g.

psychotropic drugs, analgesics and others are substrates of peroxidase and there still exists interest for selective determination of these compounds.

Acetaminophen was used as a model compound for measurements of biosensor parameters [A7]. A mathematical model of the newly created physical biosensor with dual catalase-peroxidase bioelectrode was created. This mathematical model was used to prove a concept of biosensor analytical application of such configuration. Experimental results of the biosensor response were compared with calculated results and presented in this thesis.

A specific dual biosensor with parallel substrates conversion was extensively summarized in the collaborated paper [A5]. In order to define the main governing parameters of the model, the corresponding dimensionless mathematical model was derived in this work (see Section 2.2.3).

1.6. Summary

Numerous biosensors and biosensor systems are used today to detect and analyse the concentrations of diverse compounds. Biosensors are classified according to bioreceptor and transducer elements. Enzymatic amperometric biosensors, analysed in this thesis, are amongst the most reliable ones, and are attractive because of their miniature size and structural simplicity. Low sensitivity as well as short linear parts of the calibration curves are the most serious drawbacks of this type biosensors and is the target of the research for two concrete models presented in this thesis.

The main processes taking place in enzymatic biosensors are the diffusion of the compounds and the kinetic reactions, described by reaction-diffusion equations. A multi layered approach to construct a mathematical model of biosensor is usually applied, with enzymatic reactions taking place only in the enzymatic layer, and diffusion processes present in most of the layers.

In most cases exact analytical solutions exist only for a specific set of parameter values and numerical simulation is the only way to investigate biosensor behaviour. Computational analysis of the biosensors is attractive and cost-saving solution to replace actual physical experiments. However, one of the most serious drawbacks of computational modelling is time consumption, as the digital simulations can take up to weeks and months to complete.

Distinct methods are proposed in the literature to automate and improve the creation of the biosensor modelling software and is not analysed in this thesis. Improvements to the mathematical models and computational schemes, as well as automated simulation management was employed to investigate the peculiarities of the analysed biosensors.

A mathematical model of the biosensor with chemically modified electrode acting under quasi-steady-state assumption was investigated in related literature. A generalized transient mathematical model is developed in this thesis and compared to the one found in the literature.

Various biosensors were created for the detection of psychotropic drugs, including acetaminophen (paracetamol). However, most of the existing biosensors are limited due the electrode restrictions, thus a biosensor with fundamental Clark type electrode is perspective. A mathematical model based on the application of catalase-peroxidase system utilizing parallel substrates conversion is presented in this thesis.

Chapter 2

Mathematical models of biosensors utilizing intermediate substances

As it was described in Section 1.2, mathematical modelling can be efficiently used to improve the process of new biosensors creation, as well as the improvement of the existing ones. Two mathematical models of the biosensors utilizing intermediate substances are presented in this chapter:

1. Biosensor with chemically modified electrode [A1].

2. Biosensor utilizing parallel substrates conversion [A5].

2.1. Biosensor with chemically modified electrode

Two mathematical models of the biosensor with chemically modified electrode are presented in this section [A1]. The quasi-steady-state assumption can be applied to simplify the mathematical model by reducing the number of governing equations. However, quasi-steady-state assumption must be used with precaution. A transient mathematical model originally presented here is analysed without a quasi-steady-state assumption (2.1.2) which is used in [112]. Both mathematical models are later compared (see Section 4.1.2.3) to investigate the accuracy of the quasi-steady-state approximation.

2.1.1. Biochemical background and structure

A scheme of an enzyme catalyzed substrate (S) conversion in a presence of a mediator (M) was considered,

$$E_{ox} + S \underset{k_{-1}}{\overset{k_1}{\rightleftharpoons}} ES \overset{k_2}{\longrightarrow} E_{red} + P_1, \qquad (2.1)$$

$$E_{red} + M \overset{k_3}{\longrightarrow} E_{ox} + P, \qquad (2.2)$$
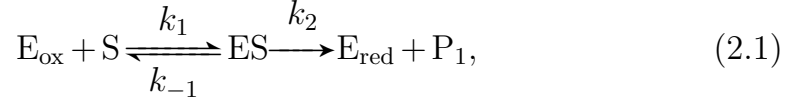
where E_{ox}, E_{red} and ES stand for the oxidized enzyme, the reduced enzyme and the enzyme substrate, respectively, P and P_1 are the reaction products [112, 162]. The biosensor is considered as a flat electrode with a thin layer of the low soluble mediator and covered with an enzyme membrane, which is attached to electrode by using dialysis membrane (see Fig. 2.1).
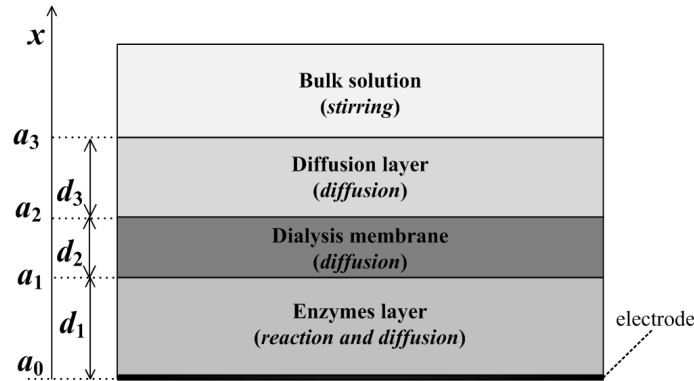
Figure 2.1. The structural scheme of the biosensor with the CME.

The model involves four regions in one dimensional space (Fig. 2.1):

1. The enzyme layer $(a_0 < x < a_1)$ where the biochemical reactions (2.1) and (2.2) as well as the mass transport by diffusion takes place.

2. A dialysis membrane $(a_1 < x < a_2)$ used to prevent the enzyme from being washed out.

3. A diffusion limiting region $(a_2 < x < a_3)$ where only the mass transport by diffusion takes place.

4. A convective region $(x > a_3)$ where the substrate concentration is maintained constant.

2.1.2. A transient mathematical model

2.1.2.1. Governing equations

Assuming a symmetrical geometry of the electrode and a homogeneous partition of the immobilized enzyme in the enzyme layer, the mathematical model of the biosensor action can be defined in a one-dimensional-in-space domain [28, 112]. Enzyme catalysed reactions (2.1) and (2.2) coupled with the one-dimensional-in-space diffusion, described by Fick's law, lead to the following equations of the reaction–diffusion type ($t > 0$, $a_0 < x < a_1$):

$$\frac{\partial s^{(1)}}{\partial t} = D_s^{(1)} \frac{\partial^2 s^{(1)}}{\partial x^2} + k_{-1} e_s - k_1 e_{ox} s^{(1)}, \tag{2.3a}$$

$$\frac{\partial m^{(1)}}{\partial t} = D_m^{(1)} \frac{\partial^2 m^{(1)}}{\partial x^2} - k_3 e_{red} m^{(1)}, \tag{2.3b}$$

$$\frac{\partial p^{(1)}}{\partial t} = D_p^{(1)} \frac{\partial^2 p_1}{\partial x^2} + k_3 e_{red} m^{(1)}, \tag{2.3c}$$

$$\frac{\partial e_{ox}}{\partial t} = k_3 e_{red} m^{(1)} + k_{-1} e_s - k_1 e_{ox} s^{(1)}, \tag{2.3d}$$

$$\frac{\partial e_{red}}{\partial t} = k_2 e_s - k_3 e_{red} m^{(1)}, \tag{2.3e}$$

$$\frac{\partial e_s}{\partial t} = k_1 e_{ox} s^{(1)} - k_{-1} e_s - k_2 e_s, \tag{2.3f}$$

where x and t stand for space and time, respectively, $s^{(1)}(x,t)$, $m^{(1)}(x,t)$, $p^{(1)}(x,t)$, $e_{red}(x,t)$, $e_{ox}(x,t)$ and $e_s(x,t)$, are the molar concentrations of the substrate S, the mediator M, the product P, the oxidized enzyme E$_{ox}$, the reduced enzyme E$_{red}$ and the enzyme substrate ES, respectively, d_1 is the thickness of the enzyme layer ($d_1 = a_1 - a_0$), and $D_s^{(1)}$, $D_m^{(1)}$, $D_p^{(1)}$ are the diffusion coefficients of corresponding substances in the enzyme ($l = 1$) layer. The enzyme and the formed ES complex are immobilized, and therefore there are no diffusion terms in the corresponding equations. The reaction product P$_1$ has no influence to the biosensor response and therefore is not described in the mathematical model.

Outside the enzyme layer only the mass transport by diffusion of the substrate, the mediator and the product takes place (enzyme does not diffuse through dialysis membrane). It was assumed that the external mass transport obeys a finite diffusion regime ($t > 0, a_l < x < a_{l+1}, l = 2,3$),

$$\frac{\partial c^{(l)}}{\partial t} = D_c^{(l)} \frac{\partial^2 c^{(l)}}{\partial x^2}, \quad c = s, m, p, \quad l = 2,3, \tag{2.4}$$

where $s^{(l)}(x,t), m^{(l)}(x,t)$ and $p^{(l)}(x,t)$ stand for the molar concentrations of the substrate, the mediator and the product in the dialysis and diffusion layers $(l=2,3)$, a_l is the according boundary of the layer (Fig. 2.1), $D_s^{(l)}, D_m^{(l)}$ and $D_p^{(l)}$ are the diffusion coefficients of substrate, product and mediator in layer l.

The diffusion layer $(a_2 < x < a_3)$ is treated as the Nernst diffusion layer [34]. According to the Nernst approach the thickness $d_3 = a_3 - a_2$ remains unchanged with time. Away from it the buffer solution is in motion and uniform in concentration.

2.1.2.2. Initial conditions

The biosensor operation starts when some substrate appears in the bulk solution $(t=0)$,

$$c^{(l)}(x,0) = 0, \quad c = s, m, p, \quad a_{l-1} < x < a_l, \quad l = 1,2,3, \tag{2.5a}$$

$$s^{(1)}(a_0,0) = 0, \qquad s^{(3)}(a_3,0) = s_0, \tag{2.5b}$$

$$m^{(1)}(a_0,0) = m_0, \quad m^{(3)}(a_3,0) = 0, \tag{2.5c}$$

$$p^{(1)}(a_0,0) = 0, \qquad p^{(3)}(a_3,0) = 0, \tag{2.5d}$$

where m_0 is the concentration of the mediator at the boundary between the electrode and the enzyme layers, s_0 is the concentration of the substrate in the bulk solution.

Only oxidized enzyme is present and only in the enzymatic membrane $(l=1)$,

$$e_{ox}(x,0) = e_0, \quad e_{red}(x,0) = 0, \quad e_s(x,0) = 0, \quad a_0 < x < a_1, \tag{2.6}$$

where e_0 is the concentration of the enzyme in the enzyme membrane.

2.1.2.3. Boundary conditions

During the biosensor operation the concentrations of the substrate, mediator and product in the bulk solution remain constant. The concentration $p^{(1)}$ of the reaction product at the electrode surface $(x = a_0)$ is being permanently reduced to zero due to the electrode polarization. Following the scheme (2.1), (2.2), the substrate is an electro-inactive substance. The constant concentration m_0 of the mediator covering the electrode surface

is achieved by permanent dissolution of the adsorbed mediator. This is described by the following boundary conditions $(t > 0)$:

$$D_s^{(1)} \frac{\partial s^{(1)}}{\partial x}\bigg|_{x=a_0} = 0, \qquad s^{(3)}(a_3, t) = s_0, \tag{2.7a}$$

$$m^{(1)}(a_0, t) = m_0, \quad m^{(3)}(a_3, t) = 0, \tag{2.7b}$$

$$p^{(1)}(a_0, t) = 0, \qquad p^{(3)}(a_3, t) = 0. \tag{2.7c}$$

2.1.2.4. Matching conditions

On the boundary between two adjacent regions having different diffusivities, the matching conditions are defined $(t > 0)$,

$$D_c^{(l)} \frac{\partial c^{(l)}}{\partial x}\bigg|_{x=a_l} = D_c^{(l+1)} \frac{\partial c^{(l+1)}}{\partial x}\bigg|_{x=a_l}, \quad c = s, m, p, \quad l = 1, 2, \tag{2.8a}$$

$$c^{(l)}(a_l, t) = c^{(l+1)}(a_l, t), \qquad c = s, m, p, \quad l = 1, 2. \tag{2.8b}$$

These conditions mean that fluxes of the substrate, mediator and product through the analysed layer l are considered to be equal to the corresponding fluxes entering the surface of the layer $l + 1$ (as it was described in Section 1.1.2.1). The partition coefficients (described in Section 1.1.2.2) of the substrate, mediator and product in all the compartments are considered to be equal ($K_c^{(1),(2)} = K_c^{(2),(3)} = 1$ for $c = s, m, p$) and therefore are not introduced in the mathematical model.

2.1.2.5. Biosensor response

The electric current is measured as a response of a biosensor in a physical experiment. The current depends on a flux of the reaction product at an electrode surface. Thus the density $i(t)$ of the current at time t is proportional to the gradient of the product at the electrode surface ($x = a_0$), as described in (1.15).

It is assumed that the system (2.3a)-(2.8b) approaches a steady-state as $t \to \infty$ (1.16)

2.1.3. Mathematical model with quasi-steady-state assumption

Reactions in the network (2.1) and (2.2) are of the different rates [2, 162, 171]. The large difference of the timescales in the reaction network creates difficulties for simulating the temporal evolution of the network and for understanding the basic principles of the biosensor operation. To sidestep these problems, the QSSA is often applied [55, 164],

$$\frac{\partial e_{ox}}{\partial t} \approx \frac{\partial e_{red}}{\partial t} \approx \frac{\partial e_s}{\partial t} \approx 0. \tag{2.9}$$

Applying the QSSA leads to a reduction of the system (2.3a)-(2.3f), presented in [112]:

$$\frac{\partial s^{(1)}}{\partial t} = D_s^{(1)} \frac{\partial^2 s^{(1)}}{\partial x^2} - v(s^{(1)}, m^{(1)}), \tag{2.10a}$$

$$\frac{\partial m^{(1)}}{\partial t} = D_m^{(1)} \frac{\partial^2 s^{(1)}}{\partial x^2} - v(s^{(1)}, m^{(1)}), \tag{2.10b}$$

$$\frac{\partial p^{(1)}}{\partial t} = D_p^{(1)} \frac{\partial^2 s^{(1)}}{\partial x^2} + v(s^{(1)}, m^{(1)}), \tag{2.10c}$$

$$v(s^{(1)}, m^{(1)}) = \frac{e_0 k_1 k_2 k_3 s^{(1)} m^{(1)}}{k_1 k_3 s^{(1)} m^{(1)} + k_1 k_3 s^{(1)} + k_3 (k_{-1} + k_2) m^{(1)}}. \tag{2.11}$$

The total sum e_0 of the concentrations of all the enzyme forms is assumed to be constant in the entire enzyme layer, $e_0 = e_{ox} + e_{red} + e_s$. In the simplest case of the biosensor operation (when only the enzyme-substrate reaction (2.3a) takes place) the sufficient condition for the QSSA to be valid is $e_0 \ll s_0 + (k_{-1} + k_2)/k_1$ [55, 164]. The conditions at which the CME operation can be simulated under QSSA for accurate calculation of the biosensor response are investigated numerically in Section 4.1.2.3. Assuming the transient mathematical model as a precise (true) mathematical model of the CME action, QSSA of the model can be validated. The relative error E_{QSSA} of the biosensor response arose due to the QSSA is defined as:

$$E_{QSSA} = \left| \int_0^\infty i_{full}(t)dt - \int_0^\infty i_{QSSA}(t)dt \right| \bigg/ \int_0^\infty i_{full}(t)dt, \tag{2.12}$$

where i_{full} is the density of the biosensor current calculated by the transient mathematical model of the CME, and i_{QSSA} is the density of the biosensor

current calculated by the corresponding model derived from the transient model by applying QSSA. The error E_{QSSA} can also be called the relative error of QSSA.

2.1.4. Parameters used for investigation

Since the reaction term depends on the concentrations s_0 and m_0 of the substrate S and the mediator M, the following dimensionless relation between these concentrations and their respective reaction rate constants can be used [112]:

$$\Sigma = \frac{s_0}{m_0}\frac{k_{red}}{k_{ox}}. \tag{2.13}$$

Two diffusion modules (see Section 1.2.3) for the biosensor with chemically modified electrode were obtained by deriving the dimensionless mathematical model in [112]. The first diffusion module is expressed as follows:

$$\sigma_1^2 = \frac{e_0 d_1^2 k_1 k_2}{D_s^{(1)}(k_{-1}+k_2))}, \tag{2.14}$$

defining the ratio between enzymatic reaction $(e_0 k_1 k_2/(k_{-1}+k_2))$ with the diffusion rate $(d_1^2/D_s^{(1)})$.

Similarly, the second diffusion module is defined,

$$\sigma_2^2 = e_0 k_3 d_e^2 / D_s^{(1)}. \tag{2.15}$$

2.2. Biosensor with parallel substrates conversion

A mathematical model of the newly created physical biosensor with dual catalase-peroxidase bioelectrode is presented in this section [A5]. Created mathematical model was used to prove a concept of bioelectrode analytical application of such configuration. The application of catalase and peroxidase allows to construct a biosensor realizing parallel substrates conversion and apply it in pharmaceutical environment. A rather unspecific electrochemical method is usually used [169, 170] for the determination acetaminophen, therefore a specifically designed biosensor is relevant.

2.2.1. Biochemical background

The biosensor containing catalase (E_1) and peroxidase (E_2) converts hydrogen peroxide (H_2O_2). The catalase catalyses hydrogen peroxide splitting with oxygen (O_2) production in the following process:

$$2H_2O_2 \rightarrow 2H_2O + O_2. \tag{2.16}$$

The peroxidase catalyses a variety of substrates (S_2) oxidation in the following peroxidase-catalysed process:

$$2H_2O_2 + 2S_2 + 2H^+ \rightarrow 2H_2O + P_2. \tag{2.17}$$
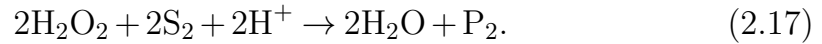
Further S_1 denotes H_2O_2, and P_1 - O_2. The remarkable feature of this conjugated system is molecular oxygen production, which can be selectively determined by Clark type electrode [172, 173].

Catalase (E_1) and peroxidase (E_2) catalyses S_2 conversion in a more complex scheme and typically includes intermediates [174]. In case of hydrogen peroxide (S_1) catalisation process (2.16), intermediate C_1 is introduced:

$$E_1 + S_1 \xrightarrow{k_{11}} C_1 + H_2O, \tag{2.18a}$$

$$C_1 + S_1 \xrightarrow{k_{12}} E_1 + P_1. \tag{2.18b}$$
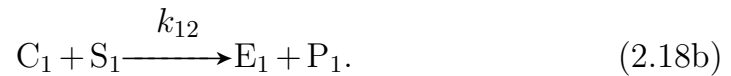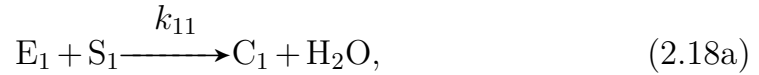
The change of E_1 and C_1 in time t can be described as follows:

$$\frac{dE_1}{dt} = -k_{11}E_1S_1 + k_{12}C_1S_1, \tag{2.19a}$$

$$\frac{dC_1}{dt} = k_{11}E_1S_1 - k_{12}C_1S_1. \tag{2.19b}$$

By adding (2.19a) with (2.19b):

$$\frac{dC_1}{dt} + \frac{dE_1}{dt} = 0, \quad \text{e.g. } E_1 + C_1 = E_{10}. \tag{2.20}$$

where E_{10} is the initial concentration of the first enzyme.

By inserting the expression of E_1 from (2.20) into (2.19b) and equalling

it to zero (by applying quasi-steady-state approximation [2, 3, 175]), C_1 can be expressed as follows:

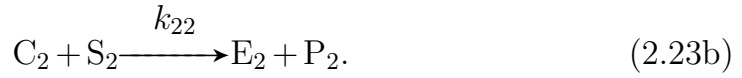$$C_1 = \frac{k_{11}E_{10}}{k_{11} + k_{12}} = \frac{E_{10}}{2}, \tag{2.21}$$

when $k_{11} = k_{12} = k_1$.

The change of hydrogen peroxide (S_1) and oxygen (P_1) concentrations can be written as follows:

$$\frac{dS_1}{dt} = -k_{11}E_1S_1 - k_{12}C_1S_1 = -k_1(E_1 + C_1)S_1 = -k_1E_{10}S_1, \tag{2.22a}$$

$$\frac{dP_1}{dt} = k_{12}C_1S_1 = k_{12}\frac{E_{10}}{2}S_1 = 0.5k_1E_{10}S_1. \tag{2.22b}$$

In case of acetaminophen (S_2) catalisation process (2.17), intermediate C_2 is introduced:

$$E_2 + S_1 \xrightarrow{k_{21}} C_2, \tag{2.23a}$$

$$C_2 + S_2 \xrightarrow{k_{22}} E_2 + P_2. \tag{2.23b}$$

The change of E_2 and C_2 in time t can be described as follows:

$$\frac{dE_2}{dt} = -k_{21}E_2S_1 + k_{22}C_2S_2, \tag{2.24a}$$

$$\frac{dC_2}{dt} = k_{21}E_2S_2 - k_{22}C_2S_2. \tag{2.24b}$$

By applying the same approach as when deriving the reactions for the first enzyme (2.20), (2.24a) is summed up with (2.24b), to obtain the following:

$$\frac{dC_2}{dt} + \frac{dE_2}{dt} = 0, \quad \text{e.g. } E_2 + C_2 = E_{20}. \tag{2.25}$$

where E_{20} is the initial concentration of the second enzyme.

By inserting the expression of E_2 from (2.25) into (2.24b) and equalling it to zero (again, by applying the quasi-steady-state approximation), C_2 can be expressed:

$$C_2 = \frac{k_{21}E_{20}S_1}{k_{21}S_1 + k_{22}S_2}. \tag{2.26}$$

The change of acetaminophen (S_1) and the second reaction product (P_2) concentrations in time t can be written as follows:

$$\frac{dS_2}{dt} = -k_{22}C_2S_2 = -\frac{k_{21}k_{22}E_{20}S_1S_2}{k_{21}S_1 + k_{22}S_2}, \tag{2.27a}$$

$$\frac{dP_2}{dt} = k_{22}C_2S_2 = \frac{k_{21}k_{22}E_{20}S_1S_2}{k_{21}S_1 + k_{22}S_2}. \tag{2.27b}$$

A following simplified kinetic scheme, utilizing two substrates (S_1 and S_2), two enzymes (E_1 and E_2) and two reaction products (P_1 and P_2) can be used for definition of the biosensor behaviour:

$$S_1 \xrightarrow{E_1} P_1, \quad S_1 + S_2 \xrightarrow{E_2} P_2. \tag{2.28}$$
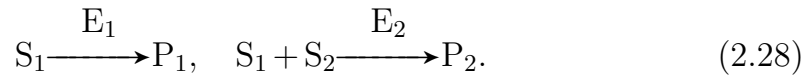
A wide variety of electrodes are used in practice for the determination of the product concentrations [95]. The molecular oxygen (P_1) can be effectively detected by applying an oxygen-sensitive electrode. A Clark-type electrode (CE) measures oxygen on a catalytic platinum surface, while the oxygen itself is not consumed to generate current [172].

In the first phase of the biosensors action, only hydrogen peroxide (S_1) is present in the solution. At the end of the first phase when the biosensor response reaches steady-state, the second substrate (S_2) is poured into the solution, and the second phase of the biosensor action starts. The relative change between the responses in the both phases is measured as the final response of the biosensor. This relative response indicates the concentration of the second substrate. The first phase is only used for the determination of the first substrate concentration and is not decisive when the concentration is known before the experiment.

2.2.2. Mathematical model with partition coefficient

Mathematical model of the biosensor utilizing parallel substrates conversion was analysed in one dimensional space, having the same three layers as CME model (see Fig. 2.1): the layer of both enzymes ($a_0 < x < a_1$), the dialysis membrane ($a_1 < x < a_2$), and the diffusion layer ($a_2 < x < a_3$).

2.2.2.1. Governing equations

Coupling the catalase (2.22) and peroxidase (2.27) catalysed reactions in the enzymatic layer with the one-dimensional-in-space diffusion, described by Fick's law, leads to the following reaction–diffusion equations describing the biosensor operation in the enzymatic layer ($a_0 < x < a_1, t > 0$):

$$\frac{\partial s_1^{(1)}}{\partial t} = D_{s_1}^{(1)}\frac{\partial^2 s_1^{(1)}}{\partial x^2} - r_1 - r_2, \quad \frac{\partial s_2^{(1)}}{\partial t} = D_{s_2}^{(1)}\frac{\partial^2 s_2^{(1)}}{\partial x^2} - r_2, \tag{2.29a}$$

$$\frac{\partial p_1^{(1)}}{\partial t} = D_{p_1}^{(1)}\frac{\partial^2 p_1^{(1)}}{\partial x^2} + \frac{1}{2}r_1, \quad \frac{\partial p_2^{(1)}}{\partial t} = D_{p_2}^{(1)}\frac{\partial^2 p_2^{(1)}}{\partial x^2} + r_2, \tag{2.29b}$$

$$r_1 = k_1 e_1 s_1^{(1)}, \qquad\qquad r_2 = \frac{k_{21}k_{22}e_2 s_1^{(1)} s_2^{(1)}}{k_{21}s_1^{(1)} + k_{22}s_2^{(1)}}, \tag{2.29c}$$

where x and t stand for space and time, respectively, $s_1^{(1)}(x,t)$, $s_2^{(1)}(x,t)$, $p_1^{(1)}(x,t)$ and $p_2^{(1)}(x,t)$ are the molar concentrations of the substrates S_1, S_2 and the products P_1, P_2 in the enzyme layer of the thickness $d_1 = a_1 - a_0$, respectively, and $D_{s_1}^{(1)}$, $D_{s_2}^{(1)}$, $D_{p_1}^{(1)}$ and $D_{p_2}^{(1)}$ are the constant diffusion coefficients.

Outside the enzyme layer, in the dialysis membrane ($a_1 < x < a_2$, $t > 0$) and in the diffusion layer ($a_2 < x < a_3$, $t > 0$) only the mass transport of all the species by the diffusion takes place,

$$\frac{\partial c^{(l)}}{\partial t} = D_c^{(l)}\frac{\partial^2 c^{(l)}}{\partial x^2}, \quad c = s_1, s_2, p_1, p_2, \quad l = 2, 3, \tag{2.30}$$

where $c^{(l)}(x,t)$ are the molar concentrations of both substrates and both products in the dialysis ($l = 2$) and diffusion ($l = 3$) layers, with the thicknesses $d_l = a_l - a_{l-1}$, and diffusion coefficients $D_c^{(l)}$.

2.2.2.2. Initial conditions

At the beginning of the biosensor operation ($t = 0$) only the first substrate is present in the solution. No concentrations of other substances are present in the enzymatic ($l = 1$), dialysis ($l = 2$) and diffusion ($l = 3$) layers:

$$c^{(l)}(x,0) = 0, \quad c = s_1, s_2, p_1, p_2, \quad a_{l-1} < x < a_l \quad l = 1,2,3, \qquad \text{(2.31a)}$$

$$s_1^{(1)}(a_0,0) = 0, \quad s_1^{(3)}(a_3,0) = s_{10}, \qquad \text{(2.31b)}$$

$$s_2^{(1)}(a_0,0) = 0, \quad s_2^{(3)}(a_3,0) = 0, \qquad \text{(2.31c)}$$

$$p_z^{(1)}(a_0,0) = 0, \quad p_z^{(3)}(a_3,0) = 0, \quad z = 1,2, \qquad \text{(2.31d)}$$

$$\text{(2.31e)}$$

where s_{10} is the concentration of the first substrate in the bulk.

2.2.2.3. Boundary conditions

Boundary conditions on the boundaries between the electrode and the enzymatic layer $(x = a_0)$, between the diffusion layer and bulk solution $(x = a_3)$ have to be defined. At the beginning $(t = 0)$ of the biosensor operation some of the first substrate appears in the bulk.

In case of the Clark electrode (CE) the molecular oxygen is not consumed at the electrode surface, therefore the boundary condition for the first product is $(t > 0)$:

$$D_{p_1}^{(1)} \frac{\partial p_1^{(1)}}{\partial x} \bigg|_{x=a_0} = 0. \qquad \text{(2.32)}$$

The substrates and the second product are also considered to be electrically inactive materials. This is defined by the following boundary condition $(t > 0)$ at the electrode surface $(x = a_0)$:

$$D_c^{(1)} \frac{\partial c^{(1)}}{\partial x} \bigg|_{x=a_0} = 0, \quad c = s_1, s_2, p_2. \qquad \text{(2.33)}$$

In the bulk the concentrations of both substrates are considered to be constant, while the concentrations of the reaction products are constantly reduced to zero,

$$s_1^{(3)}(a_3,t) = s_{10}, \qquad \text{(2.34a)}$$

$$s_2^{(3)}(a_3,t) = \begin{cases} 0, & \text{if } t < t_2 \\ s_{20}, & \text{if } t \geq t_2 \end{cases}, \qquad \text{(2.34b)}$$

$$p_z^{(3)}(a_3,t) = 0, \quad z = 1,2, \qquad \text{(2.34c)}$$

where s_{20} is the concentration of the second substrate in the buffer solution, and t_2 is the time moment when the second substrate S_2 appears in the solution.

2.2.2.4. Matching conditions

Matching conditions are defined for the boundaries between the enzymatic layer and the dialysis membrane ($x = a_1$), between the dialysis membrane and the diffusion layer ($x = a_2$).

The fluxes of the substrates and the products entering the enzymatic layer are considered to be equal to the outgoing ones. This is defined by the following matching conditions ($t > 0$):

$$D_c^{(l)} \frac{\partial c^{(l)}}{\partial x} \bigg|_{x=a_l} = K_c^{(l),(l+1)} D_c^{(l+1)} \frac{\partial c^{(l+1)}}{\partial x} \bigg|_{x=a_l}, \qquad (2.35a)$$

$$c^{(l)}(a_l, t) = K_c^{(l),(l+1)} c^{(l+1)}(a_l, t), \quad c = s_1, s_2, p_1, p_2, \quad l = 1, 2. \qquad (2.35b)$$

where $K_c^{(l),(l+1)}$ is the partition coefficient (described in section 1.1.2.2) between the neighbouring layers (l and $l+1$) of corresponding substances ($c = s_1, s_2, p_1, p_2$). When $K_c^{(l),(l+1)} > 1$, the solubility of the compound c in layer l is larger than in layer $l+1$. For the opposite case (when $K_c^{(l),(l+1)} < 1$) the solubility of substance c is larger in layer $l+1$. When no partitioning of the compounds between two neighbouring layers takes place it is considered that $K_c^{(l),(l+1)} = 1$.

2.2.2.5. Biosensor response

In case of the Clark electrode the current density is measured as the biosensor response, which is directly proportional to the product concentration at the electrode surface, and can be obtained according to Faraday's law [2],

$$i_{CE}(t) = k_s F p_1^{(1)} \bigg|_{x=a_0}, \qquad (2.36)$$

where F is Faraday's constant ($F = 96.485 \times 10^6 \, \text{CM}^{-1}\text{m}^{-3}$), n_e is a number of electrons involved in the electrochemical reaction, and k_s is the heterogenic constant calculated experimentally. In all of the simulations $n_e = 2$ was used.

2.2.3. Dimensionless mathematical model

In order to define the main governing parameters of the model, the dimensionless mathematical model was derived in this work following the similar approach presented in section 1.2.2. The list of the dimensionless parameters is presented in Table 2.1.

Table 2.1. Dimensionless model parameters.

Parameter	Dimensional	Dimensionless
Distance from electrode	x, m	$X = x/d_1$
Boundary coordinate $l = 0, 1, 2, 3$	a_l, m	$A_l = a_l/d_1$
Thickness of the layer $l = 1, 2, 3$	d_l, m	$\delta_l = d_l/d_1$
Time	t, s	$T = t(D_{s_1}^{(1)}/d_1^2)$
Time when s_{20} appears	t_2, s	$T_2 = t_2(D_{s_1}^{(1)}/d_1^2)$
Substrate concentrations	s_1, M	$S_1 = s_1/s_{10}$
	s_{10}, M	$S_{10} = s_{10}/s_{10} = 1$
	s_2, M	$S_2 = s_2(k_{22}/k_{21})/s_{10}$
	s_{20}, M	$S_{20} = s_2(k_{22}/k_{21})/s_{10}$
Product concentrations	p_1, M	$P_1 = p_1/s_{10}$
	p_2, M	$P_2 = p_2(k_{22}/k_{21})/s_{10}$
Diffusion coefficients of $c = s_1$, s_2, p_1, p_2, in layers $l = 1, 2, 3$	$D_c^{(l)}$, m/s^2	$\Phi_C^{(l)} = D_c^{(l)}/D_{s_1}^{(1)}$

As one can see from Table 2.1, the dimensionless thickness of the enzyme membrane equals one ($\delta_1 = 1$) and the partition coefficients are not included as they are already dimensionless parameters.

The governing equations (2.29) for the enzymatic ($l = 1$) layer in dimensionless coordinates are expressed as follows ($A_0 < X < A_1, T > 0$):

$$\frac{\partial S_1^{(1)}}{\partial T} = \Phi_{S_1}^{(1)}\frac{\partial^2 S_1^{(1)}}{\partial X^2} - R_1 - R_2, \quad \frac{\partial S_2^{(2)}}{\partial T} = \Phi_{S_2}^{(1)}\frac{\partial^2 S_2^{(1)}}{\partial X^2} - R_2, \qquad (2.37a)$$

$$\frac{\partial P_1^{(1)}}{\partial T} = \Phi_{P_1}^{(1)}\frac{\partial^2 P_1^{(1)}}{\partial X^2} + \frac{1}{2}R_1, \qquad \frac{\partial P_2^{(1)}}{\partial T} = \Phi_{P_2}^{(1)}\frac{\partial^2 P_2^{(1)}}{\partial X^2} + R_2, \qquad (2.37b)$$

$$R_1 = \sigma_1^2 S_1^{(1)}, \qquad\qquad R_2 = \sigma_2^2\frac{S_1^{(1)} S_2^{(1)}}{S_1^{(1)} + S_2^{(1)}}, \qquad (2.37c)$$

where $\sigma_1^2 = k_1 e_1 d_1^2/D_{s_1}^{(1)}$, $\sigma_2^2 = k_{21} e_2 d_1^2/D_{s_1}^{(1)}$ are the dimensionless factors known as the diffusion modulus (or Damköhler number) as defined in (1.25).

The governing equation (2.30) describing the action in diffusive-only

layers ($l = 2, 3$) take the following form :

$$\frac{\partial C^{(l)}}{\partial T} = \Phi_C^{(l)} \frac{\partial^2 C^{(l)}}{\partial X^2}, \quad C = S_1, S_2, P_1, P_2, \quad l = 2, 3. \tag{2.38}$$

The initial conditions (2.31) take the following form ($T = 0$):

$$C^{(l)}(X, 0) = 0, \quad C = S_1, S_2, P_1, P_2, \quad A_{l-1} < X < A_l, \quad l = 1, 2, 3, \tag{2.39a}$$

$$S_1^{(1)}(A_0, 0) = 0, \qquad\qquad S_1^{(3)}(A_3, 0) = S_{10}, \tag{2.39b}$$

$$S_2^{(1)}(A_0, 0) = 0, \qquad\qquad S_2^{(3)}(A_3, 0) = 0, \tag{2.39c}$$

$$P_Z^{(1)}(A_0, 0) = 0, \qquad\qquad P_Z^{(3)}(A_3, 0) = 0, \quad Z = 1, 2. \tag{2.39d}$$

Boundary conditions (2.32)-(2.34) are rewritten as follows ($T > 0$):

$$\Phi_{P_1}^{(1)} \frac{\partial P_1^{(1)}}{\partial X}\bigg|_{X=A_0} = 0. \tag{2.40a}$$

$$\Phi_C^{(1)} \frac{\partial C^{(1)}}{\partial X}\bigg|_{X=A_0} = 0, \quad C = S_1, S_2, P_2. \tag{2.40b}$$

$$S_1^{(3)}(A_3, T) = S_{10}, \tag{2.40c}$$

$$S_2^{(3)}(A_3, T) = \begin{cases} 0, & \text{if } T < T_2 \\ S_{20}, & \text{if } T \geq T_2 \end{cases}, \tag{2.40d}$$

$$P_Z^{(3)}(A_3, T) = 0, \quad Z = 1, 2. \tag{2.40e}$$

Finally, matching conditions (2.35) are expressed by the following equations ($T > 0$):

$$\Phi_C^{(l)} \frac{\partial C^{(l)}}{\partial X}\bigg|_{X=A_l} = K_C^{(l),(l+1)} \Phi_C^{(l+1)} \frac{\partial C^{(l+1)}}{\partial X}\bigg|_{X=A_{l+1}}, \tag{2.41a}$$

$$C^{(l)}(A_l, T) = K_C^{(l),(l+1)} C^{(l+1)}(A_l, T), \quad C = S_1, S_2, P_1, P_2, \quad l = 1, 2. \tag{2.41b}$$

2.2.4. Parameters used for investigation

The mathematical model of the biosensor with parallel substrates conversion and Clark-Type electrode involves (2.29), (2.30), (2.31), (2.32)-(2.34), (2.36) equations and it approaches the steady-state as $t \to \infty$ (as

defined in (1.16)).

A difference i_d is measured in order to evaluate the concentration s_{20} of the second substrate S_2:

$$i_d = i_{s_{10}} - i_{s_{20}}, \tag{2.42}$$

where $i_{s_{10}}$ is the steady-state response at zero concentration of the second substrate, $i_{s_{20}}$ is the steady-state response with a presence of the second substrate in the solution. The difference of the steady-state responses with the current $i_{s_{10}}$ was normalized as follows:

$$I_r = \frac{i_d}{i_{s_{10}}} = \frac{i_{s_{10}} - i_{s_{20}}}{i_{s_{10}}}, \tag{2.43}$$

where I_r is the relative steady-state biosensor current or the relative response.

As it was mentioned in (Section 1.2.3), the sensitivity (1.19) is one of the most important characteristics of biosensor. In case of the catalase-peroxidase biosensor, the dimensionless sensitivity (1.20) was analysed,

$$B_{rs} = \frac{di_d(s_{20})}{ds_{20}} \times \frac{s_{20}}{i_d(s_{20})} = \frac{dI_r(s_{20})}{ds_{20}} \times \frac{s_{20}}{i_r(s_{20})}. \tag{2.44}$$

The half-time of the steady-state can be used to investigate the behaviour of the response time [176–180]. The half-time of the second operational phase steady-state is described as follows:

$$t_h = \min_{t > t_2} \left\{ t : i(t) < i(t_2) - \frac{i(t_2) - i(t_R)}{2} \right\} - t_2, \tag{2.45}$$

where t_h is the time difference between the time when the reaction-diffusion process reaches the medium in the second operational phase and the time when the second substrate is poured into the bulk (t_2). It is the time moment of occurrence of the half of the steady-state current in the second phase of the biosensor action. The half-time of the response was investigated extensively in [A8].

The influence of both enzymes on the relative response was investigated. The following dimensionless reaction rate ξ_1 between the concentrations of the catalase and peroxidase and their kinetic reaction rates was

introduced:

$$\xi_1 = \frac{k_1 e_1}{k_{21} e_2}. \tag{2.46}$$

In some cases, only the ration between the enzyme concentrations can be used, excluding the kinetic reaction rates, as they usually remain constant during the calculations:

$$\xi_2 = \frac{e_1}{e_2}. \tag{2.47}$$

In case of the biosensors with parallel substrates conversion, diffusion module (1.25) is defined according to the dimensionless mathematical model (see Section 2.2.3) as follows:

$$\sigma_1^2 = \frac{k_1 e_1 d_1^2}{D_{s_1}^{(1)}}, \quad \sigma_2^2 = \frac{k_{21} e_2 d_1^2}{D_{s_1}^{(1)}}. \tag{2.48}$$

The diffusion modules σ_1 and σ_2 compare the rates of the enzymatic reactions $k_1 e_1$ and $k_{21} e_2$, respectively, with the diffusion rate $D_{s_1}^{(1)}/d_1^2$.

The half-maximal effective concentration (1.24) was defined as the concentration s_{20} of the second substrate S_2 at which the response of the biosensor reaches half of the maximal steady-state response keeping the concentration s_{10} of S_1 constant,

$$\begin{aligned}
C_{50} &= \left\{ s_{20}^* : i_{s_{20}}(s_{20}^*) = 0.5 \lim_{s_{20} \to \infty} i_{s_{20}}(s_{20}) \right\} = \\
&= \left\{ s_{20}^* : I_r(s_{20}^*) = 0.5 \lim_{s_{20} \to \infty} I_r(s_{20}) \right\},
\end{aligned} \tag{2.49}$$

where $I_r(s_{20})$ is the relative current (2.43) at the steady-state achieved with the concentration s_{20} of the second substrate S_2.

2.3. Summary

Two mathematical models (transient and based on the quasi-steady-state assumption) were presented for the biosensor with chemically modified electrode. Mathematical model of the biosensor utilizing parallel substrates conversion was presented by introducing partition coefficient for the neighbouring layers. A dimensionless mathematical model was derived in order to determine the main governing parameters. The derivation of the reac-

tion terms describing the kinetic biosensor action was provided based on the quasi-steady-state assumption.

The parameters usually used for the investigation of the biosensor action (see Section 1.2.3) were customized for both analysed biosensors. The developed mathematical models were later successfully used to investigate the peculiarities of the biosensor action (see Chapter 4).

Chapter 3

Solving the mathematical models

Analytical solutions of one and two compartment models of amperometric biosensors are known only for a specific set of parameter values. To solve the problems presented by the mathematical models in Chapter 2 in general case, a computational modelling is used. The results of this chapter were presented in papers [A1, A2, A6].

3.1. Biosensor with chemically modified electrode

A mathematical model of the biosensor with chemically modified electrode is solved numerically in this section. To validate the achieved results, numerically obtained solutions are compared to known analytical solutions, as well as to the existing results [112]. The possibility of the variable space step usage in the computational scheme is investigated and evaluated. The results presented in this section were published in [A2].

3.1.1. Analytical solution

The analytical solutions of the mathematical model with quasi-steady-state assumption exist when non-linear term v (2.11) becomes linear. When the dimensionless ratio Σ, defined in (2.13) is relatively small ($\Sigma \ll 1$), the

steady-state response is calculated as follows [28]:

$$
\begin{aligned}
i_{s1} = {} & \frac{n_e F D_p^{(1)} s_0}{(d_1 + d_2)(D_p^{(2)} d_1 + D_p^{(1)} d_2)} \times \\
& \left(d_1 + d_2 \frac{(D_s^{(2)} - \sigma_1 D_s^{(1)} \sinh(\sigma_1)/\cosh(\sigma_1)}{D_s^{(2)} + \sigma_1 D_s^{(1)}(d_2/d_1)\sinh(\sigma_1)/\cosh(\sigma_1)} \right) \times \\
& \left(\sigma_1 D_s^{(1)} \frac{d_2}{d_1} \times \frac{\sinh(\sigma_1)}{\cosh(\sigma_1)} + \frac{D_s^{(1)} D_p^{(2)}}{D_p^{(1)}} \left(1 - \frac{1}{\cosh(\sigma_1)} \right) \right),
\end{aligned}
\tag{3.1}
$$

where σ_1^2 is the first diffusion module defined in Section 2.1.4.

When $\Sigma \gg 1$, the steady-state current is known for single-layered biosensor:

$$
i_{s2} = n_e F D_p^{(1)} m_0 (\sigma_2 \coth(\sigma_2) - 1),
\tag{3.2}
$$

where σ_2^2 is the second diffusion module defined in Section 2.1.4.

3.1.2. Numerical solution

A rectangular mesh of intersecting lines in space and time is used to cover the domain of the solved problem when using a finite difference scheme. A following uniform mesh is defined according to (1.26) with $L = 3$, for the problem (2.3a)-(2.8b) in the domain $[a_0, a_3] \times [0, T]$, where T is the total time of biosensor action:

$$
\Omega_{h\tau} = \{ (x_i^{(l)}, t_j) : x_i^{(l)} = h_l i + \sum_{ii=1}^{l-1} a_{ii}; \ t_j = j\tau; \ i = 1, ..., N_l, \ j = 1, ..., M \},
\tag{3.3}
$$

where N_l - space step count in layer, $h_l = N_l/d_l$ - the size of time step in layer l ($l = 1, 2, 3$). To have an accurate and stable result, it is required to use a very small step size in x direction at the boundaries where boundary and matching conditions are defined. Assumption was made in [112] that further from all these peculiar boundaries, the step size may increase. However, the efficiency of the variable space step was not analysed, as well as the accuracy issue was not investigated. When using variable space step a total amount of space points is decreased by $R\%$,

$$
R = \frac{N_{const} - N_{var}}{N_{const}} \times 100\%,
\tag{3.4}
$$

where N_{var} is the total amount of space points when using the variable space step, N_{const} - when using a constant one.

When reaching the middle $((a_{l+1} - a_l)/2)$ of each layer l, the space step is increased exponentially,

$$h_i^{(l)} = \begin{cases} h_l q_l^{i-1}, & i = 1, 2, ..., (N_{var,l} - 1)/2, \\ h_l q_l^{N_{var,l} - i}, & i = (N_{var,l} - 1)/2 + 1, (N_{var,l} - 1)/2 + 2, ..., N_{var,l}, \end{cases} \tag{3.5}$$

where $N_{var,l}$ is the variable space step count in layer l, and q_l is the experimentally chosen scale values of geometric progression, that for each analysed layer l the following condition would be satisfied:

$$d_l = \sum_{i=1}^{N_{var,l}} h_i^{(l)}, \quad l = 1, 2, 3. \tag{3.6}$$

Explicit scheme was chosen because of it's simplicity and low computational cost for the investigation of the variable space step. It was numerically proved in [A6] that the errors of the variable space step usage for implicit, explicit and Crank-Nicolson finite difference methods are totally the same.

For the explicit scheme to be numerically stable, requirement for the time step must be satisfied. By changing size of the space step exponentially, the stability condition (1.30) takes the following form:

$$\tau < min\left(\frac{h_1^{(l)} h_2^{(l)}}{D_c^{(l)}}\right) = min\left(\frac{h_1^{(l)^2} q}{D_c^{(l)}}\right), \quad l = 1, 2, 3, \quad c = s, m, p. \tag{3.7}$$

When using the variable space step the requirement for the time step is weakened q times, comparing to the constant space step scheme. This difference affects the speed of calculations (presented in Section 3.1.2.2) noticeably.

During the digital simulation, the response was considered to have reached a steady-state current (1.16) when the change in current was relatively low compared to the change in time. Time t_r defining a moment in time, when the sufficient enough response change is detected was used as defined in (1.31). In the calculations $\varepsilon = 10^{-3}$ was used.

3.1.2.1. Comparison of the schemes with variable and constant space steps

Time used to calculate the steady-state response is directly proportional to the nod count in finite difference scheme, independently of the space step selection algorithm complexity [44],

$$SK = M \times N, \quad N = N_{var}, \ N_{const}, \tag{3.8}$$

where M is total count of the time steps defined in (3.3), N – total count of space steps.

Calculation error, occurring because of the variable space step is evaluated by the following formula:

$$\varepsilon_R = \frac{|i_{sA} - i_{s,var}|}{i_{sA}} \times 100\%, \quad i_{sA} = \begin{cases} i_{s1}, & \text{from (3.1)}, \quad \Sigma \ll 1, \\ i_{s2}, & \text{from (3.2)}, \quad \Sigma \gg 1, \\ i_{s,const}, & \Sigma \approx 1, \end{cases} \tag{3.9}$$

where $i_{s,const}$ is the digitally calculated steady-state response with a constant space step, and $i_{s,var}$ is calculated with a variable space step.

The accuracy of the computational model with variable space step size (when $N_{const} = 1000$ and $R = 0\%$) was investigated with a two-layered mathematical model, with a membrane thicknesses $d_{23} = d_1 = 10^{-4}$m, the diffusion coefficient were $D^{(23)} = 2 \times D^{(1)} = 6 \times 10^{-10}$ m^{2}s^{-1} and other parameter values as defined in Table 4.1. The computed steady-state response with a constant space step size was compared to the analytical solutions (3.1) and (3.2). The extended information regarding models validity is provided in Section 4.1.1.2. For both cases the relative error of the computed response was less than 2%.

3.1.2.2. Effectiveness of variable space step

Efficiency of the variable step use was investigated by changing the total amount of space points N_{const} for the constant space step. The results presented in this section were published in [A2]. The similar research regarding the application of the variable space step on the biosensor based on the Michaelis-Menten kinetics was presented in [A6]. The total amount of space points (3.8) needed to calculate the response with a desired accuracy ε_R (3.9) was evaluated. The analysis were carried out for different

concentrations e_0 of enzyme E and different decrease sizes R (3.4).

The dependency of the total points used in the simulation (3.8) on the desired calculation accuracy is presented in Fig. 3.1. The substrate concentration s_0 was relatively low compared to the mediator concentration m_0 ($\Sigma \ll 1$), while the other parameter values were the same as in Table 4.1.
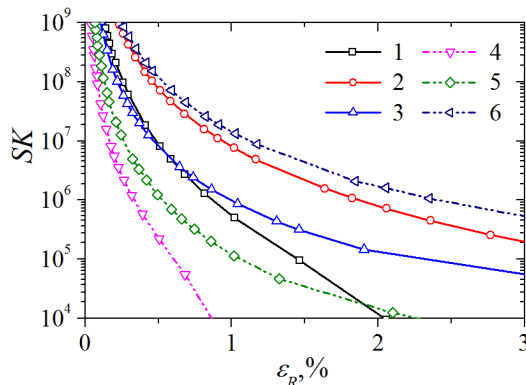

Figure 3.1. The dependency of the total points count SK on the desired accuracy ε_R, when $\Sigma \ll 1$, for different concentrations e_0 of enzyme: 10^{-6}M (1, 2, 3), 10^{-5}M (4, 5, 6), and different decrease sizes R: 0% (3, 6), 60% (2, 5) and 90% (1, 4).

It is noticeable in Fig. 3.1 that for the higher concentrations of the enzyme ($e_0 = 10^{-5}$M, curves 4-6) with a loss of $\varepsilon_R = 0.5\%$ the variable space step calculations can be improved approximately 1000 times.

Both decreased counts of the space steps (because of the variable size) and the time steps (because of the changed stability requirement (3.7)) play a role in such an increased calculation performance. For the relatively high enzyme concentrations variable step size calculations have an improved performance of at least 100 times for all the analysed accuracies ε_R, therefore it is highly recommended.

However, for the lower concentrations of the enzyme ($e_0 = 10^{-6}$M, curves 1-3) the variable space step calculations can only be used for approximate calculations (when $\varepsilon_R > 1\%$) and for the large decrease in space steps ($R = 90\%$).

For the relatively low concentrations of the mediator ($m_0 = 10^{-6}$M) and relatively high concentrations of the substrate ($s_0 = 0.1$M) (when $\Sigma \gg 1$, Fig. 3.2), the variable space step predetermines lower amount of computational points (3.8). To achieve the same accuracy with a constant space step, at
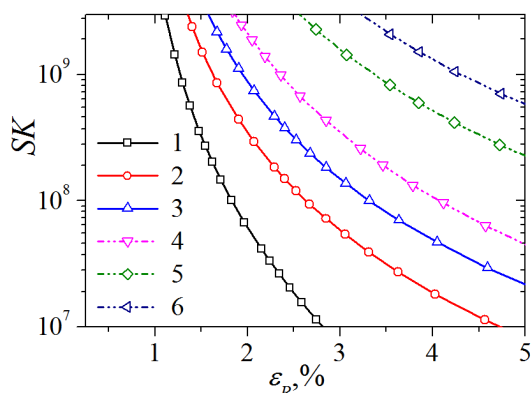
Figure 3.2. The dependency of the total points count SK on the desired accuracy ε_R, when $\Sigma \gg 1$. Values of e_0 and R are the same as in Fig. 3.1.

least 10 times increased SK is needed, therefore the use of the variable time step assures more efficient computational modelling when $\Sigma \gg 1$. For the highest analysed values of $R = 90\%$ (curves 1 and 4) an impact of enzyme concentration can be noted: for the lower concentrations lesser amount of the computational points is needed.
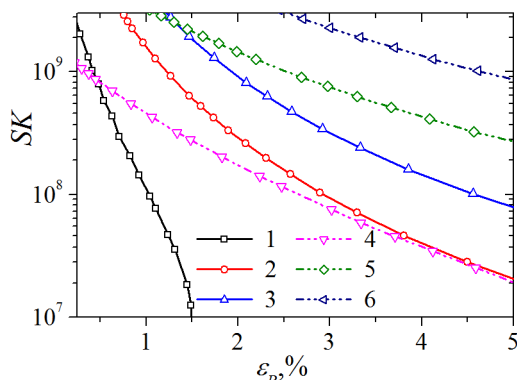

Figure 3.3. The dependency of the total points count SK on the desired accuracy ε_R, when $\Sigma = 1$. Values of e_0 and R are the same as in Fig. 3.1.

When $\Sigma = 1$ the values of the substrate and mediator concentration were $s_0 = 10^{-3}$ M, $m_0 = 10^{-6}$ M (Fig. 3.3). One can see, that the variable space step assures more efficient calculations as in (Fig. 3.2). The steady-state response calculated with a constant space step (calculated at $N_{const} = 1000$) was considered to be accurate when evaluating the error. A direct influence of the enzyme concentration also can be noted, the same as for the second case ($\Sigma \gg 1$). However, when $\Sigma = 1$, the speed-up provided by the variable step calculations is approximately 10 for the most values of ε_R.

The following mathematical model parameters were used as input pa-

rameters in developed software tool:

$$D_s^{(l)}, D_m^{(l)}, D_p^{(l)}, d_l, \quad l = 1, 2, 3,$$
$$k_{-1}, k_1, k_2, k_3, m_0, s_0. \tag{3.10}$$

3.2. Biosensor utilizing parallel substrates conversion

3.2.1. Analytical solution

The analytical solutions of the mathematical model of biosensor utilizing parallel substrates conversion (see Section 2.2.2) exist when the second reaction term r_2 in equation (2.29c) becomes linear, e.g.:

1. When $s_{20} = 0$, then non-linear reaction term r_2 (2.29c) is equal to zero and the concentration of the first reaction product at the electrode surface $(x = a_0)$ can be calculated analytically, as the system approaches a steady-state at $t \to \infty$,

$$p_1^{(1)} = s_{10} \times \frac{D_{s_1}^{(1)}}{2D_{p_1}^{(1)}} \times$$
$$\frac{\sigma_1 \sinh(\sigma_1)(d_2/d_1)(D_{p_1}^{(1)}/D_{p_1}^{(2)}) + \cosh(\sigma_1) - 1}{\sigma_1 \sinh(\sigma_1)(d_2/d_1)(D_{s_1}^{(1)}/D_{s_1}^{(2)}) + \cosh(\sigma_1)}. \tag{3.11}$$

2. When $k_{21}s_{10} \ll k_{22}s_{20}$, then $r_2 = k_{21}e_1 s_1^{(1)}$ and the solution is obtained by the following formula:

$$p_1^{(1)} = s_{10} \times \frac{D_{s_1}^{(1)}}{2D_{p_1}^{(1)}} \times \frac{k_1 e_1}{k_1 e_1 + k_{21}e_2} \times$$
$$\frac{\sigma_1 \sinh(\sigma_1)(d_2/d_1)(D_{p_1}^{(1)}/D_{p_1}^{(2)}) + \cosh(\sigma_1) - 1}{\sigma_1 \sinh(\sigma_1)(d_2/d_1)(D_{s_1}^{(1)}/D_{s_1}^{(2)}) + \cosh(\sigma_1)}, \tag{3.12}$$

   additionally, when $k_1 e_1 \gg k_{21}e_2$ the solution (3.12) becomes the same as (3.11).

3. When $k_{21}s_{10} \gg k_{22}s_{20}$ and $k_1 e_1 s_{10} \gg k_{21}e_2 s_{20}$, the solution is again obtained by (3.11).

3.2.2. Numerical solution

Mathematical model of the biosensor utilizing parallel substrates conversion (defined in Section 2.2.2) was solved in the similar numerical manner as described in previous Section. A uniform in space and time dimensions mesh was used when constructing a computational scheme. Explicit and Crank-Nicolson methods were used for the calculations, with their processing being described in the following Section.

The following mathematical model parameters were used as input parameters in developed software tool:

$$
\begin{aligned}
&k_1, k_{21}, k_{22}, e_{10}, e_{20}, s_{10}, s_{20}, \\
&D_c^{(l)}, d_l, \quad l = 1, 2, 3, \\
&K_c^{(1),(2)}, K_c^{(2),(3)}, \quad c = s_1, s_2, p_1, p_2.
\end{aligned}
\tag{3.13}
$$

3.3. Single calculation processing

For each single calculation a set of parameter values must be provided. Since the simulation process might take place in various environments, including remote ones (e.g. computational grid), a software tool implementing computational models was built to work in a command-line interface, with parameter values being provided through the input file. The provided input parameters might be divided by their origin into three following groups:

1. *Parameters of the mathematical model.* Parameters defined in (3.10) are used for model of biosensor with chemically modified electrode and in (3.13) - for the model of biosensor utilizing parallel substrates conversion.

2. *Parameters of the computational model.* These are: space step sizes N_l of l layers, the accuracy of calculations ε_R defined in (1.31), parameter-flag, showing if the merger of two diffusive-only layers is needed and decrease of space step count R defined in (3.4) for the variable space step calculations.

3. *Simulation parameters.* These parameters are used to define the behaviour of the software tool, including: time intervals defining how often to write currents and concentrations to the output, simulation number, simulation accuracy (for the early calculations, defined in Fig.

3.5), etc.

Computational results are written to output file, with output parameters being divided in the similar manner, except the computational model parameters:

1. *Governing parameters of the mathematical model.* These parameters include half-time of the response, the response itself, sensitivity, half maximal effective concentration, etc.

2. *Simulation parameters.* Two parameters are used as simulation result: simulation number, used to match input parameter values with output parameter values, and parameter-flag, determining weather the simulation was successful.

The computational model is solved according to the UML activity diagram scheme presented in Fig. 3.4.
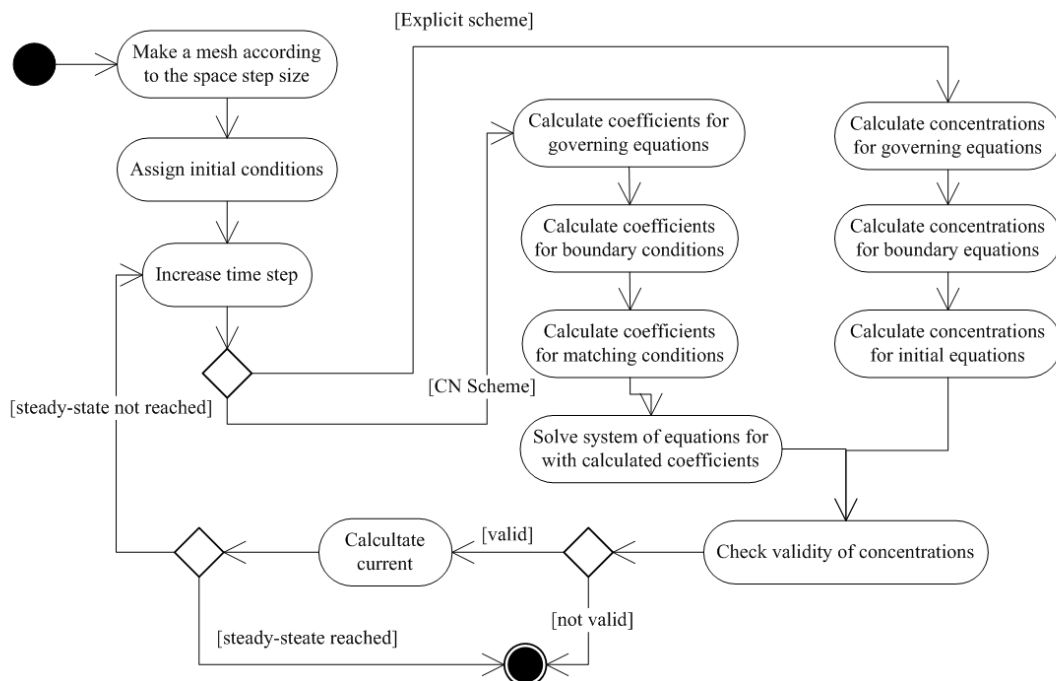

Figure 3.4. Solving of the computational model.

The solution starts by applying initial conditions at time moment $t = 0$. Mesh points at the time row $j = 0$ are calculated according to the discretized initial conditions of the mathematical model. Time step is increased, and new row of the concentration values is calculated according to the approximated governing, boundary and matching conditions. In case of the explicit finite difference scheme, new values are calculated explicitly, while for Crank-Nicolson method the coefficients for tridiagonal matrix algorithm are

calculated on the first step (forward sweep) and the solution of concentrations is later solved by back substitution. When the concentrations for all the compounds at all mesh points of the new time step are calculated, validation of the concentrations is executed. For the analysed mathematical models, validation of concentrations is carried out by checking if the concentrations do not contain any sudden spikes in the inner sections of the layer. Additionally, the transient mathematical model of biosensor with chemically modified electrode, was validated by ensuring the following restriction:

$$\forall x \in [a_{l-1}, a_l], l = 1, 2, 3, t \in [0, M] :$$
$$e_{red}^{(l)}(x,t) + e_{ox}^{(l)}(x,t) + p_s^{(l)}(x,t) = e_0. \tag{3.14}$$

This additional check of the concentrations might not seem necessary because of the stability condition (1.30). However, the stability condition is not sufficient enough, as it is accurate only for the diffusion equation. If the validation of concentrations does not fail (as it is a mandatory requirement), the calculations are continued. If the newly calculated current does not satisfy condition (1.31), the time step is increased again repeatedly, while the condition (1.31) is satisfied.

When computationally analysing newly developed mathematical model, large sets of input parameter values are varied. In the beginning of the investigations, more often than not, no high accuracy is needed. In that case, calculations are carried out as displayed in Fig. 3.5. Term "ac-
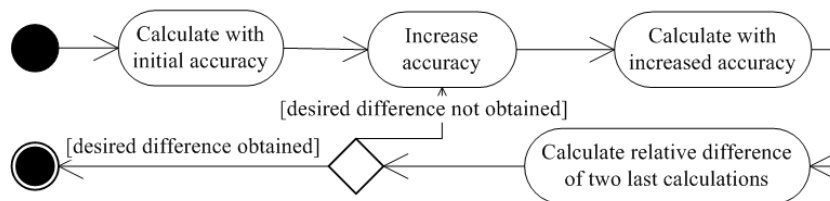

Figure 3.5. Simulation process in the beginning of investigations.

curacy" here is used to describe the group of ε (described in (1.31)) and N_l (the space step count for numerical approximation) values. This approach is not reasonable for final and accurate results (and therefore, it was not used for any of the figures displaying biosensor behaviour), however, it was highly useful when determining dependencies in general sense. Sometimes accurate calculation (e.g. with relatively small ε and relatively large space step counts N_l) is not needed, as the solution obtained with less accurate calculations does not change by increasing the accuracy. After calculating two

solutions of the computational model, the relative difference between them is analysed. If relative difference is less than desired, than ε is decreased and group of N_l is increased correspondingly. After the third solution is calculated, the same relative difference is checked for desired accuracy. This process is repeated until desired accuracy of the results is obtained.

The scheme presented in Fig. 3.5 was especially useful when calculating dimensionless sensitivity (2.44) displayed in Figs. 4.10b and 4.12b, as the relative sensitivities of $B_{rs} = 1$ and $B_{rs} = 0$ are calculated at relatively low calculation accuracy, and does not change upon increasing it.

3.4. Using computational grids to model the behaviour of the biosensors

A parameter sweep approach was used to model the behaviour of the biosensor by using computational grids. The developed technique is presented in Section 3.4.2. Efficiency of *BalticGrid* computational grid usage is presented in Section 3.4.3. The results presented in this section were published in [A1].

3.4.1. Parameter sweep approach

Computer modelling software has to meet specific requirements in order to ensure the efficient and convenient usage of grid computing. The most important requirements for passing parameters and the environment of software are the following ones:

- Data input and output. The ability to change model's parameters without changing model itself is crucial. The most efficient way to assure this requirement is to develop the software which would read modelling data from a file defined in models parameters. Data input and output must be independent of the operating system.

- Operation of the software. Computer models have to operate in command line mode as in the computational grids they are executed automatically. Occurring mistakes should be logged to the error log file because it is the only way to assure that no information is lost during the process.

The parameter sweep approach, described in Section 1.4.2 was applied for the investigation of the biosensors behaviour, since computer models designed to investigate the peculiarities of biosensors are parametrized as well.

To perform the parametrized simulation in the computational grid a group G of total N_G tasks is submitted to the grid:

$$G = \{M, PS_i\}, \qquad (3.15)$$

where G stands for a group of tasks, M is the software implementing computational model, PS_i is the smaller parameter sweep, $i = 1, 2, ..., N_G$. Each of these smaller parameter sweeps consist of parameter queues with parameters p_1, p_2,..., p_N in each queue.

Utilization of grid computing to solve the parametrized tasks can be defined by the following steps:

- The rules to form parameter sweep are defined. The parameter sweep can be enumerated by hands, generated using progression or both ways can be used at the same time. In such case, a part of the parameter queues are generated and part of them are enumerated manually.

- The main parameter sweep is prepared according to the defined rules.

- Produced parameter sweep is divided into N_G amount of smaller sweeps. It is recommended to seek that smaller sweeps would be similar in size.

- The group of tasks (3.15) is submitted to the computational grid.

- The results are retrieved after the simulation is finished.

3.4.2. Computational grid usage scheme

It is commonly required that some parameter values would be enumerated, some to be generated and some to remain constant in all parameter queues. In order to meet this requirement, a method for the parameter sweep generation was developed. Directions for the generation of parame-

ters are provided in the parameter description file in the following syntax:

$$
\left.
\begin{aligned}
&M_{PQ} \\
&Type; Guidelines; \\
&... \\
&Type; Guidelines;
\end{aligned}
\right\} N_P,
\tag{3.16}
$$

where M_{PQ} stands for the number of the desired parameter queues in the main parameter sweep (which also equals to the total number of simulations), N_P is the total number of parameters, $Type$ defines the type of parameter generation and $Guidelines$ define an additional information needed for the current parameter. Values allowed for $Type$ and $Guidelines$ are defined in Table 3.1.

Table 3.1. Parameter values defined in the description file.

$Type$	$Type$ description	$Guidelines$	$Guidelines$ description
0	Parameter is not changed during the simulations.	$ConcreteValue$;	A single value with semicolon at the end.
1	Parameter is changed by enumerating its values.	$ListOfValues$;	The enumerated list of parameter values separated by semicolons. If $ListOfValues$ count is less than M_{PQ}, then the last value of the given list is used for the remaining parameter queues, if $ListOfValues$ count is more than M_{PQ}, then the remaining values are ignored.
2	Parameter is generated using arithmetic progression.	$StartingValue$; $EndValue$;	$StartingValue$ stands for the first value in desired interval of parameter's values; $EndValue$ is the final value (number M_{PQ}) in mentioned interval.
3	Parameter is generated using geometric progression.	$StartingValue$; $EndValue$;	$StartingValue$ stands for the first value in desired interval of parameter's values; $EndValue$ is the final value (number M_{PQ}) in mentioned interval.

A computer program was developed to generate the main parameter

sweep using parameter description file. Entire scheme of computational grid usage was implemented as follows:

- The main parameter sweep is generated using the above mentioned syntax.

- The main parameter sweep of M_{PQ} parameter queues is divided into N_G smaller parameter sweeps. An average amount of parameter queues in the smaller parameter sweep is found:

$$N_{avg} = M_{PQ}/N_G. \tag{3.17}$$

Let $N_{avg,int}$ be the integer part of the average N_{avg}. Then a total number of A parameter sweeps will have $N_{avg,int}$ parameter queues. A total number of B parameter sweeps will have $N_{avg,int} + 1$ parameter queues. A and B stands for integer numbers satisfying the following equation:

$$M_{PQ} = AN_{avg,int} + B(N_{avg,int} + 1). \tag{3.18}$$

In accordance with the equation (3.18) it is assured that every smaller parameter sweep would be similar in the size.

- The group of N_G tasks (3.15) is submitted to the computational grid.

- The modelling software writes results to the output file independently in its own computing node.

- The output files from different computing nodes are collected and joined after the separate modelling tasks are completed.

3.4.3. Efficiency of computational grid usage

The recommendations for an efficient and convenient usage of the grid computing were developed and presented in [A1]. By applying the developed technique to model chemically modified biosensors, the computing time required to complete specific simulation locally was compared with the time consumed in the *BalticGrid*. Local simulations were carried out on a computer with the processor of 2 GHz speed and a memory of 1 GB of RAM. The acceleration R of the simulations in the computational grid is described as follows:

$$R = (M_{PQ}T_S - T)/T \times 100\%, \tag{3.19}$$

where T_S stands for duration of simulation with a single parameter queue in local computer, T is the duration of the calculations with all parameter queues in the computational grid. T was measured as time between submission of groups of tasks G and the receiving of the results.

Comparisons were carried out by changing the amount of total tasks N_G submitted to the grid between 2 and 15 as well as with different durations $M_{PQ} \times T_S = 30, 40, 60, 120, 240$ and 480 minutes. Accelerations R dependency on N_G is displayed in Fig. 3.6a.

The efficiency of simulations in the computational grid was measured by submitting the same tasks and by calculating the average durations. In some cases, values of T were much larger than the calculated average and it caused some non-monotonicity as it is seen in the Fig. 3.6a. This can be attributed to the constantly changing load of the grid environment.
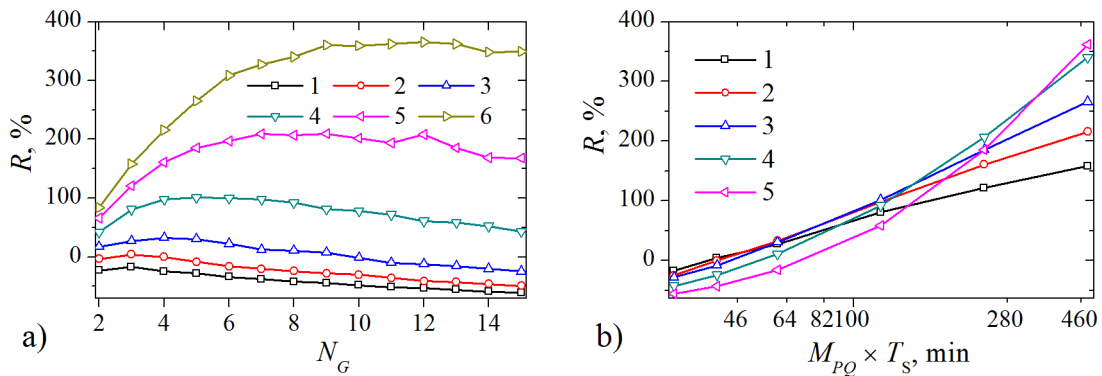

Figure 3.6. Acceleration R dependence on total count of tasks N_G (a) and on calculations durations on local computer $M_{PQ} \times T_S$ (b). For (a) six values of calculations durations on local computer were used: $M_{PQ} \times T_S = 30$ (1), 40 (2), 60 (3), 120 (4), 240 (5) and 480 (6) min. For (b) five total count of tasks N_G were used: 3 (1), 4 (2), 5 (3), 8 (4) and 13 (5).

As one can see in Fig. 3.6a, the efficiency of the developed technique of computational grid usage depends on the volume of the task. The smallest task efficiently solved in *BalticGrid* was with a duration of $M_{PQ} \times T_S = 40$ minutes. Calculations were faster than in the local computer but the task was divided into three parts and three remote computers were used instead of one local computer. By dividing the same task into more parts calculations were even slower than in the local computer because the time required to assign concrete task to its node increases more that decreases the time of calculations. The task in local computer solved in 120 minutes was efficiently solved in *BalticGrid* environment with all analysed total count of tasks N_G. The task of 480 minutes was also solved efficiently with all

analysed total number N_G of tasks, but the most efficiently when N_G is between 9 and 13 (curve 6, Fig. 3.6a).

Fig. 3.6b shows that the larger is the task $M_{PQ} \times T_S$ the larger becomes optimal count of tasks submitted to the grid N_G. 60 minutes duration task was solved most efficiently when N_G is 3, 4 and 5. Larger, 8 hours task, was solved most efficiently when N_G is 13. Accelerations differ slightly for the tasks with durations between 1 and 4 hours, when N_G is between 3 and 8 (curves 1–4, Fig. 3.6b).

Relatively small division size N_G and acceleration R can be attributed to the fact that resource broker used in *BalticGrid* environment is centralized. The centralized resource brokers can cause a noticeable delay. It was noticed during the studies that the delay is caused mainly by two reasons:

- The time required for middleware to assign concrete task to its computational node. This delay remains roughly constant during the experiments and is caused by the configuration of the computational grid and the middleware itself.

- Random time when one or more computational tasks are finished later than the others. This delay depends on the load of the computational grid and the difference in capacities of computational nodes.

3.5. Summary

The efficiency of the finite difference scheme with the variable space step usage was investigated depending on the biosensor with chemically modified electrode parameters. The variable space step can be used in most cases, however the restrictions are dependant on the biosensor parameters.

The scheme presented for the early investigation process of the mathematical models of biosensors was effectively used when determining main tendencies of the biosensor dynamics. Parameter sweep calculations presented in this Chapter were successfully applied to investigate the behaviour of both biosensors.

Chapter 4

Investigation of the biosensor peculiarities

By using developed software the peculiarities of the biosensors utilizing intermediate substances are investigated in this chapter:

1. Biosensor with chemically modified electrode.

2. Biosensor utilizing parallel substrates conversion.

The dependencies of the biosensor characteristics, including the sensitivity (1.20) and the half maximal effective concentration (1.24) on the various parameters presented in Sections 1.2.3, 2.1.4 and 2.2.4 are analysed in this Chapter. Possible modifications of the presented mathematical models are explored and analysed. The presented results can be applied for the creation of the new biosensors as well as for the optimization of the existing ones.

4.1. Peculiarities of the biosensor with chemically modified electrode

A transient mathematical model (see Section 2.1.2) and the mathematical model with quasi-steady-state assumption (defined in Section 2.1.3) of the biosensor with chemically modified electrode are analysed in this section digitally. The results presented in this section are presented in two articles [A1, A2]. The results of digital simulation are compared to the known analytical solutions as well as to the pre-existing research results. A possibility to use the effective diffusion coefficient to simplify the mathematical

model is investigated. Accuracy of the quasi-steady-state approximation is analysed and proved digitally to be accurate in most cases.

4.1.1. Digital simulation

A software implementing the computational scheme described in Section 3.1.2 was developed. By using a total number of $N = 900$ space points in the majority of the calculations and $\varepsilon = 10^{-3}$ (as defined in (1.31) equation) the behaviour of the biosensor with chemically modified electrode was investigated digitally.

Digital simulation was carried out by implementing the schemes defined in Section 3.3 to compare both models as well as to investigate the dependency of half maximal effective concentration on the mediator concentration. A computational grid was used by applying parameter sweep approach described in Section 3.4.2.

4.1.1.1. Parameters used for simulation

The sizes of the substrate, mediator and product molecules are considered to be in similar sizes. Therefore the diffusion coefficients are considered equal in the respective layers, in order to decrease the large number of the parameters,

$$D_c^{(l)} = D^{(l)}, \quad c = s, m, p, \quad l = 1, 2, 3. \tag{4.1}$$

The values of the parameters used in the digital investigation process are provided in Table 4.1.

4.1.1.2. Model validation

The accuracy of the two-layered mathematical model with quasi-steady-state assumption (defined in Section 2.1.3) was compared with two analytical solutions for known parameter values. When the dimensionless ratio Σ, defined in (2.13) is relatively small ($\Sigma \ll 1$), the steady-state response is calculated as defined in (3.1) for a two-layered mathematical model. By changing the values of layer thicknesses d_1 and d_2 between 10^{-6} and 10^{-3}m, and keeping the concentrations $m_0 = 10^{-4}$M, $s_0 = 10^{-5}$M and $e_0 = 1^{-6}$M, while other parameter values the same as in Table 4.1, the

Table 4.1. Model parameter values.

Description	Notation	Value	Dimension
Diffusion coefficient in the enzyme layer	$D^{(1)}$	3.4×10^{-10}	$\mathrm{m^2s^{-1}}$
Diffusion coefficient in the dialysis membrane	$D^{(2)}$	4.4×10^{-11}	$\mathrm{m^2s^{-1}}$
Diffusion coefficient in the diffusion layer	$D^{(3)}$	6.3×10^{-10}	$\mathrm{m^2s^{-1}}$
Reaction rate of E_{ox} reduction	k_{-1}	1.0×10^4	$\mathrm{s^{-1}}$
Reaction rate of E_{ox} oxidation	k_1	1.1×10^5	$\mathrm{M^{-1}s^{-1}}$
Reaction rate of ES conversion	k_2	1.0×10^3	$\mathrm{s^{-1}}$
Reaction rate of the enzyme interaction with the mediator	k_3	1.0×10^7	$\mathrm{M^{-1}s^{-1}}$
Number of electrodes	n_e	1	-
Enzyme concentration	e_0	1.0×10^{-6}	M

largest relative difference between analytical and simulated responses was less than 2%.

When $\Sigma \gg 1$, the steady-state current is calculated by (3.2) for the single layered biosensor. By keeping the thickness of the enzymatic layer relativelly large ($d_1 = 10^{-3}$) and the values of concentrations constant at $m_0 = 10^{-6}$M, $s_0 = 1$M and $e_0 = 1^{-6}$M, while lowering the thickness of diffusion layer, the relative difference lowers to zero.

Additionally, the transient mathematical model was validated computationally by ensuring that the sum of all enzyme concentrations would be equal at all time moments as defined in (3.14).

4.1.1.3. Biosensor response

The dependency of the biosensor response on time was investigated at five different values of the dimensionless rate (2.13), $\Sigma = 10^{-4}$, 10^{-2}, 1, 10^2, 10^4. The responses of the two-layered (2L) and three-layered (3L) mathematical models are displayed in the Fig. 4.1.

Values of Σ were calculated by changing mediator and substrate concentrations in the bulk solution: $s_0 = 10^{-4}$, 10^{-3}, 10^{-2}, 10^{-1}, 1M and $m_0 = 10^{-7}$, 10^{-6}, 10^{-5}, 10^{-4}, 10^{-3}M. The thickness of the enzyme and diffusion layers were $d_1 = d_3 = 10^{-4}$m, dialysis membrane thickness was $d_2 = 5 \times 10^{-5}$m, other values were kept as in Table 4.1.

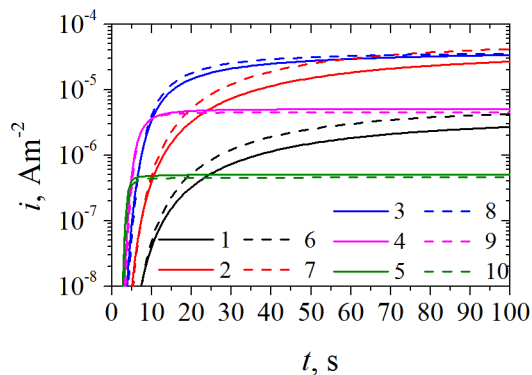As one can see from Fig. 4.1, the higher values of Σ correspond to the

Figure 4.1. The dependency of the biosensor response on time at five different values of $\Sigma = 10^{-4}$ (1, 6), 10^{-2} (2, 7), 1 (3, 8), 10^2 (4, 9) and 10^4 (5, 10). Solid lines (1-5) show the dependence calculated for 3L model and the dashed ones (6-10) shows the results for the 2L model.

shorter times when steady-state is achieved. The smallest and the largest analysed values of Σ represent the smallest overall responses, as the largest response is reached when $\Sigma \approx 1$. The difference between the responses of 3L and 2L models is larger when $\Sigma < 1$, compared to those when $\Sigma > 1$. For the smallest analysed value of $\Sigma = 10^{-4}$ the difference between the steady-state responses of 3L and 2L models was the largest and calculated to be approximately 20%.

4.1.2. Results and discussion

4.1.2.1. The application of effective diffusion coefficient

To further investigate the possibility of the two layers merger by applying the effective diffusion coefficient approach (see Section 1.1.2.3), the normalized concentration profiles were analysed. The impact of the dimensionless rate Σ on the steady-state response and the accuracy of the simplified 2L model response were evaluated.

The concentrations were normalized as follows:

$$s_N = s/s_0, \quad m_N = m/m_0, \quad p_N = p/s_0. \tag{4.2}$$

The simulation results of the normalized concentration profiles are displayed in Fig. 4.2. The thickness of the enzymatic layer was $d_1 = 10^{-4}$m, the thicknesses of the outer layers were equal, at $d_2 = d_3 = 5 \times 10^{-5}$m. The substrate concentration in the bulk solution was $s_0 = 10^{-5}$M, the mediator

70

concentration was $m_0 = 10^{-4}$M, other parameter values as in Table 4.1.
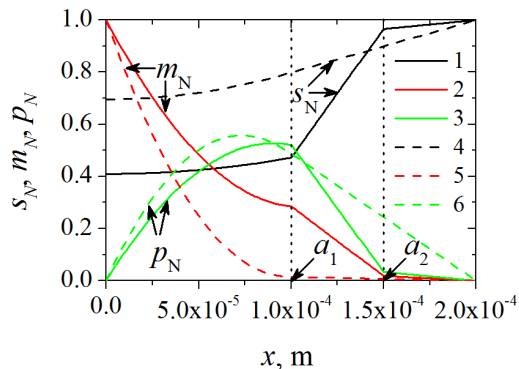

Figure 4.2. The profiles of the normalized substrate (1, 3), mediator (2, 5) and product (3, 6) concentrations for three-layered (1-3) and two-layered (4-6) models.

As it is seen from Fig. 4.2, two-layered approximation has the biggest impact on the substrate concentration (curves 1 and 4), where a difference of approximately 40% is noticeable at the boundary of $x = a_1 = 10^{-4}$m. The difference between mediator concentrations at the same coordinate is approximately 30%. The difference between normalized profiles of the product concentration is mostly noticeable at the boundary of $x = a_2 = 1.5 \times 10^{-4}$m. However this difference does not significantly affect the accuracy of 2L model in the enzyme layer ($a_0 < x < a_1$), as the concentrations in this layer do not differ more than 10% at any point in space (curves 3 and 6). The concentration profiles of the product are the most important, since the product is directly included in the response equation. The impact of the dialysis membrane relative thickness v (defined in (1.12)) on the 2L approximation was less than 1% at all analysed parameter values, therefore it is not presented. A relative error of less than 10% is considered accurate enough when analysing dependencies of the various biosensors [33, 67].

The impact of the dimensionless concentration rate (2.13) is crucial when designing new biosensors and improving existing ones. The dependency of the biosensor steady-state response on the rate Σ is displayed in Fig. 4.3a with a calculations carried out using 3L model. The relative error (1.23) of the calculations carried out using 2L model, compared to those carried out in 3L model is displayed in Fig. 4.3b.

By changing the concentration s_0 of substrate S in the bulk solution between 10^{-4}M and 1M and mediator concentration m_0 between 10^{-7}M and 10^{-3}M, the rate Σ changes in nine orders of magnitude. The simulation was

carried out at four different values of the dimensionless diffusion module $\sigma_1^2 = 10^{-4}$, 10^{-2}, 1 and 100. The values of the diffusion module were varied by changing enzyme concentration and enzymatic layer thickness.
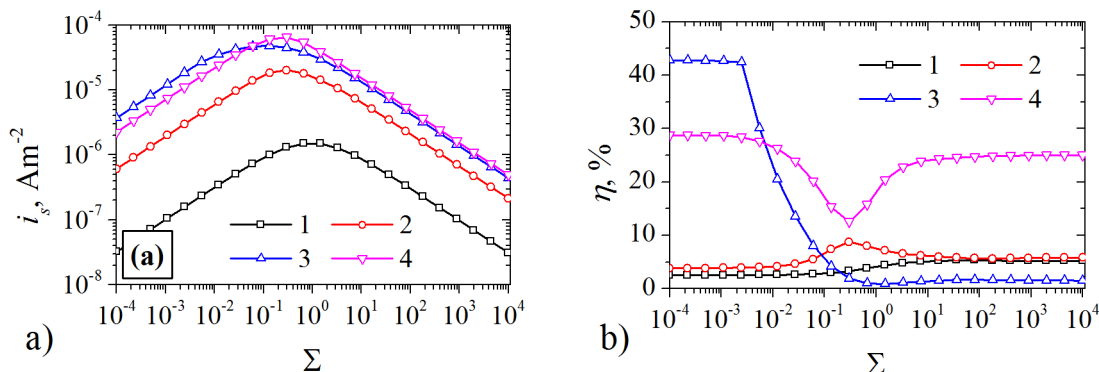

Figure 4.3. The steady-state response is versus the dimensionless concentration ratio Σ of 3L model calculations (a) and the relative error of 2L calculations (b) at four different values of the diffusion module $\sigma_1^2 = 10^{-4}$, 10^{-2}, 1 and 100. Other parameter values were as in Fig. 4.1 and Table 4.1.

As one can see from Fig. 4.3b, when the diffusion module is less than unity ($\sigma_1^2 < 1$), the relative error of 2L model approximation is less than 10% for all the analysed values of rate Σ (Fig. 4.3b, curves 1 and 2). For the lowest analysed diffusion module of $\sigma_1^2 = 10^{-4}$ the relative error is more than 10% for any value of Σ, with a noticeable breaking point at $\Sigma = 3 \times 10^{-1}$. A sudden change of 2L model approximation error appears because of the modulus in (1.23) equation. When $\sigma_1^2 = 10^{-2}$ and $\Sigma < 0.1$, the relative error is $\eta > 10\%$ (curve 3, Fig. 4.3b). However, the error considerably lowers when $\Sigma > 1$ and is less than 3%.

When $\Sigma < 1$, the steady-state current is approximately steadily increasing function of Σ (Fig. 4.3a) for all the analysed values of the diffusion modules – a result corresponding with the result discussed in [112] , Fig. 10. However, when $\Sigma > 1$, the steady-state response is decreasing function of Σ – the feature not noticeable in [112]. This could be attributed to the fact, than in [112], the values of Σ were varied by changing only the concentrations s_0, but keeping m_0 concentration constant.

There is also a noticeable difference in the absolute values of steady-state response in Fig. 4.3a and Fig. 10 in [112], as the lowest values in Fig. 4.3a are less than 10^{-7}Am^{-2} – more than 1000 times less than in the discussed paper. The way of varying diffusion module corresponds to such a large difference: in this research, values of the diffusion modulus σ_1^2 were

calculated by varying enzymatic layer thickness d_1 and the concentration e_0 of enzyme, while in [112] only the values of the thickness d_1 were varied. The relative thickness v (1.12) of the dialysis membrane affects the accuracy of 2L model calculations less than by 1%, therefore it is not presented in this paper.

4.1.2.2. Half maximal effective concentration

The influence of the mediator concentration on the half maximal effective concentration (described in Section 1.2.3) was investigated. A two-layered mathematical model (with diffusion and dialysis layers being merged) was used. Enzymatic membrane thickness was $d_1 = 10^{-4}$m, and the diffusion coefficient was $D^{(1)} = 3 \times 10^{-10}$ m^{2}s^{-1}. The merged layer was of the same thickness ($d_{23} = d_1$) with twice as big diffusion coefficient $D^{(23)}$ $= 2 \times D^{(1)}$. The calculations were carried out for four different enzymatic concentrations e_0: 10^{-8} (1), 10^{-7} (2), 10^{-6} M (3) and 10^{-5}M (4). Other parameters were the same as in Table 4.1. The results are displayed in Fig. 4.4.
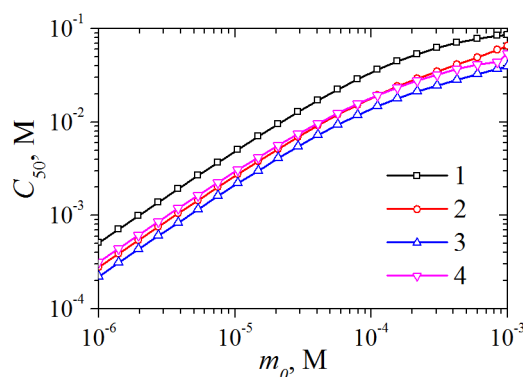

Figure 4.4. The dependency of the half maximal effective concentration C_{50} on the mediator concentration m_0 at different values of the enzymatic concentration: e_0: 10^{-8} (1), 10^{-7} (2), 10^{-6} (3) and 10^{-5}M (4).

A monotonic dependency of the half maximal effective concentration on the mediator concentration is noticeable in Fig. 4.4: the larger mediator concentration corresponds to the larger values of C_{50}. By changing the mediator concentration in three orders of magnitude, C_{50} increases 1000 times.

The influence of the enzymatic concentration is minimal, as the difference between C_{50} values for the smallest and the largest values of e_0 is less than 10 times, and remains constant for all analysed values of m_0.

73

The largest values of C_{50} are achieved at the largest mediator concentrations m_0 and the smallest enzymatic concentrations e_0. One can notice, that the dependency of half maximal effective concentration on the mediator concentration is influenced by diffusion modulus:

- when $\sigma_1^2 < 1$ (curves 1, 2 and 3), the values of C_{50} decreases while decreasing the values of σ_1^2, at the same m_0 concentration;

- when $\sigma_1^2 > 1$ (curve 4), the values of the half maximal effective concentration increases by increasing the diffusion modulus.

4.1.2.3. The accuracy of quasi-steady-state approximation

Two-layered mathematical model was used for the investigation of QSSA approximation, keeping the same parameter values as in previous section, except for mediator and substrate concentrations: $m_0 = 1 \times 10^{-5}$, $s_0 = 10^{-4}$m. The normalized steady-state current (1.22) versus the Biot number Bi was calculated at the following six values of the thickness d_1 of the enzyme layer: 17.3×10^{-5}, 24.4×10^{-5}, 34.6×10^{-5}, 48.9×10^{-5}, 69.2×10^{-5} and 97.9×10^{-5}m and six values of the enzyme concentration e_0 in the enzyme membrane: 10^{-8}, 5×10^{-8}, 2.5×10^{-7}, 1.25×10^{-6}, 6.25×10^{-6}, 3.125×10^{-5}M. At each value of d_1 as well as e_0 the Biot number Bi was changed from 0.1 up to 100. At these values of d_1 and e_0, keeping other parameters unchanged, the diffusion modules (σ_1^2 and σ_2^2) change in five orders of magnitude. Thus, the behaviour of the biosensor response was calculated at different limitations of the response.

One can see in Fig. 4.5a that the normalized steady-state biosensor current I_N (defined in Section 2.1.4) is a monotonous increasing function of the Biot number Bi when $\sigma_1^2 \geq 1$. I_N is non-monotonous when $\sigma_1^2 \leq 1$. The normalized steady-state current only slightly varies for different diffusion modules when $Bi > 10$.

The dependence of error (2.12) on the dimensionless Biot number Bi is shown in Fig. 4.5b. The responses were calculated by changing the values of d_1 and e_0 in the same way as in Fig. 4.5a. There can be seen an effect of the dimensionless Biot number Bi on the modeling error E_{QSSA}. The larger Biot number corresponds to the larger error of QSSA calculations. The error of the QSSA may be neglected with all the values of diffusion module except the case of small diffusion module for relatively large Biot number (curve 1). When $\sigma_1^2 = 10^{-4}$ and $Bi > 30$ the error of QSSA calculations is bigger
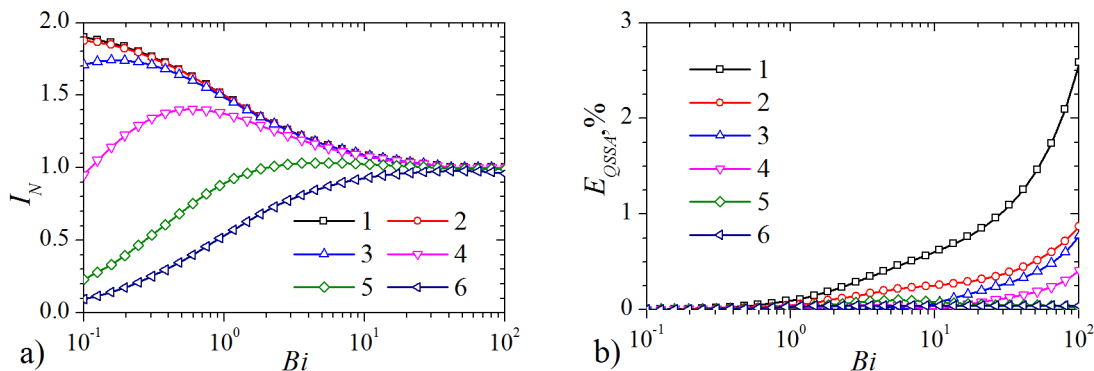
Figure 4.5. The normalized steady-state current I_N versus the Biot number Bi (a) and versus the error of the QSSA (b) at six values of the diffusion module σ_1^2: 10^{-4} (1), 10^{-3} (2), 10^{-2} (3), 0.1 (4), 1 (5) and 10 (6), $\sigma_2^2 = 1000\ \sigma_1^2$.

than 1% with even bigger E_{QSSA} for larger Biot numbers.

4.1.3. Efficiency of the used tool

The parameters affecting the error of the mathematical model based on QSSA were calculated using computational grid by applying the parameter sweep approach described in Section 3.4.2. The same problem with different sets of parameter-values was solved more than 1000 times by comparing two models in the computational grid. The analysis carried out in Section 4.1.2.3 was solved more than 10 times faster by using the computational grid than it would be solved on a local computer. The efficiency of the parameter sweep calculations on *BalticGrid* environment for lower simulation amounts was presented in Section 3.4.3.

4.2. Peculiarities of the biosensor with parallel substrates conversion

A mathematical model (see Section 2.2.2) of biosensor utilizing parallel substrates conversion is analysed in this section. The results of the digital simulation are compared to the known analytical solutions as well as to the experimental data [A7]. A possibility to use effective diffusion coefficient to simplify the mathematical model is investigated [A3]. Half maximal effective concentration is determined at various model parameter values [A5]. The

impact of the diffusion modulus [A8] and Biot number [A4] on the biosensor response and sensitivity is investigated.

4.2.1. Digital simulation

A software implementing the computational schemes described in Section 3.2.2 was developed and used to investigate the biosensor with parallel substrates conversion. A total number of $N = 900$ space points was used in majority of the calculations and $\varepsilon = 10^{-3}$ was used as defined in (1.31).

A software tool for automated calculations described in Chapter 3 was used to investigate the biosensor behaviour.

4.2.1.1. Parameters used for simulation

Constant parameter values used in validation and simulation processes are listed in Tables 4.2 and 4.3. The diffusion coefficients of the second product $(D_{p2}^{(1)}, D_{p2}^{(2)}, D_{p2}^{(3)})$ does not play any role in the investigated peculiarities, therefore the values of the first reaction product were used. The values of the reaction constants k_1 and k_{22} were obtained by physical experiments.

The value of heterogenic constant k_s was obtained in the experiments. Due the presence of oxygen in the solution at the initial state, a response of the biosensor is non-zero. In the experiments, the initial condition of oxygen was $p_1 = 2.5 \times 10^{-4}$M and it corresponded to the current of $i \approx 0.85 \mu$A By dividing these values heterogenic constant was obtained.

4.2.1.2. Model validation

Analytical solutions (3.11) and (3.12) are known only for the two-layered mathematical model. By keeping the diffusion coefficients of the dialysis and the diffusion layers equal for corresponding compounds and by considering the partition coefficients of all substances to be equal to unity, and by choosing the values of the substrate concentrations (s_{10} and s_{20}) as well as enzyme concentrations (e_1 and e_2) as defined in Table 4.3, so that the analytical solutions would exist, and keeping other parameters constant as listed in Table 4.2, and changing the remaining parameter values as displayed in Table 4.3, the relative difference between the analytical

Table 4.2. Constant values of the biosensor parameters.

Parameters	Notation	Value	Dimension	Ref.
Diffusion coefficient of S_1 in enzymatic membrane	$D_{s_1}^{(1)}$	3.1×10^{-10}	m^2s^{-1}	[57]
Diffusion coefficient of S_1 in dialysis membrane	$D_{s_1}^{(2)}$	9.8×10^{-11}	m^2s^{-1}	[181]
Diffusion coefficient of S_1 in diffusion layer	$D_{s_1}^{(3)}$	1.4×10^{-9}	m^2s^{-1}	[57]
Diffusion coefficient of S_2 in enzymatic membrane	$D_{s_1}^{(1)}$	3.4×10^{-10}	m^2s^{-1}	[182]
Diffusion coefficient of S_2 in dialysis membrane	$D_{s_1}^{(2)}$	4.4×10^{-11}	m^2s^{-1}	[181]
Diffusion coefficient of S_2 in diffusion layer	$D_{s_1}^{(3)}$	6.3×10^{-10}	m^2s^{-1}	[181]
Diffusion coefficient of P_1 in enzymatic membrane	$D_{p_1}^{(1)}$	1.4×10^{-9}	m^2s^{-1}	[183]
Diffusion coefficient of P_1 in dialysis membrane	$D_{p_1}^{(2)}$	1.43×10^{-11}	m^2s^{-1}	[184]
Diffusion coefficient of P_1 in diffusion layer	$D_{p_1}^{(3)}$	2.12×10^{-9}	m^2s^{-1}	[183]
Diffusion coefficient of P_2 in enzymatic membrane	$D_{p_2}^{(1)}$	1.4×10^{-9}	m^2s^{-1}	this work
Diffusion coefficient of P_2 in dialysis membrane	$D_{p_2}^{(2)}$	1.43×10^{-11}	m^2s^{-1}	this work
Diffusion coefficient of P_2 in diffusion layer	$D_{p_2}^{(3)}$	2.12×10^{-9}	m^2s^{-1}	this work
Heterogenic constant	k_s	3.4×10^{-3}	AM^{-1}	this work
e_1 reaction rate	k_1	1.3×10^6	$M^{-1}s^{-1}$	this work
e_2 reaction rate	k_{21}	7.1×10^6	$M^{-1}s^{-1}$	[185]
e_2 reaction rate	k_{22}	6.0×10^6	$M^{-1}s^{-1}$	this work

and computational steady-state current densities was less than 1% for the mathematical model defined in Section 2.2.2.

Additionally, the model was validated computationally by ensuring that at the steady-state the sum of all the concentrations would be equal to the sum of initial concentrations of both substrates in the bulk solution:

$$\forall x \in [a_{l-1}, a_l], l = 1, 2, 3, t \to \infty :$$
$$s_1^{(l)}(x,t) + s_2^{(l)}(x,t) + 2p_1^{(l)}(x,t) + 2p_2^{(l)}(x,t) = s_{10} + s_{20}. \quad (4.3)$$

Table 4.3. Variable values of the biosensor parameters.

Parameters	Notation	Interval	Dimension
First substrate concentration	s_{10}	$[10^{-4}, 10^{-2}]$	M
Second substrate concentration	s_{20}	$[10^{-6}, 10^{-1}]$	M
First enzyme concentration	e_1	$[3 \times 10^{-8}, 3 \times 10^{-5}]$	M
Second enzyme concentration	e_2	$[3 \times 10^{-8}, 3 \times 10^{-5}]$	M
Enzyme layer thickness	d_1	$[5 \times 10^{-6}, 5 \times 10^{-4}]$	m
Dialysis membrane thickness	d_2	$[1 \times 10^{-5}, 5 \times 10^{-5}]$	m
Diffusion layer thickness	d_3	$[5 \times 10^{-6}, 1.9 \times 10^{-4}]$	m

4.2.2.   Comparison with the experimental results

The addition of hydrogen peroxide increased the bioelectrode current that is associated with oxygen production (see Fig. 4.6). The increase of the current depends on the hydrogen peroxide concentration. The experimentally measured half-time of the steady-state current was 36.3s for all analysed hydrogen peroxide concentrations.
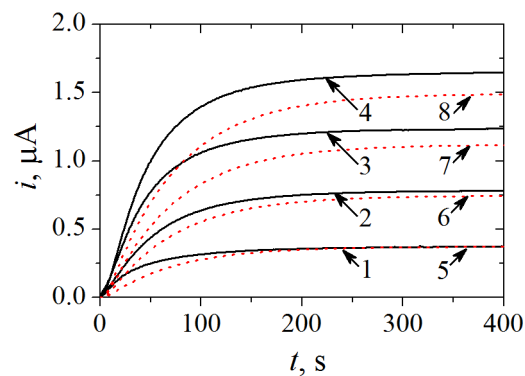
Figure 4.6. The dynamics of the biosensor response to the first substrate. Comparison of experimental data (curves 1-4) against the simulated results (curves 5–8). The concentration of s_{10} was 3.4 $\times 10^{-4}$ (curves 1 and 5), 6.8 $\times 10^{-4}$ (2, 6), 10^{-3} (3, 7) and 1.36 $\times 10^{-3}$ (4, 8)M. The concentrations of enzymes were $e_1 = e_2 = 3.2 \times 10^{-5}$M, the thickness of enzymatic membrane was $d_1 = 2.66 \times 10^{-4}$m.

The calculated steady-state response of the biosensor to hydrogen peroxide (of concentration s_{10}) was $i_s \approx 0.38 \mu$A for the smallest concentration of $s_{10} = 3.4 \times 10^{-4}$M (5 curve) and $i_s \approx 1.49 \mu$A for the largest concentration

of $s_{10} = 1.36 \times 10^{-3}$M (8 curve). The value of $i_s \approx 1.49\mu$A is just 11% less in comparison to the experimentally determined one (Fig. 4.6), while the difference for the lowest concentrations of the first substrate is even smaller and non-existing for the smallest one ($s_{10} = 3.4 \times 10^{-4}$M).

The simulation of the dynamics of the biosensor response gave a half-time value of 55s for all hydrogen peroxide concentrations. The calculated half-time is 53% higher in comparison to the experimentally determined. The increase of the half-time can be explained by the decrease of the bio-catalytical membrane thickness under dialysis membrane. The additional calculations showed that at the high concentrations of catalase and per-oxidase the decrease of the membrane thickness of 19% can decrease the half-time by almost 53%. It has been discovered, that by lowering the diffusion coefficient of the external diffusion layer (or, alternatively, by enlarging the thickness of this layer), a steady-state response can be manipulated in various ways [186]. The diffusion coefficients of hydrogen peroxide in all three layers were taken from different sources (see Table 4.2), so this might effect the difference noticeable in Fig. 4.6. Additionally, the impact of the diffusion layer peculiarities on the half-time of the steady-state response is known to be non-monotonous (see [186], Figs. 4 and 5).

The steady-state response is less sensitive to the membrane thickness, but the decrease of it will cause an almost proportional decrease of the steady-state response, if the biosensor is acting under internal diffusion lim-itation, as it was investigated in [A5] (Fig. 5, parts a and b).

The addition of S_2 decreased the steady-state response (Fig. 4.7). Four approximately equal portions of the second substrate were added to the so-lution at time moments of 585, 750, 945 and 1135s during the conducted experiment (represented by curve 1). The total concentration of the second substrate at the mentioned time moments was increased to $s_{20} = 4 \times 10^{-5}$, 8×10^{-5}, 1.19×10^{-4} and 1.57×10^{-4}M. The thickness of the enzymatic membrane was $d_1 = 2.66 \times 10^{-6}$m, the concentrations of catalase and per-oxidase were, correspondingly $e_1 = 3.18 \times 10^{-6}$M and $e_2 = 3.2 \times 10^{-6}$M. The concentration of hydrogen peroxide was $s_{10} = 6.6 \times 10^{-4}$M.

The digitally simulated response (curve 2, Fig. 4.7) was larger for all analysed time domain. The relative difference of 13% between the simulated and experimental steady-state responses to the hydrogen peroxide (S_1, $t <$ 600s) is noticeable. However, the difference of this magnitude can be ignored because of the error in the experiment, as the curves 1 and 2 in Fig. 4.7 are
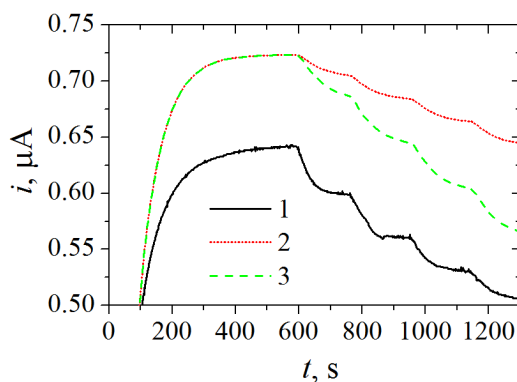
Figure 4.7. The dynamics of the biosensor response to both substrates. Solid curve (1) shows the experimental data, dotted curve (2) shows digital simulation without the partition approach, dashed curve (3) shows the results with partition coefficients $K_{s_1}^{(1),(2)} = 0.5$ and $K_{s_1}^{(1),(2)} = 4$. The concentration s_{10} was 6.6 $\times 10^{-4}$M, concentration s_{20} was increased for times by approximately 4×10^{-5}M. The concentrations of enzymes were $e_1 = e_2 = 3.2 \times 10^{-5}$M, the thickness of the enzymatic membrane was $d_1 = 2.66 \times 10^{-4}$m.

achieved at the same parameter values as curves 2 and 6 in Fig. 4.6, where the experimentally obtained response is higher than the computed one.

The other issue can be noted in Fig. 4.7: by increasing concentration of S_2 at four different time moments, the difference between the simulated and experimental data is increasing at each step.

The comparison of the experimental and simulation results revealed that the partition of compounds in the membranes should be considered during simulations of the biosensor action [A7]. The application of the partition coefficients $K_{s_2}^{(1),(2)} = 0.5$ and $K_{s_2}^{(2),(3)} = 4$, while keeping the partition coefficients of other compounds equal to unity at both boundaries is displayed by curve 3, Fig. 4.7.

The values of the partition coefficients $K_{s_2}^{(1),(2)} = 0.5$ and $K_{s_2}^{(2),(3)} = 4$ were chosen to have a best matching with the experimental result. The partition coefficient of acetaminophen in enzymatic layer ($K_{s_2}^{(1),(2)}$) is with slight accordance to [61], as in this article values of 0.85 and 0.9 are analysed. However, partition coefficient is unique for each analysed system, and physically accurate partition coefficient can be obtained only by physical experiments [187].

4.2.3. Results and discussion

4.2.3.1. Influence of partition coefficient

The influence of the partition coefficient was investigated extensively, by analysing its impact on the biosensors normalized concentration profiles, response and sensitivity. The calculations were carried out for the first operational phase of the biosensor, when only the first substrate was present in the solution. The concentrations of first substrate and first product were normalized as follows:

$$s_{1,N} = s_1/s_{10}, \quad p_{1,N} = p_1/s_{10}. \tag{4.4}$$

The partition coefficient $K_{s_1}^{(l),(l+1)}$ of the first substrate was investigated for both boundaries, while always keeping the partition coefficient of p_1 constant at $K_{p_1}^{(l),(l+1)} = 1$ $(l = 1, 2)$. The results displayed in Fig. 4.8 are for three different combinations of $K_{s_1}^{(l),(l+1)}$:

1. $K_{s_1}^{(1),(2)} = 1$ and $K_{s_1}^{(2),(3)} = 1$ (non-existing partitioning) (curves 1S and 1P in Fig. 4.8a and curve 1R in Fig. 4.8b).

2. $K_{s_1}^{(1),(2)} = 0.5$ and $K_{s_1}^{(2),(3)} = 4$ (increasing partitioning) (curves 2S and 2P in Fig. 4.8a and curve 2R in Fig. 4.8b).

3. $K_{s_1}^{(1),(2)} = 2$ and $K_{s_1}^{(2),(3)} = 2$ (constant partitioning) (curves 3S and 3P in Fig. 4.8a and curve 3R in Fig. 4.8b).
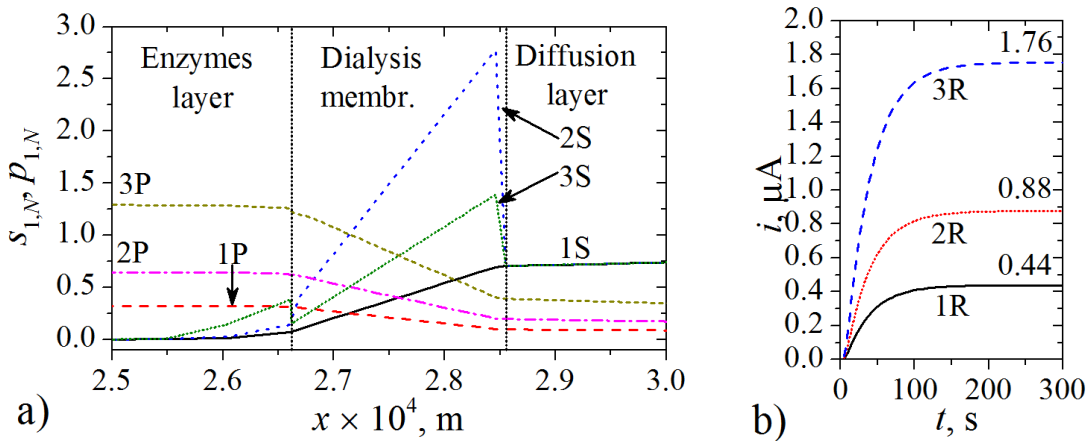

Figure 4.8. The normalized concentration profiles (a) and biosensor response (b) at three different combinations of first substrate partition coefficient.

As one can see from Fig. 4.8a, the partition coefficient of the first substrate affects not only s_1 concentrations, but p_1 as well. The constant partitioning configuration (curves 3S and 3P) has the largest impact on the biosensor response (curve 3R, Fig. 4.8b). The increase of the response, as well as the reaction product, is approximately proportional to the partition coefficient for S_1 in the enzymatic layer, as by enlarging the partition co-efficient from $K_{s_1}^{(1),(2)} = 1$ to $K_{s_1}^{(1),(2)} = 4$, the response increases from $i_s = 0.44$ to $i_s = 1.76$ (curves 1R and 3R, Fig. 4.8b).

To further investigate the impact of both partition coefficients, influ-ence of their ratio is analysed,

$$K_c = K_c^{(1),(2)}/K_c^{(2),(3)}, \quad c = s_1, s_2, p_1, p_2. \tag{4.5}$$

The impact of the dimensionless partition coefficient of the first sub-strate (K_{s_1}) on the steady-state response is displayed in Fig. 4.9. The investigation was carried out for two different concentrations of the first substrate (s_{10}: 3.4×10^{-4}M and 1.36×10^{-3}M) and two different concen-trations of the first enzyme (s_{10}: 3.2×10^{-8}M and 3.2×10^{-5}M), other parameter values were the same as in Table 4.2 and Fig. 4.6. By changing the partition coefficients $K_{s_1}^{(1),(2)}$ and $K_{s_1}^{(2),(3)}$ between 0.5 and 5, the dimen-sionless partition coefficient (4.5) changes in two orders of magnitude from 0.1 and 10.
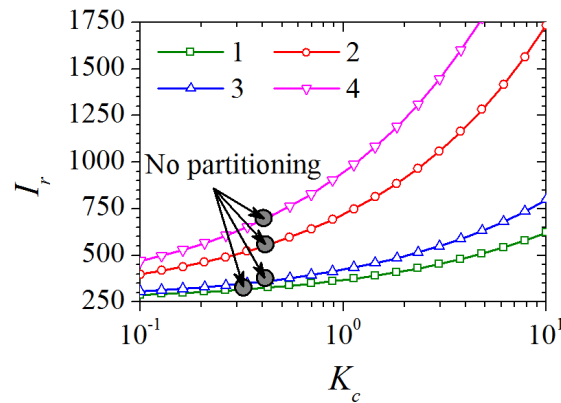

Figure 4.9. The impact of the dimensionless partition coefficient on the steady-state response of the first phase of the biosensor action at two differ-ent concentrations of the first substrate s_{10}: 3.4×10^{-4}M (curves 1 and 3) and 1.36×10^{-3}M (2, 4) and two different concentrations of the first enzyme e_1: 3.2×10^{-8}M (1, 2) and 3.2×10^{-5}M (3, 4).

The steady-state response is monotonically increasing non-linear function of dimensionless partition coefficient (4.5) for all the analysed parameter values (Fig. 4.9). The largest increase of approximately five times is achieved for the largest analysed concentrations of $e_1 = 3.2 \times 10^{-5}$M and $s_{10} = 1.36 \times 10^{-3}$M (curve 4), while the smallest of approximately two times is for the smallest concentrations.

The concentrations of the first substrate are more sensitive to the partition coefficient change, than the concentrations of the first enzyme. For the largest value of $K_{s_1} = 1$, the increase of e_1 by 1000 times leads to slight change (the pairs of curves 1 with 3, and 2 with 4). By changing the concentration of the first substrate 4 times, and keeping the enzymatic concentration constant, the increase is much more noticeable (the pairs of curves 1 with 2, and 3 with 4).

The dependency of the relative biosensor response (2.43) and relative sensitivity (2.44) on the second substrate concentration is displayed in Fig. 4.10. The calculations were carried out for three different dimensionless enzymatic concentrations (2.47). Modelling approach with a partition coefficient equal to unity ($K_{s_1}^{(1,2)} = K_{s_1}^{(2,3)} = 1$, curves 2, 4 and 6) was compared to the one, where partition coefficient is present ($K_{s_1}^{(1,2)} = 0.5$ $K_{s_1}^{(2,3)} = 2$, curves 1, 3 and 5). The concentration of the first substrate was $s_{10} = 1.36 \times 10^{-3}$M, while other parameter values were the same as in Table 4.2 and Fig. 4.6.
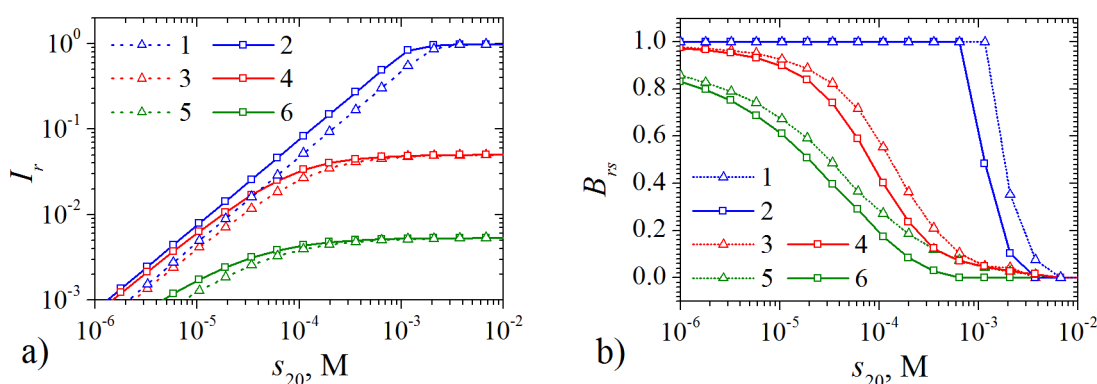

Figure 4.10. The relative response (a) and relative sensitivity (b) of the biosensor for three different values of $\xi_2 = 10^{-3}$ (curves 1 and 2), 10^{-2} (3 and 4), 10 (5 and 6) and with (1, 3 and 5) and without (2, 4 and 6) the partitioning of compounds approach.

As one can see in Fig. 4.10a, the values of the steady-state relative current I_r are less than 0.1 when $\xi_2 \leq 10^{-1}$ (curves 3–6). This applies to both

cases: with and without the partition approach applied. The steady-state biosensor response varies in several orders of magnitude for the opposite case (curves 1–2).

It is noticeable that the concentration s_{10} of the first substrate highly affects the calibration curves. When $s_{20} > s_{10}$, the steady-state response of the biosensor is practically independent from the concentration s_{20} of the second substrate, while for $s_{20} < s_{10}$ this dependence is approximately linear. The highest biosensor sensitivity B_{rs} is achieved at the smallest enzymatic ratio ξ_2 (curves 1 and 2, in Fig. 4.10b). The ratio between the substrates concentrations s_{10} and s_{20} is also very important for the biosensor sensitivity. In case of the relatively large concentrations of the second substrate ($s_{20} > s_{10}$), the biosensor sensitivity B_{rs} is relatively small for all the concentrations of both enzymes (Fig. 4.10b). In the opposite case (when $s_{20} < s_{10}$) the biosensor sensitivity increases with decreasing the ratio s_{20}/s_{10}.

For all the analysed values of ξ_2, the addition of the partition coefficient decreases the relative response (Fig. 4.10a), but increases the relative sensitivity (Fig. 4.10b). The impact of the partition coefficient on the relative response is more noticeable when $s_{20} < s_{10}$.

4.2.3.2.   The application of effective diffusion coefficient

The effective diffusion coefficient approach (see Section 1.1.2.3) was applied for external diffusion layers of the biosensor utilizing parallel substrates conversion. In the simulations, the concentrations of both enzymes were considered equal at $e_1 = e_2 = 10^{-5}$M, other parameter values were the same as in Table 4.2, except no partition coefficient was applied and in order of simplicity the diffusion coefficients for all the materials were considered equal in corresponding layers:

$$D_c^{(l)} = D^{(l)}, \quad c = s_1, s_2, p_1, p_2, \quad l = 1, 2, 3, \tag{4.6}$$

having $D^{(1)} = 3.1 \times 10^{-10}$ m^{2}s^{-1}, $D^{(2)} = 9.8 \times 10^{-11}$ m^{2}s^{-1} and $D^{(3)} = 1.4 \times 10^{-9}$ m^{2}s^{-1}.

The impact of the enzymatic layer thickness d_1 and the second substrate S$_2$ concentration s_{20} on the two-layered model accuracy and relative response is displayed in Fig. 4.11. The results presented in this Section were published in [A3].

In the calculations, the dimensionless reaction rate $\xi_2 = 1000$ was used, as it corresponded to the largest errors of two-layered model as investigated in [A3]. It was also determined, that the effective diffusion coefficient application on the dialysis and diffusion layers is possible whenever $\xi_2 < 10$.

The thicknesses of diffusion and dialysis layers were considered to be equal, at $d_2 = d_3 = 3 \times 10^{-5}$ m.
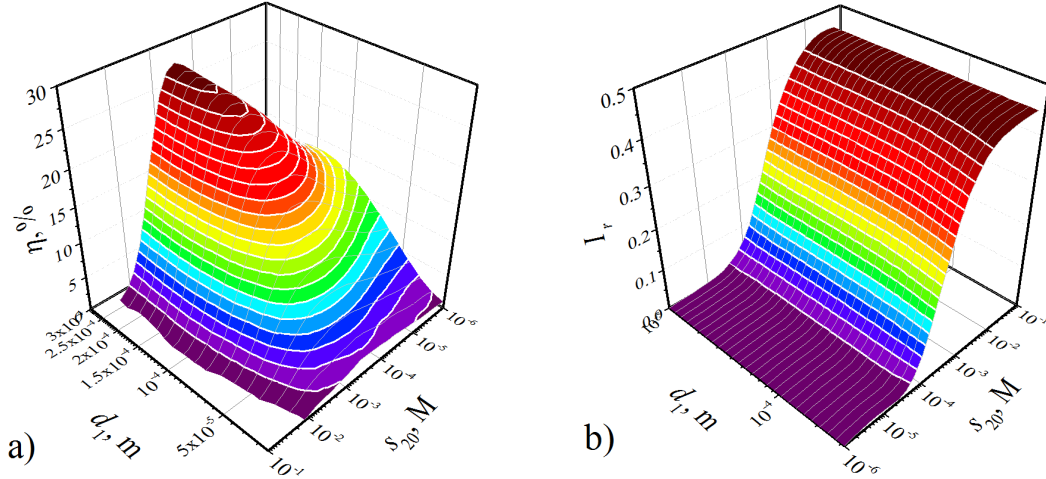

Figure 4.11. The dependency of the relative error of two-layered model calculations (a) as well as the relative response (b) on the enzymatic layer thickness d_1 and second substrate concentration s_{20}.

As one can see from Fig. 4.11a, the relative error is a non-monotonous function of the second substrate concentration, reaching the maximal values when $10^{-4}\text{M} < s_{20} < 10^{-3}\text{M}$ and $d_1 = 3 \times 10^{-4}\text{m}$. The maximal value of η = 27% is reached when the concentrations s_{20} of the second substrate are approximately equal to the first ones (s_{10}).

The relative response is the increasing function of the second substrate concentration, with the largest alteration in the above mentioned interval ($10^{-4}\text{M} < s_{20} < 10^{-3}\text{M}$, Fig. 4.11b).

4.2.3.3. Impact of the Biot number

Two-layered mathematical model was used to investigate the impact of the Biot number on the relative response and sensitivity [A4]. Fig. 4.12a shows the influence of the Biot number at eight concentrations (s_{20}) of the second substrate: 1×10^{-6}, 3.2×10^{-6}, 10^{-5}, 3.2×10^{-5}, 10^{-4}, 3.2×10^{-4}, 10^{-3} and 0.1M. The Biot number Bi was varied by changing the thickness

d_{23} of the merged diffusion layer between 2×10^{-6}m and 2×10^{-3}m. The concentration of catalase was kept constant at $e_1 = 10 \times 10^{-9}M$. The magnitude of Bi is directly proportional to the intensity of solution stirring as described in Section 1.2.3: the greater values correspond to more intensive stirring and vice versa.
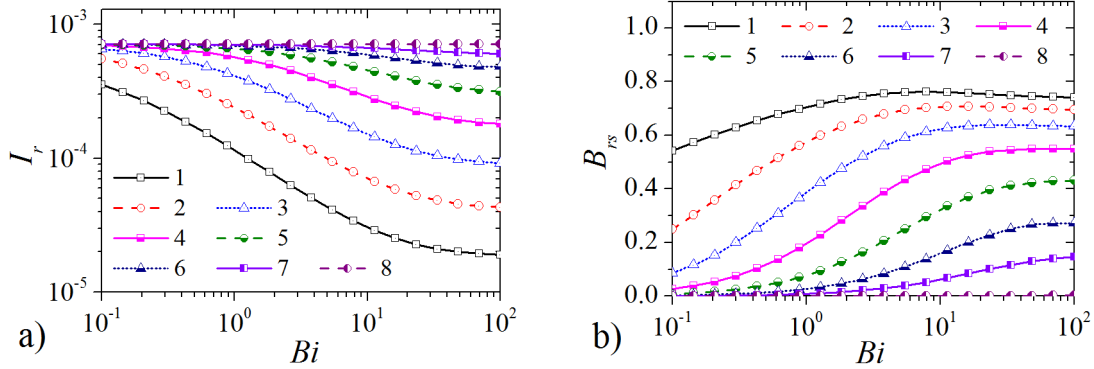

Figure 4.12. The dependence of the relative response (a) and relative sensitivity (b) on the Biot number Bi at eight concentrations of the second substrate: 10^{-6} (1), 3.2×10^{-6} (2), 10^{-5} (3), 3.2×10^{-5} (4), 10^{-4} (5), 3.2×10^{-4} (6), 10^{-3} (7) and 0.1M (8).

As seen from Fig. 4.12a, the normalized steady-state current is an increasing function of the concentration s_{20} of the second substrate S_2 and is a monotonous decreasing function of the Biot number Bi. The decrease is mostly noticeable for the smaller concentrations of the second substrate. The relative response for the smallest value of analysed concentration ($s_{20} = 1 \times 10^{-6}$M, curve 1) of the second substrate changes approximately tenfold by changing the intensity of the stirring. The normalised current I_r becomes practically stagnant at high values of s_{20} (curves 7 and 8).

As it is seen from Fig. 4.12b, the biosensor sensitivity B_{rs} is higher at greater values of Bi rather than at lower ones, meaning that the sensitivity can be increased by increasing the intensity of the stirring in the bulk solution. However, at extremely low concentrations of S_2 (curves 1 and 2), B_{rs} becomes slightly non-monotonous function of Bi. The sensitivity decreases with the increase of s_{20} concentration. The dimensionless sensitivity is less than 0.2 in the whole domain of analysed Biot numbers for the largest concentrations ($s_{20} > 10^{-3}$M) of the second substrate S_2.

4.2.3.4.   Half maximal effective concentration

As it was mentioned in section 1.2.3, the half-maximal effective concentration C_{50} is one of the most important parameters, describing the selectivity of the analysed biosensor. The dependence of C_{50} for the biosensor utilizing parallel substrates conversion (as defined in Section 2.2.4) on the dimensionless reaction rate ξ_1 and enzymatic layer thickness d_1 was investigated with two layered mathematical model~citeAseris2012. The diffusion coefficients were considered equal (4.6) for all the substances, $D^{(1)} = 3.0 \times 10^{-10}$ m^{2}s^{-1}, $D^{(23)} = 6.0 \times 10^{-10}$ m^{2}s^{-1}. The merged layer thickness was considered to be $d_{23} = 10^{-4}$m, while other parameters were as defined in Table 4.2.

Fig. 4.13 shows the half maximal effective concentration C_{50} versus the dimensionless reaction rate ξ_1 (a) as well as the enzymatic membrane thickness d_1 (b). The following three concentrations s_{10} of the first substrate were analysed: 10^{-3}, 3.16×10^{-3} and 10^{-2}M. The dimensionless reaction rate ξ_1 was varied in seven orders of magnitude by changing the values of e_1 and e_2 as defined in 4.3.
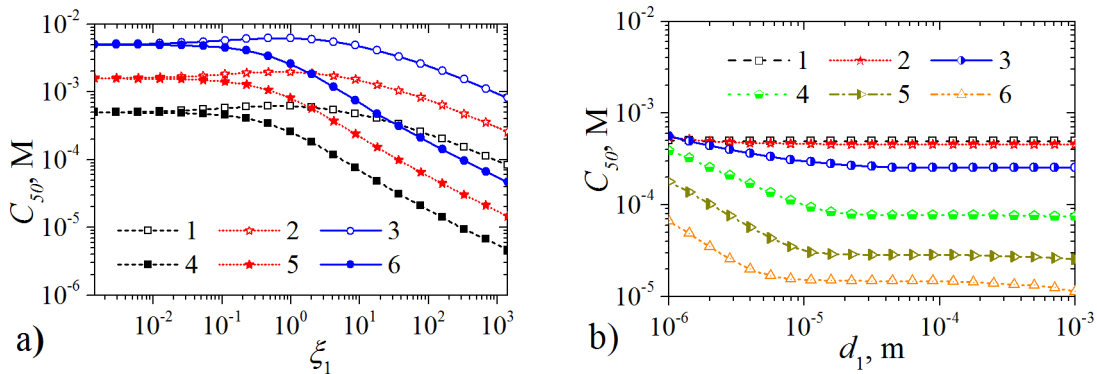

Figure 4.13.   The half maximal effective concentration C_{50} versus the dimensionless reaction rate ξ_1 (a) and versus the enzyme layer thickness d_1 (b). Changed values were: s_{10} (a): 10^{-3} (1, 4), 3.16×10^{-3} (2, 5) and 10^{-2} (3, 6)M, d_1 (a): 10^{-6} (1-3) and 10^{-3} (4-6) m. and ξ_1 (b): 10^{-3} (1), 10^{-1} (2), 1 (3), 10 (4), 10^2 (5) and 10^3 (6).

As one can see from Fig. 4.13a, the half maximal effective concentration is slightly non-monotonous function of the dimensionless reaction rate for the smaller values of the enzyme thickness ($d_1 = 10^{-6}$ m, curves 1-3). The highest value of the half maximal effective concentration $C_{50} \approx 5 \times 10^{-3}$M is reached with the smallest value of the enzyme thickness d_1 and the largest concentration of the first substrate (curve 3) at $\xi_1 = 1$ dimen-

sionless reaction rate. The relative difference between the values of C_{50} for any of the two neighbouring curves remains the same in all the interval of the dimensionless reaction rate.

The dimensionless reaction rate affects the half maximal effective concentration when $\xi_1 > 0.1$ for all the analysed concentrations of the first substrate. The greater dimensionless reaction rate represents smaller values of C_{50}. When $\xi_1 \in [1; 10^3]$ the values of the half maximal effective concentration lowers by one order of magnitude for the smaller thickness of enzyme layer ($d_1 = 10^{-6}$m, curves 1-3) and by more than 2 orders of magnitude for the larger one ($d_1 = 10^{-3}$m, curves 4-6). For the smaller values of the dimensionless reaction rate ($\xi_1 < 1$) and both analysed enzyme layer thicknesses d_1, C_{50} remains almost constant.

The results displayed in Fig. 4.13b confirm the results shown in Fig. 4.13a: the largest half maximal effective concentration C_{50} can be reached by choosing the thinnest possible enzyme layer. The maximal effective concentration C_{50} is practically invariant to changes in the thickness d_1 of the enzyme layer at low values of the dimensionless reaction rate ($\xi_1 < 1$) as well as when the biosensor response is under diffusion limitation ($\sigma_1^2 \gg 1$ and $\sigma_2^2 \gg 1$). Otherwise, the concentration C_{50} increases with decreasing the thickness d_1.

4.2.3.5. Impact of the diffusion modulus

The influence of the second diffusion module on the relative response (Fig. 4.14a) and the relative sensitivity (Fig. 4.14b) was investigated at three different concentrations s_{20} of the second substrate (10^{-6}, 10^{-4} and 10^{-2}M) and three different concentrations e_1 of the first enzyme (10^{-8}, 5×10^{-7} and 10^{-6}M) for the biosensor utilizing parallel substrates conversion [A8]. By changing the thickness of the enzymatic layer between 5 $\times 10^6$m and 5 $\times 10^6$m and the concentration of the second substrate as defined in Table 4.3, the values σ_2^2 of the second diffusion module changes in 7 orders of magnitude.

As one can see from Fig. 4.14a, the relative response is a monotonous increasing function of the second diffusion module for all the analysed values of the biosensor parameters. The smallest concentrations ($s_{20} = 10^{-6}$M) of the second substrate (curves 1-3) correspond to the lowest relative responses of the biosensor without any considerable effect of the first enzyme concen-
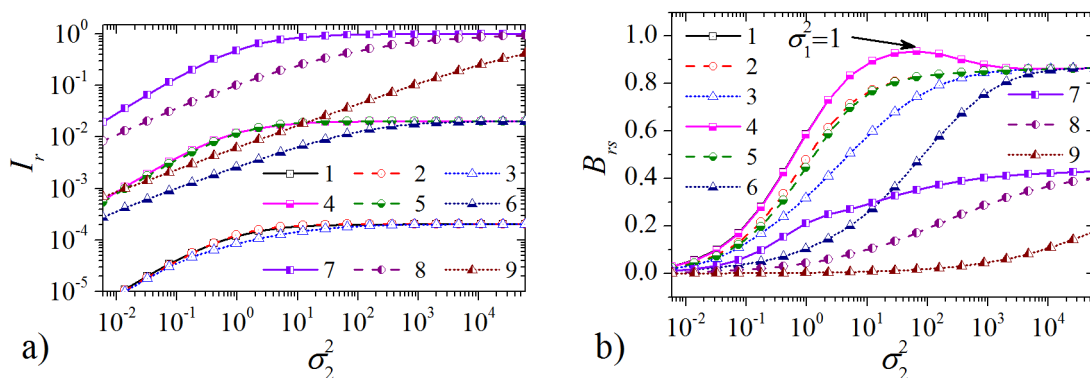
Figure 4.14. The dependence of the relative response (a) and relative sensitivity (b) on the second diffusion module σ_2^2 at three different concentrations s_{20} of the second substrate: 10^{-6} (1-3), 10^{-4} (4-6), 10^{-2} (7-9)M. The concentration e_1 of the first substrate was 10^{-8} (1,4,7), 5×10^{-7} and 10^{-6}M. The other parameters were as in Table 4.2.

tration. For the largest analysed concentrations ($s_{20} = 10^{-2}$M) of the second substrate (curves 7-9) the relative responses are considerably larger, with a noticeable impact of the first enzyme concentration. The lowest analysed concentration $e_1 = 10^{-8}$M of the first enzyme (curve 7) corresponds to the largest possible response ($I_r \approx 1$), when $\sigma_2^2 > 10$. The increase of the first enzyme concentration leads to the lower values of the relative response (curves 7-9 corresponding to $e_1 = 10^{-8}, 5 \times 10^{-7}, 10^{-5}$M). The biggest relative difference between the responses for $s_{20} = 10^{-2}$ is approximately 100, reached at $\sigma_2^2 = 1$ for the largest and smallest concentrations of the first enzyme (curves 7 and 9).

However, for the largest relative responses the sensitivities are the lowest (curves 7-9, Fig. 4.14b), with a small increase for the larger values of the diffusion module. The sensitivity B_{rs} is more than 0.4 when $s_{20} \leq 10^{-4}$ M and $\sigma_2^2 > 1$ (curves 1-5). For the smallest concentrations of the first enzyme ($e_1 = 10^{-8}$M) and the smallest concentrations of the second substrate ($s_{20} \leq 10^{-4}$ M) largest overall sensitivity is achieved (curves 1 and 4). A non-monotonicity is noticeable at $\sigma_2^2 \approx 100$ for the mentioned curves, as the point of extrema corresponds to the unity of the first diffusion module σ_1^2.

4.3. Summary

The mathematical models provided in Chapter 2 were solved numerically in this section. Most of the simulations were performed by applying

schemes and algorithms provided in Chapter 3. The adequacy of the simulation results were validate in different manners.

The transient and quasi-steady-state mathematical models of the biosensor with chemically modified electrode were compared by using computational grids and applying parameter sweep approach. The biosensor action was analysed in stirred and non-stirred solutions. The parameters affecting the error of quasi-steady-state modelling were determined. The dependency of the half maximal effective concentration was investigated based on the concentration of the mediator.

The simulation results of mathematical model of biosensor with parallel substrates conversion presented in Section 2.2.2 were relatively close to the experimental ones. A partition coefficient between neighbouring layers was analysed. It was digitally proved, that partition coefficient can be used to improve the accuracy of the mathematical model. The impact of the enzymatic membrane thickness, enzyme concentrations and Biot number on the biosensor response, sensitivity and half-maximal effective concentrations was investigated.

A possibility to apply an effective diffusion coefficient to mathematical models of both biosensors was analysed. The parameters affecting the error of modelling with such an approach were determined.

Conclusions

1. The transient mathematical model of biosensor with chemically modified electrode is more accurate than one with a quasi-steady-state assumption (QSSA) for a practically meaningful set of parameter values. The error of the QSSA is the largest for relatively small diffusion module and relatively large Biot number. A quasi-steady-state assumption can be applied for other parameter values with relative error being less than 1%.

2. The developed mathematical model of the biosensor with parallel substrates conversion can be successfully used to investigate the kinetic peculiarities of the biosensor behaviour. Only the concentrations of the substrate to be determined (the second substrate) less than the concentration of the hydrogen peroxide (the first substrate) can be suitably recognised. The largest half-maximal effective concentrations are achieved at the largest concentrations of first substrate and the lowest ratio of the catalase to the peroxidase.

3. The partition coefficient is a response altering parameter for the mathematical model of biosensor utilizing parallel substrates conversion. The involvement of the partition coefficient impacts the relative response and relative sensitivity, but does not change general tendencies of the biosensor behaviour.

4. Effective diffusion coefficient can be successfully applied to merge two diffusion-based regions into one for both analysed mathematical models. Numerical investigation showed that in most cases the error of the merger is less than 10%.

Author publications

[A1] V. Ašeris, R. Baronas. Using GRID Computing to Model Biosensors Acting in Stirred and Non-Stirred Solutions. *Proceedings of the 5th european conference on computational fluid dynamics (eccomas cfd 2010)*. C. F. Pereira, A. Sequeira, J. M. C. Pereira, editors. Lisbon, Portugal, 2010, pp. 14–17 (cit. on pp. 6, 33, 51, 61, 64, 67).

[A2] V. Ašeris, R. Baronas. Kintamo diskrečiosios gardelės erdvės žingsnio taikymas biojutiklio su chemiškai modifikuotu elektrodu kompiuteriniam modeliavimui (Using variable space step of the discrete grid to model the biosensor with chemically modified electrode). Lithuanian. *Xv kompiuterininkų konferencijos mokslo darbai.* Žara, Klaipėda, 2011, pp. 7–18 (cit. on pp. 6, 51, 54, 67).

[A3] V. Ašeris. Biojutiklio su lygiagrečiu substratų virsmu ir dializės membrana kompiuterinis modeliavimas (Computational modelling of the biosensor acting under parallel substrates conversion with dialysis membrane). Lithuanian. *Lietuvos matematikos rinkinys. lmd darbai. serija b.*, 53:1–6, 2012 (cit. on pp. 6, 75, 84, 85).

[A4] V. Ašeris, R. Baronas, J. Kulys. Effect of Diffusion Limitations of the Response of Biosensors Utilizing Parallel Substrates Conversion. *Proceedings of the 6th european congress on computational methods in applied sciences and engineering.* Vienna, Austria, 2012, pp. 1–10 (cit. on pp. 6, 76, 85).

[A5] V. Ašeris, R. Baronas, J. Kulys. Modelling the Biosensor utilizing parallel substrates conversion. *Journal of electroanalytical chemistry*, 685(1):63–71, 2012. DOI: http://dx.doi.org/10.1016/j.jelechem.2012.06.025 (cit. on pp. 5, 6, 31, 33, 39, 75, 79).

[A6] I. Paužaitė, V. Ašeris. Kompiuterinis biojutiklių modeliavimas taikant kintamą diskrečiosios gardelės erdvės žingsnį (Computational Modeling of Biosensors using variable space step of the discrete grid).

Lithuanian. *17-osios tarpuniversitetinės magistrantų ir doktorantų konferencijos „informacinės technologijos 2012" mokslo darbai*:1–4, 2012 (cit. on pp. 6, 51, 53, 54).

[A7] J. Kulys, I. Bratkovskaja, V. Ašeris, R. Baronas. Electrochemical Peroxidase-Catalase Clark-Type Biosensor: Computed and Experimental Response. *Electroanalysis*, 25(6):1491–1496, 2013. DOI: 10 . 1002/elan.201300070 (cit. on pp. 5, 6, 31, 75, 80).

[A8] V. Ašeris, R. Baronas, J. Kulys. Computational Modeling of Bienzyme Biosensor with Different Initial and Boundary Conditions. *Informatica*:accepted (cit. on pp. 6, 48, 76, 88).

Bibliography

[1] J. Cooper, A. Cass. *Biosensors: A Practical Approach*. Oxford University Press, Oxford, UK, 2004 (cit. on pp. 1, 9, 20).

[2] F. Scheller, F. Schubert. *Biosensors*. Elsevier, Amsterdam, Netherlands, 1992 (cit. on pp. 1, 9, 20, 38, 41, 45).

[3] A. P. Turner, I. Karube, G. S. Wilson. *Biosensors: fundamentals and applications*. Oxford University Press, Oxford, UK, 1987 (cit. on pp. 1, 9, 41).

[4] F. Scheller, J. Fedrowitz. *Frontiers in Biosensorics*. Birkhauser Varloy, 1997 (cit. on pp. 1, 9, 18).

[5] G. I. A. Inc. Biosensors in Medical Diagnostics - a Global Strategic Business Report. Tech. rep. Global Industry Analysts, Inc., 2012 (cit. on p. 1).

[6] L. D. Ciana, G. Bernacca, F. Bordin. Highly sensitive amperometric measurement of alkaline phosphatase activity with glucose oxidase amplification. *Journal of electroanalytical chemistry*, 382:129–135, 1995 (cit. on p. 1).

[7] R. A. C. Jr., S. Vaddiraju, F. Papadimitrakopoulos, F. C. Jain. Theoretical Analysis of the Performance of Glucose Sensors with Layer-by-Layer Assembled Outer Membranes. *Sensors*, 12(10):13402–13416, 2012. DOI: 10.3390/s121013402 (cit. on pp. 1, 16).

[8] J. Rickus. Impact of coenzyme regeneration on the performance of an enzyme-based optical biosensor: a computational study. *Biosensors & bioelectronics*, 21(6):965–72, 2005. DOI: 10.1016/j.bios.2005.01.023 (cit. on p. 1).

[9] D. Fraser. *Biosensors in the Body: Continuous in Vivo Monitoring*. Wiley, 1997 (cit. on p. 1).

[10] L. D. Mello, L. T. Kubota. Review of the use of biosensors as analytical tools in the food and drink industries. *Food chemistry*, 77(2):237–256, 2002. DOI: 10.1016/S0308-8146(02)00104-8 (cit. on pp. 1, 10).

[11] A. Sadana, N. Sadana. *Handbook of biosensors and biosensor kinetics*. Elsevier, 2010 (cit. on pp. 1, 9, 20, 21).

[12] T. Schulmeister, J. Rose, F. W. Scheller. Mathematical modelling of exponential amplification in membrane-based enzyme sensors. *Biosensors and bioelectronics*, 12(9-10):1021–1030, 1997. DOI: 10.1016/S0956-5663(97)00058-4 (cit. on pp. 1, 18).

[13] H. Nakamura, I. Karube. Current research activity in biosensors. *Analytical and bioanalytical chemistry*, 377(3):446–468, 2003. DOI: 10.1007/s00216-003-1947-5 (cit. on p. 2).

[14] V. Scognamiglio, G. Pezzotti, I. Pezzotti, J. Cano, et al. Biosensors for effective environmental and agrifood protection and commercialization: from research to market. *Microchimica acta*, 170(3-4):215–225, 2010. DOI: 10.1007/s00604-010-0313-5 (cit. on p. 2).

[15] A. Akkaya, C. Altug, N. K. Pazarlioglu, E. Dinckaya. Determination of 5-Aminosalicylic Acid by Catalase-Peroxidase Based Biosensor. *Electroanalysis*, 21(16):1805–1810, 2009. DOI: 10.1002/elan.200904606 (cit. on pp. 2, 29).

[16] J. Castillo, S. Gáspár, I. Sakharov, E. Csöregi. Bienzyme biosensors for glucose, ethanol and putrescine built on oxidase and sweet potato peroxidase. *Biosensors and bioelectronics*, 18(5-6):705–714, 2003. DOI: 10.1016/S0956-5663(03)00011-3 (cit. on pp. 2, 29).

[17] R. M. Ianniello, A. M. Yacynych. Immobilized enzyme chemically modified electrode as an amperometric sensor. *Analytical chemistry*, 53(13):2090–2095, 1981. DOI: 10.1021/ac00236a033 (cit. on pp. 2, 29).

[18] J. Kulys, V. Sorochinskii, R. Vidziunaite. Transient response of bienzyme electrodes. *Biosensors*, 2(3):135–46, 1986 (cit. on p. 2).

[19] R. W. Murray. Chemically Modified Electrodes. *Accounts of chemical research*, 117(1979):135–141, 1980 (cit. on pp. 2, 29).

[20] R. Baronas. Computer Simulation of Diffusion Processes in Nonhomogeneous Media. PhD Thesis, Summary. Vilnius University, 2000 (cit. on p. 2).

[21] A. Rabner, E. Martinez, R. Pedhazur, T. Elad, et al. Mathematical Modeling of a Bioluminescent E. Coli Based Biosensor. *Nonlinear analysis: modelling and control*, 14(4):505–529, 2009 (cit. on pp. 2, 16).

[22] G. Rahamathunissa, L. Rajendran. Application of He's variational iteration method in nonlinear boundary value problems in enzyme–substrate reaction diffusion processes: part 1. The steady-state amperometric response. *Journal of mathematical chemistry*, 44(3):849–861, 2008. DOI: 10.1007/s10910-007-9340-9 (cit. on pp. 2, 16).

[23] S. Rosini, E. Siebert. Electrochemical sensors for detection of hydrogen in air: model of the non-Nernstian potentiometric response of platinum gas diffusion electrodes. *Electrochimica acta*, 50(14):2943–2953, 2005. DOI: 10.1016/j.electacta.2004.11.044 (cit. on p. 2).

[24] J. P. Kernevez, D. Thomas. Numerical analysis and control of some biochemical systems. *Applied mathematics and optimization*, 1(3):222–285, 1975. DOI: 10.1007/BF01448182 (cit. on pp. 2, 16).

[25] L. D. Mell, J. Maloy. A model for the amperometric enzyme electrode obtained through digital simulation and applied to the immobilized glucose oxidase system. *Analytical chemistry*, 47(2):299–307, 1975. DOI: 10.1021/ac60352a006 (cit. on p. 2).

[26] J. Kernevez. *Enzyme mathematics*. Elsevier, 1980 (cit. on p. 2).

[27] J. Kulys. Development of new analytical systems based on biocatalysers. *Enzyme and microbial technology*, 3(4):344–352, 1981 (cit. on p. 2).

[28] T. Schulmeister. Mathematical modelling of the dynamic behaviour of amperometric enzyme electrodes. *Selective electrode reviews*, 12(2):203–260, 1990 (cit. on pp. 2, 18, 20, 29, 35, 52).

[29] S. W. Feldberg. Digital simulation: a general method for solving electrochemical diffusion-kinetic problems. *Electroanalytical chemistry*, 3:199–296, 1969 (cit. on p. 2).

[30] B. Flanagan, L. Marcoux. Digital simulation of edge effects at planar disc electrodes. *Journal of physical chemistry*, 77(8):1051–1055, 1973 (cit. on p. 2).

[31] P. Bartlett, K. Pratt. Theoretical treatment of diffusion and kinetics in amperometric immobilized enzyme electrodes Part I: Redox mediator entrapped within the film. *Journal of electroanalytical chemistry*, 397(1-2):61–78, 1995. DOI: 10.1016/0022-0728(95)04236-7 (cit. on pp. 2, 16).

[32] P. Bartlett. *Bioelectrochemistry*. John Wiley & Sons, 2008 (cit. on p. 2).

[33] R. Baronas, F. Ivanauskas, J. Kulys. *Mathematical Modeling of Biosensors*. Springer, Dordrecht, Netherlands, 2010. DOI: 10.3390/s6040453 (cit. on pp. 2, 16, 19, 20, 22, 24, 29, 71).

[34] D. Britz. *Digital Simulation in Electrochemistry*. Springer Berlin Heidelberg, Berlin, Germany, 2005. DOI: 10.1007/b97996 (cit. on pp. 2, 20, 36).

[35] A. Pradeep. *Introduction to Numerical Methods in Chemical Engineering*. PHI Learning Private Limited, 2010 (cit. on p. 2).

[36] L. K. Bieniasz, D. Britz. Recent developments in digital simulation of electroanalytical experiments. eng. *Polish journal of chemistry*, 78(9):1195–1219, 2004 (cit. on p. 2).

[37] D. Britz, R. Baronas, E. Gaidamauskaite, F. Ivanauskas. Further comparisons of finite difference schemes for computational modelling of biosensors. *Nonlinear analysis: modelling and control*, 14(4):419–433, 2009 (cit. on p. 2).

[38] E. Gaidamauskaite, R. Baronas. A comparison of finite difference schemes for computational modelling of biosensors. *Nonlinear analysis: modelling and control*, 12(3):359–369, 2007 (cit. on pp. 2, 24).

[39] L. K. Bieniasz. Use of dynamically adaptive grid techniques for the solution of electrochemical kinetic equations Part 1 . Introductory exploration of the finite-difference adaptive moving grid solution of the one-dimensional fast homogeneous reaction-diffusion problem w. *Journal of electroanalytical chemistry*, 360(1-2):119–138, 1993. DOI: http://dx.doi.org/10.1016/0022-0728(93)87008-J (cit. on pp. 2, 25).

[40] L. K. Bieniasz. Use of dynamically adaptive grid techniques for the solution of electrochemical kinetic equations Part 16: Patch-adaptive strategy combined with the extended Numerov spatial discretisation. *Electrochimica acta*, 52(12):3929–3940, 2007. DOI: 10.1016/j.electacta.2006.11.008 (cit. on pp. 2, 25).

[41] D. Britz, O. Østerby, J. Strutwolf. Comparison of flux approximations in electrochemical digital simulation. Part 2: Complications due to homogeneous chemical reactions, charge estimation and application to the ultramicrodisk electrode. *Journal of electroanalytical chemistry*, 622(1):51–58, 2008. DOI: 10.1016/j.jelechem.2008.05.013 (cit. on p. 2).

[42] D. Britz, O. Østerby, J. Strutwolf. Minimum grid digital simulation of chronoamperometry at a disk electrode. *Electrochimica acta*, 78:365–376, 2012. DOI: 10.1016/j.electacta.2012.06.009 (cit. on p. 2).

[43] R. Čiegis. *Diferencialinių lygčių skaitiniai sprendimo metodai (Numercal Methods for Differential Equations)*. Lithuanian. Technika, Vilnius, Lithuania, 2003 (cit. on pp. 2, 22, 24).

[44] A. A. Samarskij. *The theory of difference schemes*. Marcel Dekker, New York, New York, USA, 2001 (cit. on pp. 2, 22, 54).

[45] A. A. Samarskij, P. N. Vabishchevich. *Numerical methods for solving inverse problems of mathematical physics*. Walter de Gruyter, Berlin, Germany, 2007 (cit. on pp. 2, 22, 24).

[46] M. Sapagovas, B. Kvedaras. *Skaičiavimo metodai*. Mintis, Vilnius, 1974 (cit. on pp. 2, 22–24).

[47] V. Giedrimas, A. Varoneckas, A. Juozapavičius. The Grid and Cloud Computing Facilities in Lithuania. *Scalable computing: practice and experience*, 12(4):417–421, 2012 (cit. on pp. 2, 26).

[48] L. C.Clark Jr., R. Wolf, D. Granger, Z. Taylor. Continuous recording of blood oxygen tensions by polarography. *Journal of applied physiology*, 6(3):189–193, 1953 (cit. on pp. 9, 30).

[49] L. C.Clark Jr., C. Lyons. Electrode Systems For Continuous Monitoring In Cardiovascular Surgery. *Annals of the new york academy of sciences*, 102(1):29–45, 1962. DOI: 10.1111/j.1749-6632.1962.tb13623.x (cit. on p. 9).

[50] J. D. Newman, S. J. Setford. Enzymatic biosensors. *Molecular biotechnology*, 32(3):249–268, 2006. DOI: 10.1385/MB:32:3:249 (cit. on p. 9).

[51] J. Davis, D. H. Vaughan, M. F. Cardosi. Elements of biosensor construction. *Enzyme and microbial technology*, 17(12):1030–1035, 1995 (cit. on p. 9).

[52] R. Monošík, M. Streďanský, E. Šturdík. Biosensors - classification, characterization and new trends. *Acta chimica slovaca*, 5(1):109–120, 2012. DOI: 10.2478/v10188-012-0017-z (cit. on p. 10).

[53] L. Michaelis, M. Menten. Die kinetik der invertinwirkung (The Kinetics of Invertase Action). German. *Biochem. z*, 49:333–369, 1913 (cit. on pp. 10, 16).

[54] G. E. Briggs, J. B. S. H. Haldane. A note on the kinetics of enzyme action. *Biochemical journal*, 19(2):338–339, 1925 (cit. on p. 10).

[55] L. A.Segel, M. M. Slemrod. The Quasi-Steady-State Assumption: A Case Study in Perturbation. *Siam review*, 31(3):446–477, 1989. DOI: 10.1137/1031091 (cit. on pp. 11, 19, 38).

[56] M. Nič, J. Jirát, B. Košata, A. Jenkins, et al., eds. *IUPAC Compendium of Chemical Terminology*. IUPAC, Research Triangle Park, NC, 2009. DOI: 10.1351/goldbook (cit. on p. 14).

[57] v. S. A. Stroe-Biezen, F. M. Everaerts, L. J. Janssen, Roland A. Tacken. Diffusion coefficients of oxygen, hydrogen peroxide and glucose in a hydrogel. *Analytica chimica acta*, 273(1-2):553–560, 1993. DOI: 10.1016/0003-2670(93)80202-V (cit. on pp. 14, 77).

[58] D. C. Scott, J. W. Clymer. Estimation of Distribution Coefficients from the Partition Coefficient and pKa. *Pharmaceutical technology*, 26(11):30–40, 2002 (cit. on p. 14).

[59] A. Kousba, L. G. Sultatos. Continuous system modeling of equilibrium dialysis for determinations of tissue partitioning of parathion and paraoxon. *Toxicology letters*, 133(2-3):153–9, 2002 (cit. on p. 14).

[60] M. Sales-Cruz, E. Perez-Cisneros, J. Ochoa-Tapia. An analytic solution for the transient diffusion problem in a multi-layer system. *Revista mexicana de ingeniería química*, 1(1-2):57–72, 2002 (cit. on pp. 14, 20).

[61] A. Abd. Aziz. Mathematical Modeling Of An Amperometric Glucose Sensor: The Effect Of Membrane Permeability And Selectivity On Performance. *Jurnal teknologi*, 51(1):77–94, 2009. DOI: 10.11113/jt.v51.148 (cit. on pp. 14, 80).

[62] L. Coche-Guerente, P. Labbé, V. Mengeaud. Amplification of amperometric biosensor responses by electrochemical substrate recycling. 3. Theoretical and experimental study of the phenol-polyphenol oxidase system immobilized in Laponite hydrogels and layer-by-layer self-assembled structures. *Analytical chemistry*, 73(14):3206–18, 2001 (cit. on pp. 14, 16).

[63] M. Velkovsky, R. Snider, D. E. Cliffel, J. P. Wikswo. Modeling the measurements of cellular fluxes in microbioreactor devices using thin enzyme electrodes. *Journal of mathematical chemistry*, 49(1):251–275, 2010. DOI: `10.1007/s10910-010-9744-9` (cit. on pp. 14, 16).

[64] N. S. Bakhvalov, G. Panasenko. *Homogenisation: Averaging Processes in Periodic Media: Mathematical Problems in the Mechanics of Composite Materials.* Springer, 1989 (cit. on p. 15).

[65] L. Dormieux, E. Lemarchand. An Homogenization Approach Of Advection And Diffusion In Cracked Porous Material. *Journal of engineering mechanics*, 127(12):1267–1274, 2001 (cit. on p. 15).

[66] S. Whitaker. *The Method of Volume Averaging.* Springer, 1999 (cit. on p. 15).

[67] K. Petrauskas, R. Baronas. Computational Modelling of Biosensors with an Outer Perforated Membrane. *Nonlinear analysis: modelling and control*, 14(1):85–102, 2009 (cit. on pp. 15, 71).

[68] K. Petrauskas, R. Baronas. One-dimensional modelling of a carbon nanotube-based biosensor. *Proceedings of the 26th european conference on modelling and simulation (ecms 2012).* U. L. Klaus G. Troitzsch, Michael Möhring, editor. Koblenz, Germany, 2009, pp. 121–127 (cit. on pp. 15, 27).

[69] A. C. Fowler. *Mathematical Models in the Applied Sciences.* Cambridge University Press, 1997 (cit. on pp. 16, 19).

[70] U. D'Ambrosio. Mathematical Modeling: Cognitive, Pedagogical, Historical And Political Dimensions. *Journal of mathematical modelling and application*, 1(1):89–98, 2009 (cit. on p. 16).

[71] S. Rutkauskas. *Ivadas į diferencialinių lygčių teoriją (Introduction to the differential equation theory).* Lithuanian. Vilniaus pedagoginio universiteto leidykla, Vilnius, 2006 (cit. on p. 16).

[72] R. Baronas, F. Ivanauskas, J. Kulys, M. Sapagovas, et al. The influence of diffusion space geometry on behavior of some processes in biochemistry and electrochemistry. *Nonlinear analysis: modelling and control*, 5:3–38, 2000 (cit. on p. 16).

[73] R. Baronas, F. Ivanauskas, A. Survila. Simulation of electrochemical behavior of partially blocked electrodes under linear potential sweep conditions. *Journal of mathematical chemistry*, 27(4):267–278, 2000 (cit. on p. 16).

[74] R. Baronas, F. Ivanauskas, J. Kulys, M. Sapagovas. Computational Modelling of a Sensor Based on an Array of Enzyme Microreactors. *Nonlinear analysis: modelling and control*, 9(3):203–218, 2004 (cit. on p. 16).

[75] R. Baronas, F. Ivanauskas, J. Kulys. Mathematical Modeling of Biosensors Based on an Array of Enzyme Microreactors. *Sensors*, 6(4):453–465, 2006. DOI: `10.3390/s6040453` (cit. on p. 16).

[76] R. Baronas, J. Kulys, K. Petrauskas, J. Razumienė. Modelling carbon nanotube based biosensor. *Journal of mathematical chemistry*, 49(5):995–1010, 2010. DOI: `10.1007/s10910-010-9791-2` (cit. on p. 16).

[77] D. Simelevicius, R. Baronas, J. Kulys. Modelling of amperometric biosensor used for synergistic substrates determination. *Sensors (basel, switzerland)*, 12(4):4897–917, 2012. DOI: `10.3390/s120404897` (cit. on p. 16).

[78] E. Gaidamauskaite, R. Baronas, J. Kulys. Modelling synergistic action of laccase-based biosensor utilizing simultaneous substrates conversion. *Journal of mathematical chemistry*, 49(8):1573–1586, 2011. DOI: `10.1007/s10910-011-9844-1` (cit. on p. 16).

[79] A. Cambiaso, L. Delfino, M. Grattarola, G. Verreschia, et al. Modelling and simulation of a diffusion limited glucose biosensor. *Sensors and actuators b: chemical*, 33(1-3):203–207, 1996 (cit. on p. 16).

[80] A. Eswari, L. Rajendran. Application of variational iteration method and electron transfer mediator/catalyst composites in modified electrodes. *Natural science*, 02(06):612–625, 2010. DOI: `10.4236/ns.2010.26076` (cit. on p. 16).

[81] N. Kohli, I. Lee, R. J. Richardson, R. M. Worden. Theoretical and experimental study of bi-enzyme electrodes with substrate recycling. *Journal of electroanalytical chemistry*, 641(1-2):104–110, 2010. DOI: `10.1016/j.jelechem.2009.12.010` (cit. on p. 16).

[82] T. D. Rane, P. S. Gandhi. Modeling and Simulation of Cantilever Biosensor (for MI) Based on Molecular Electrostatic Interactions. *Proceedings of the type or paste your content heremicrofluidics, biomems, and medical microsystems iii.* I. Papautsky, I. Chartier, editors, 2005, pp. 255–264. DOI: `10.1117/12.590862` (cit. on p. 16).

[83] L. Ferreira, M. De Souza, J. Trierweiler, O. Broxtermann, et al. Aspects concerning the use of biosensors for process control: experimental and simulation investigations. *Computers & chemical engineering*, 27(8-9):1165–1173, 2003. DOI: `10.1016/S0098-1354(03)00044-9` (cit. on p. 16).

[84] K. Babu, D. Rao. Mathematical Modeling of Amperometric Biosensors. *Ijca proceedings on international conference on vlsi, communications and instrumentation (icvci)*, (2), 2011 (cit. on p. 16).

[85] N. Botkin, V. Turova. Mathematical models of a biosensor. *Applied mathematical modelling*, 28(6):573–589, 2004. DOI: `10.1016/j.apm.2003.10.012` (cit. on pp. 16, 22).

[86] M. E. Lyons. Modelling the Transport and Kinetics of Electroenzymes at the Electrode/Solution Interface. *Sensors*, 6(12):1765–1790, 2006. DOI: `10.3390/s6121765` (cit. on p. 16).

[87]   A. Meena, L. Rajendran. Mathematical modeling of amperometric and potentiometric biosensors and system of non-linear equations – Homotopy perturbation approach. *Journal of electroanalytical chemistry*, 644(1):50–59, 2010. DOI: `10.1016/j.jelechem.2010.03.027` (cit. on pp. 16, 21).

[88]   Y. Liu. Mathematical and Computational Modelling for Biosensors: A Modular Approach. PhD Thesis. Dublin Institute of Technology, 2012 (cit. on p. 16).

[89]   Q. Wang. Mathematical Methods for Biosensor Models. PhD Thesis. Dublin Institute of Technology, 2011 (cit. on pp. 16, 19).

[90]   D. Mackey, A. J. Killard, A. Ambrosi, M. R. Smyth. Optimizing the ratio of horseradish peroxidase and glucose oxidase on a bienzyme electrode: Comparison of a theoretical and experimental approach. *Sensors and actuators b: chemical*, 122(2):395–402, 2007. DOI: `10.1016/j.snb.2006.06.006` (cit. on p. 16).

[91]   D. Mackey, T. Killard. Optimising Design Parameters of Enzyme-Channelling Biosensors. *Proceedings of the progress in industrial mathematics at ecmi 2006.* Vol. 12. Springer, 2008 (cit. on p. 16).

[92]   P. Bartlett, C. Toh, E. Calvo, V. Flexer. Modelling Biosensor Responses, *Bioelectrochemistry*, pp. 267–325. John Wiley & Sons, Ltd, 2008. DOI: `10.1002/9780470753842.ch8`. arXiv: `9780470753842.ch8 [10.1002]` (cit. on pp. 16, 18).

[93]   D. Baronas, F. Ivanauskas, R. Baronas. Mechanisms controlling the sensitivity of amperometric biosensors in flow injection analysis systems. *Journal of mathematical chemistry*, 49(8):1521–1534, 2011. DOI: `10.1007/s10910-011-9838-z` (cit. on pp. 16, 20).

[94]   S. Loghambal, L. Rajendran. Mathematical modeling of diffusion and kinetics in amperometric immobilized enzyme electrodes. *Electrochimica acta*, 55(18):5230–5238, 2010. DOI: `10.1016/j.electacta.2010.04.050` (cit. on p. 16).

[95]   W. E. Morf, P. D. v. d. Wal, E. Pretsch, N. d. Rooij. Theoretical treatment and numerical simulation of potentiometric and amperometric enzyme electrodes and of enzyme reactors. Part 1: Steady-state concentration profiles, fluxes, and responses. *Journal of electroanalytical chemistry*, 657(1-2):1–12, 2011. DOI: `10.1016/j.jelechem.2011.02.007` (cit. on pp. 16, 42).

[96]   S. D. Schnell, P. K. Maini. A Century of Enzyme Kinetics: Reliability of the KM and vmax Estimates. *Comments on theoretical biology*, 8(2-3):169–187, 2003. DOI: `10.1080/08948550390206768` (cit. on p. 16).

[97]   V. Sorochinskii, B. Kurganov. Steady-state kinetics of cyclic conversions of substrate in amperometric bienzyme sensors. *Biosensors and bioelectronics*, 11(3):225–238, 1996. DOI: `10.1016/0956-5663(96)88409-0` (cit. on pp. 16, 21).

[98] O. Štikoniene, F. Ivanauskas. Numerical simulation of the influence of the fluctuations of the biosensor's parameters on its response. *Lietuvos matematikos rinkinys. lmd darbai.*, 50:345–350, 2009 (cit. on p. 16).

[99] O. Štikoniene, F. Ivanauskas, V. Laurinavičius. The influence of external factors on the operational stability of the biosensor response. *Talanta*, 81(4-5):1245–1249, 2010. DOI: 10.1016/j.talanta.2010.02.016 (cit. on pp. 16, 21).

[100] J. Wang. *Analytical electrochemistry.* Vol. 3. Wiley, 2004 (cit. on p. 17).

[101] L. A. Pribe, A. J. Welch. A dimensionless model for the calculation of temperature increase in biologic tissues exposed to nonionizing radiation. *Ieee transactions on bio-medical engineering*, 26(4):244–50, 1979 (cit. on p. 19).

[102] R. E. Tsai, A. Seibert, R. Eldridge, G. T. Rochelle. A dimensionless model for predicting the mass-transfer area of structured packing. *Aiche journal*, 57(5):1173–1184, 2011. DOI: 10.1002/aic.12345 (cit. on p. 19).

[103] H. Yeh, H. Yeh. A Dimensionless Mathematical Model for Studying the Physical Parameters of Composite Laminates - Part I. *Journal of reinforced plastics and composites*, 22:83–99, 2003. DOI: 10.1177/0731684403022001489 (cit. on p. 19).

[104] F. Heineken, H. Tsuchiya, R. Aris. On the mathematical status of the pseudo-steady state hypothesis of biochemical kinetics. *Mathematical biosciences*, 1(1):95–113, 1967. DOI: 10.1016/0025-5564(67)90029-6 (cit. on p. 19).

[105] E. Gaidamauskaite. A Computational Investigation of the Optical Biosensor by a Dimensionless Model. *Information sciences*, 50:306–310, 2009 (cit. on p. 19).

[106] D. Šimelevičius, R. Baronas. Computational modelling of amperometric biosensors in the case of substrate and product inhibition. *Journal of mathematical chemistry*, 47(1):430–445, 2009. DOI: 10.1007/s10910-009-9581-x (cit. on pp. 19, 20).

[107] R. Baronas, R. Šimkus. Modeling the bacterial self-organization in a circular container along the contact line as detected by bioluminescence imaging. *Nonlinear analysis: modelling and control*, 16(3):270–282, 2011 (cit. on p. 19).

[108] L. K. Bieniasz. Use of dynamically adaptive grid techniques for the solution of electrochemical kinetic equations Part 11. Patch-adaptive simulation of example transient experiments described by kinetic models involving simultaneously distributed and localised unknowns, *Journal of electroanalytical chemistry*, 527(1-2):11–20, 2002. DOI: 10.1016/S0022-0728(02)00812-4 (cit. on p. 19).

[109] L. K. Bieniasz. Use of dynamically adaptive grid techniques for the solution of electrochemical kinetic equations. Part 15: patch-adaptive simulation of example transient experiments described by Nernst–Planck–electroneutrality equations in one-dimensional space geometry. *Journal of electroanalytical chemistry*, 565(2):273–285, 2004. DOI: `10.1016/j.jelechem.2003.10.019` (cit. on p. 19).

[110] A. Deutsch, L. Brusch, H. Byrne, G. d. Vries, et al. *Mathematical Modeling of Biological Systems*. Vol. 1. Birkhauser, Boston, 2007 (cit. on p. 19).

[111] R. Šimkus, R. Baronas, Ž. Ledas. A multi-cellular network of metabolically active E. coli as a weak gel of living Janus particles. *Soft matter*, 9(17):4489, 2013. DOI: `10.1039/c3sm27786k` (cit. on p. 19).

[112] R. Baronas, J. Kulys. Modelling Amperometric Biosensors Based on Chemically Modified Electrodes. *Sensors*, 8(8):4800–4820, 2008. DOI: `10.3390/s8084800` (cit. on pp. 20, 25, 29, 30, 33–35, 38, 39, 51, 52, 72, 73).

[113] F. Ivanauskas, R. Baronas. Numerical simulation of a plate-gap biosensor with an outer porous membrane. *Simulation modelling practice and theory*, 16(8):962–970, 2008. DOI: `10.1016/j.simpat.2008.05.004` (cit. on p. 20).

[114] R. Baronas, F. Ivanauskas, J. Kulys. The Influence of the Enzyme Membrane Thickness on the Response of Amperometric Biosensors. *Sensors*, 3(7):248–262, 2003. DOI: `10.3390/s30700248` (cit. on p. 20).

[115] F. Ivanauskas, R. Baronas. Modelling an amperometric biosensor acting in a flowing liquid. *International journal for numerical methods in fluids*, 56(8):1313–1319, 2008. DOI: `10.1002/fld` (cit. on pp. 20, 21).

[116] M. E. Lyons, T. Bannon, G. Hinds, S. Rebouillat. Reaction/diffusion at conducting polymer ultramicroelectrodes. *The analyst*, 123(10):1947–1959, 1998. DOI: `10.1039/a803274b` (cit. on p. 20).

[117] D. Šimelevičius, R. Baronas. Mechanisms Controlling the Sensitivity of Amperometric Biosensors in the Case of Substrate and Product Inhibition. *Proceedings of the 3rd international conference on advances in system simulation (simul 2011)*. Barcelona, Spain, 2011, pp. 69–74 (cit. on p. 20).

[118] A. Benyahia, S. Bacha. Numerical Simulation Of Amperometric Biosensors Performances. *Proceedings of the 16th european simulation symposium*. G. Lipovszki, I. Molnár, editors. Budapest, Hungary, 2004, pp. 1–7 (cit. on p. 21).

[119] H. Bisswanger. *Enzyme Kinetics: Priciples and Methods*. Wiley-VCH Verlag GmbH & Co. KGaA, Weinheim, Germany, 2008. DOI: `10.1002/9783527622023` (cit. on p. 21).

[120] F. Ivanauskas, I. Kaunietis, V. Laurinavičius, J. Razumienė, et al. Computer simulation of the steady state currents at enzyme doped carbon paste electrodes. *Journal of mathematical chemistry*, 38(3):355–366, 2005. DOI: 10.1007/s10910-005-5825-6 (cit. on p. 21).

[121] M. Puida, A. Malinauskas, F. Ivanauskas. Modeling of electrocatalysis at conducting polymer modified electrodes: nonlinear current-concentration profiles. *Journal of mathematical chemistry*, 49(6):1151–1162, 2011. DOI: 10.1007/s10910-011-9802-y (cit. on p. 21).

[122] M. Puida, A. Malinauskas, F. Ivanauskas. Modeling of electrocatalysis at chemically modified electrodes: a combination of second-order and Michaelis-type chemical kinetics. *Journal of mathematical chemistry*, 50(7):2001–2011, 2012. DOI: 10.1007/s10910-012-0016-8 (cit. on pp. 21, 29).

[123] J. Kulys, L. Tetianec. Synergistic substrates determination with biosensors. *Biosensors & bioelectronics*, 21(1):152–158, 2005. DOI: 10.1016/j.bios.2004.08.013 (cit. on p. 21).

[124] K. Kriaučiūnas, J. Kulys. Macrokinetic Model of Catalase Electrode with Biphasic Enzyme Inhibition. *Nonlinear analysis: modelling and control*, 9(3):241–246, 2004 (cit. on p. 21).

[125] M. Sapagovas, A. Štikonas, O. Štikonienė. Alternating direction method for the Poisson equation with variable weight coefficients in an integral condition. *Differential equations*, 47(8):1176–1187, 2011. DOI: 10.1134/S0012266111080118 (cit. on p. 22).

[126] F. Ivanauskas, T. Meškauskas, M. Sapagovas. Stability of difference schemes for two-dimensional parabolic equations with nonlocal boundary conditions. *Applied mathematics and computation*, 215(7):2716–2732, 2009. DOI: 10.1016/j.amc.2009.09.012 (cit. on p. 22).

[127] V. Skakauskas, P. Katauskis. Numerical solving of coupled systems of parabolic and ordinary differential equations. *Nonlinear analysis: modelling and control*, 15(3):351–360, 2010 (cit. on p. 22).

[128] I. Basov, D. Švitra. A possibility of taking into consideration of insulin "age structure" for modeling blood glucose dynamics. *Informatica*, 11(1):87–96, 2000 (cit. on p. 22).

[129] J. Kleiza, M. Sapagovas, V. Kleiza. The Extension of the Van Der Pauw Method to Anisotropic Media. *Informatica*, 18(2):253–266, 2007 (cit. on p. 22).

[130] R. Baronas, F. Ivanauskas, M. Sapagovas. Reliability of one dimensional model of moisture diffusion in wood. *Informatica*, 13(4):405–416, 2002 (cit. on p. 22).

[131] I. Tumasoniene, G. Kulvietis, D. Mazeika, R. Bansevicius. The eigenvalue problem and its relevance to the optimal configuration of electrodes for ultrasound actuators. *Journal of sound and vibration*, 308(3-5):683–691, 2007. DOI: 10.1016/j.jsv.2007.04.036 (cit. on p. 22).

[132] P. Vasiljev, D. Mazeika, G. Kulvietis. Modelling and analysis of omnidirectional piezoelectric actuator. *Journal of sound and vibration*, 308(3-5):867–878, 2007. DOI: 10.1016/j.jsv.2007.03.074 (cit. on p. 22).

[133] D. Matuzevičius, A. Serackis, D. Navakauskas. Mathematical models of oversaturated protein spots. *Electronics and electrical engineering*, 1:63–68, 2007 (cit. on p. 22).

[134] S. Bacha, A. Bergel, M. Comtat. Modeling of amperometric biosensors by a finite-volume method. *Journal of electroanalytical chemistry*, 359(1-2):21–38, 1993 (cit. on p. 22).

[135] B. Sheeparamatti, M. Hebbal, R. Sheeparamatti, V. Math, et al. Simulation of Biosensor using FEM. *Journal of physics: conference series*, 34:241–246, 2006. DOI: 10.1088/1742-6596/34/1/040 (cit. on p. 22).

[136] B. Fornberg. Generation of finite difference formulas on arbitrarily spaced grids. *Mathematics of computation*, 51(184):699–706, 1988. DOI: 10.1090/S0025-5718-1988-0935077-0 (cit. on p. 23).

[137] R. Čiegis. *Lygiagretieji algoritmai (Parallel algorithms)*. Lithuanian. Technika, Vilnius, Lithuania, 2003 (cit. on pp. 26, 28).

[138] R. Čiegis. *Lygiagretieji algoritmai ir tinklinės technologijos (Parallel algorithms and network technologies)*. Lithuanian. Technika, Vilnius, Lithuania, 2005 (cit. on pp. 26, 28).

[139] B. Wilkinson, M. Allen. *Parallel Programming*. Pearson/Prentice Hall, 2005 (cit. on p. 26).

[140] A. Y. Zomaya. *Parallel computing for bioinformatics and computational biology*. John Wiley & Sons, Hoboken, NJ, USA, 2005 (cit. on p. 26).

[141] S. Ivanikovas, G. Dzemyda. Evaluation of the hyper-threading technology for heat conduction-type problems. *Mathematical modelling and analysis*, (September 2013):37–41, 2007 (cit. on p. 26).

[142] M. Mackevičius. Cheminių sintezių prie aukštų temperatūrų modeliavimas (Computer modeling of chemical synthesis at high temperatures). Lithuanian. PhD Thesis. Vilnius University, 2013 (cit. on p. 26).

[143] H. H. Wang. A Parallel Method for Tridiagonal Equations. *Acm transactions on mathematical software*, 7(2):170–183, 1981. DOI: 10.1145/355945.355947 (cit. on pp. 26, 28).

[144] W. Gander, J. Hřebíček. *Solving Problems in Scientific Computing Using Maple and MATLAB*. Springer Berlin Heidelberg, Berlin, Heidelberg, 2004. DOI: 10.1007/978-3-642-18873-2 (cit. on p. 26).

[145] V. Galvanauskas, R. Simutis. Software tool for efficient hybrid model-based design of biochemical processes. *Wseas transactions on biology and biomedicine*, 4(9):136–144, 2007 (cit. on p. 26).

[146] E. Gaidamauskaite. Computational Modeling Of Complex Reactions Kinetics In Biosensors. PhD Thesis. Vilnius University, 2011 (cit. on p. 27).

[147] M. Hucka, A. Finney, H. M. Sauro, H. Bolouri, et al. The systems biology markup language (SBML): a medium for representation and exchange of biochemical network models. *Bioinformatics*, 19(4):524–531, 2003. DOI: 10.1093/bioinformatics/btg015 (cit. on p. 27).

[148] A. Jouraku, N. Le Novère, A. Zell, M. Hucka, et al. JSBML: a flexible and entirely Java-based library for working with SBML. *Nature precedings*:3, 2011. DOI: 10.1038/npre.2011.6718 (cit. on p. 27).

[149] Geometry in SBML (cit. on p. 27).

[150] M. Hucka, F. T.Bergmann, S. Hoops, S. M.Keating, et al. The Systems Biology Markup Language (SBML): Language Specification for Level 3 Version 1 Core. Tech. rep. smbl.org, 2010. DOI: 10.1038/npre.2010.4959.1 (cit. on p. 27).

[151] K. Petrauskas. Kompiuterinis sudėtinės geometrijos biojutiklių modeliavimas (Computational Modelling of Biosensors of Complex Geometry). Lithuanian. PhD Thesis. Vilnius University, 2011 (cit. on p. 27).

[152] R. Baronas, K. Petrauskas. Sudėtinės geometrinės struktūros biojutiklių kompiuterinis modeliavimas (Computer-aided modeling of biosensors with a complex geometrical structure). Lithuanian. *Information sciences*, 56:156–162, 2011 (cit. on p. 27).

[153] D. Šimelevičius. Kompiuterinis sudėtingų biokatalizės procesų biojutikliuose modeliavimas (Computational Modelling of Complex Biocatalytic Processes in Biosensors). Lithuanian. PhD Thesis. Vilnius University, 2013 (cit. on p. 27).

[154] A. Kurtinaitis, R. Vaicekauskas, F. Ivanauskas. FDVis: the Interactive Visualization and Steering Environment for the Computational Processes Using the Finite-Difference Method. *Nonlinear analysis: modelling and control control*, 8(2):71–82, 2003 (cit. on p. 27).

[155] I. Foster. What is the grid?-a three point checklist. *Gridtoday*, 1(6), 2002 (cit. on p. 28).

[156] D. Abramson, J. P. Giddy, L. Kotler. High performance parametric modeling with Nimrod/G: Killer application for the global grid? *Proceedings of the 14th international parallel and distributed processing symposium (ipdps 2000).* Los Alamitos, Calif. : IEEE Computer Society, Cancun, Mexico, 2000, pp. 520–528. DOI: `10.1109/IPDPS.2000.846030` (cit. on p. 28).

[157] D. Abramson. Applications Development for the Computational Grid. *Proceedings of the 8th asia-pacific web conference on frontiers of www research and development. apweb 2006.* X. Zhou, J. Li, H. T. Shen, M. Kitsuregawa, et al., editors. Springer Berlin Heidelberg, Harbin, China, 2006, pp. 1–12. DOI: `10.1007/11610113\_1` (cit. on p. 28).

[158] H. Casanova, F. Berman. Parameter Sweeps on the Grid with APST. *Concurrency, practice and experience*, 1(1):1–15, 2003. DOI: `10.1002/0470867167` (cit. on p. 28).

[159] M. Yarrow, K. M. McCann, R. Biswas, R. F. V. DerWijngaart, et al. An advanced user interface approach for complex parameter study process specification on the information power grid. *Proceedings of the first ieee/acm international workshop on grid computing. grid 2000.* R. Buyya, M. Baker, editors. Springer Berlin Heidelberg, Bangalore, India, 2000, pp. 146–157. DOI: `10.1007/3-540-44444-0\_14` (cit. on p. 28).

[160] D. Abramson, T. Peachey, A. Lewis. Model Optimization and Parameter Estimation with Nimrod / O. *Proceedings of the 6th international conference on computational science (iccs'06).* V. N. Alexandrov, G. Dick, P. A. Sloot, J. Dongarra, editors. Vol. 1. Springer-Verlag Berlin, Heidelberg, Reading, United Kingdom, 2006, pp. 720–727. DOI: `10.1007/11758501\_96` (cit. on p. 28).

[161] W. Sudholt, K. K. Baldridge, D. Abramson, C. Enticott. Applying Grid Computing to the Parameter Sweep of a Group Difference Pseudopotential. *Proceedings of the 4th international conference on computa tional science [iccs 2004], volume 3036 of lecture notes in computer science.* Marian Bubak, G. D. v. Albada, P. M. A. Sloot, J. Dongarra, editors. Springer, Kraków, Poland, 2004, pp. 148–155 (cit. on p. 29).

[162] N. Čenas, J. Kulys. Biocatalytic oxidation of glucose on the conductive charge transfer complexes. *Bioelectrochemistry and bioenergetics*, 8(1):103–113, 1981. DOI: `10.1016/0302-4598(81)85011-8` (cit. on pp. 29, 34, 38).

[163] L.-C. Chen, K.-S. Tseng, K.-C. Ho. General Kinetic Model for Amperometric Sensors Based on Prussian Blue Mediator and Its Analogs: Application to Cysteine Detection. English. *Electroanalysis*, 18(13-14):1313–1321, 2006. DOI: `10.1002/elan.200603530` (cit. on p. 29).

[164] B. Li, Y. Shen, B. Li. Quasi-steady-state laws in enzyme kinetics. *The journal of physical chemistry. a*, 112(11):2311–2321, 2008. DOI: `10.1021/jp077597q` (cit. on pp. 29, 38).

[165] E. Hazai, L. Vereczkey, K. Monostory. Reduction of toxic metabolite formation of acetaminophen. *Biochemical and biophysical research communications*, 291(4):1089–94, 2002. DOI: `10.1006/bbrc.2002.6541` (cit. on p. 30).

[166] A. K. Rowden, J. Norvell, D. L. Eldridge, M. A. Kirk. Updates on acetaminophen toxicity. *The medical clinics of north america*, 89(6):1145–59, 2005. DOI: `10.1016/j.mcna.2005.06.009` (cit. on p. 30).

[167] A. K. Rowden, J. Norvell, D. L. Eldridge, M. A. Kirk. Acetaminophen poisoning. *Clinics in laboratory medicine*, 26(1):49–65, 2006 (cit. on p. 30).

[168] J. E. Sullivan, H. C. Farrar. Fever and antipyretic use in children. *Pediatrics*, 127(3):580–7, 2011. DOI: `10.1542/peds.2010-3852` (cit. on p. 30).

[169] M. Espinosa Bosch, A. Ruiz Sánchez, F. Sánchez Rojas, C. Bosch Ojeda. Determination of paracetamol: historical evolution. *Journal of pharmaceutical and biomedical analysis*, 42(3):291–321, 2006. DOI: `10.1016/j.jpba.2006.04.007` (cit. on pp. 30, 39).

[170] A. A. Ensafi, H. Karimi-Maleh, S. Mallakpour, M. Hatami. Simultaneous determination of N-acetylcysteine and acetaminophen by voltammetric method using N-(3,4-dihydroxyphenethyl)-3,5-dinitrobenzamide modified multiwall carbon nanotubes paste electrode. *Sensors and actuators b: chemical*, 155(2):464–472, 2011. DOI: `10.1016/j.snb.2010.12.048` (cit. on pp. 30, 39).

[171] H. Gutfreund. *Kinetics for the Life Sciences*. Cambridge University Press, 1995 (cit. on p. 38).

[172] J. N. Rodriguez-Lopez, J. R. Ros-Martinez, R. Varon, F. Garcia-Canovas. Calibration of a Clark-Type Oxygen Electrode by Oxidation of 4-tert-Butylcatechol. *Analytical biochemistry*, 202(2):356–360, 1992 (cit. on pp. 40, 42).

[173] H. Suzuki, A. Sugama, N. Kojima, F. Takei, et al. A miniature Clark-type oxygen electrode using a polyelectrolyte and its application as a glucose sensor. *Biosensors & bioelectronics*, 6(5):395–400, 1991 (cit. on p. 40).

[174] J. Kulys, K. Krikstopaitis, A. Ziemys. Kinetics and thermodynamics of peroxidase- and laccase-catalyzed oxidation of N-substituted phenothiazines and phenoxazines. *Journal of biological inorganic chemistry*, 5(3):333–40, 2000 (cit. on p. 40).

[175] R. Aris. *The Mathematical Theory of Diffusion and Reaction in Permeable Catalysts: The theory of the steady state*. Clarendon Press, 1975 (cit. on p. 41).

[176] R. Baronas, F. Ivanauskas, J. Kulys, M. Sapagovas. Modelling of amperometric biosensors with rough surface of the enzyme membrane. *Journal of mathematical chemistry*, 34(3-4):227–242, 2003 (cit. on p. 48).

[177] R. Baronas, J. Kulys, F. Ivanauskas. Computational Modelling of Biosensors with Perforated and Selective Membranes. *Journal of mathematical chemistry*, 39(2):345–362, 2005. DOI: 10 . 1007 / s10910-005-9034-0 (cit. on p. 48).

[178] Z. Farhagrazi, B. R. Copeland, T. Nakayama, T. Amachi, et al. Oxidation-Reduction Properties of Compounds I and II of Arthromyces ramosus Peroxidase. *Biochemistry*, 33:5647–5652, 1994 (cit. on p. 48).

[179] J. Kulys. Modeling Trienzyme Biosensor at Internal Diffusion Limitation. *Nonlinear analysis: modelling and control*, 9(1):139–144, 2004 (cit. on p. 48).

[180] M. Mackevičius, F. Ivanauskas, A. Kareiva, D. Jasaitis. A closer look at the computer modeling and sintering optimization in the preparation of YAG. *Journal of mathematical chemistry*, 50(8):2291–2302, 2012. DOI: 10.1007/s10910-012-0031-9 (cit. on p. 48).

[181] D. A. Gough, J. K. Leypoldt. Membrane-covered, rotated disk electrode. *Analytical chemistry*, 51(3):439–444, 1979. DOI: 10 . 1021 / ac50039a028 (cit. on p. 77).

[182] H.-C. Chang, C.-C. Wu, S.-J. Ding, I.-S. Lin, et al. Measurement of diffusion and partition coefficients of ferrocyanide in protein-immobilized membranes. *Analytica chimica acta*, 532(2):209–214, 2005. DOI: 10.1016/j.aca.2004.10.063 (cit. on p. 77).

[183] J. MacDougall, M. McCabe. Diffusion Coefficient of Oxygen through Tissues. *Nature*, 215:1173–1174, 1967. DOI: 10.1038/2151173a0 (cit. on p. 77).

[184] J. Wu, Q. Yuan. Gas permeability of a novel cellulose membrane. *Journal of membrane science*, 204(January):185–194, 2002 (cit. on p. 77).

[185] M. B. Andersen, Y. Hsuanyu, K. G. Welinder, P. Schneider, et al. Spectral and kinetic properties of oxidized intermediates of Coprinus cinereus peroxidase. *Acta chemica scandinavica*, 45:1080–1086, 1991 (cit. on p. 77).

[186] R. Baronas, F. Ivanauskas, J. Kulys. Computer simulation of the response of amperometric biosensors in stirred and non stirred solution. *Nonlinear analysis: modelling and control*, 8(1):3–18, 2003 (cit. on p. 79).

[187] A. Leo, C. Hansch, D. Elkins. Partition coefficients and their uses. *Chemical reviews*, 71(6):525–616, 1971 (cit. on p. 80).

Curriculum vitae

PERSONAL INFORMATION

	Vytautas Ašeris
Email	vytautas.aseris@gmail.com
Birth	1984-04-30. Panevėžys, Lithuania

EDUCTATION

PhD	2009-now	Informatics, to be defended on 2013-12-19
MsC	2007-2009	Software engineering
BsC	2003-2007	Software engineering
School	1995-2003	Juozas Balčikonis Gymnasium

WORK EXPERIENCE

NPSYS	2012-now	Founder, director, account manager
JMSYS	2009-2012	Developer, account manager
Affecto	2007-2008	Developer
Naviranta	2006-2007	Developer, analyst

TEACHING AND RESEARCH EXPERIENCE

VU MIF	2011-now	Junior researcher, Biomoda
VU MIF	2008-now	Assistant
VU MIF	2008-2010	Junior researcher, BIOSA

SCHOLARSHIPS

2012,2013	Lithuanian research council
2012	ECCOMAS Congress
2011	"Infobalt"